



University of
BRISTOL

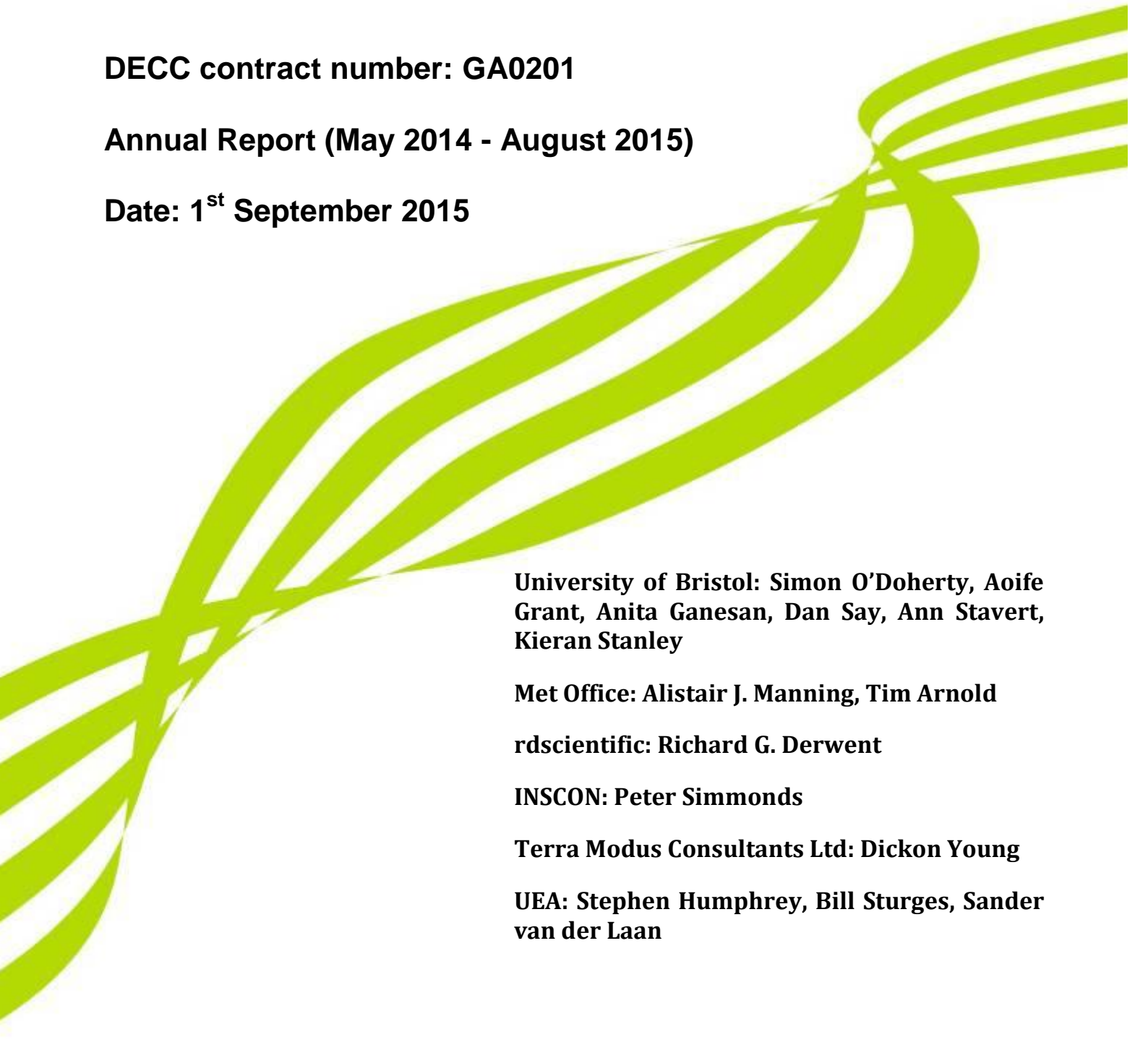
REPORT TO DECC

LONG-TERM ATMOSPHERIC MEASUREMENT AND INTERPRETATION (OF RADIATIVELY ACTIVE TRACE GASES)

DECC contract number: GA0201

Annual Report (May 2014 - August 2015)

Date: 1st September 2015



University of Bristol: Simon O'Doherty, Aoife Grant, Anita Ganesan, Dan Say, Ann Stavert, Kieran Stanley

Met Office: Alistair J. Manning, Tim Arnold

rdscientific: Richard G. Derwent

INSCON: Peter Simmonds

Terra Modus Consultants Ltd: Dickon Young

UEA: Stephen Humphrey, Bill Sturges, Sander van der Laan

Contents

1	Executive Summary	3
1.1	Project Summary.....	3
1.2	Background atmospheric trends	4
1.3	Estimates of regional emissions	5
1.4	Summary of the main findings	7
1.5	Summary of headline progress.....	8
2	Introduction	10
2.1	Objectives	10
2.2	Detail on Specific Work Programme Items	11
2.3	Recent Publications.....	15
2.4	Related information	17
3	Instrumentation	18
3.1	Sites.....	18
3.1.1	Mace Head (MHD).....	18
3.1.2	Ridge Hill (RGL)	18
3.1.3	Tacolneston (TAC)	18
3.1.4	Angus (TTA)	18
4	Description of data analysis methods.....	20
4.1	Introduction	20
4.2	Northern Hemisphere Atmospheric Baseline Trend Analysis.....	20
4.2.1	Summary.....	20
4.2.2	Introduction.....	20
4.2.3	Methodology	20
4.2.4	Baseline Mole Fractions	24
4.3	Regional emission estimation.....	28
4.3.1	Summary.....	28
4.3.2	InTEM (Inversion Technique for Emission Modelling)	28
5	Results and analysis of gases reported to the UNFCCC	32
5.1	Introduction	32
5.2	Methane (CH_4)	33
5.3	Nitrous oxide (N_2O)	36
5.4	Carbon dioxide (CO_2)	38
5.5	HFC-125	39
5.6	HFC-134a	41
5.7	HFC-143a	43
5.8	HFC-152a	45
5.9	HFC-23	47
5.10	HFC-32	49
5.11	HFC-227ea	51
5.12	HFC-43-10mee	53
5.13	HFC-365mfc.....	55
5.14	PFC-14 (CF_4)	57
5.15	PFC-116.....	59
5.16	PFC-218.....	61
5.17	PFC-318.....	63
5.18	SF_6	65
5.19	NF_3	67
6	Results and analysis of additional gases.....	68
6.1	Introduction	68
6.2	CFC-11	69
6.3	CFC-12	70
6.4	CFC-113	71
6.5	HCFC-124.....	72
6.6	HCFC-141b.....	73
6.7	HCFC-142b.....	74
6.8	HCFC-22.....	75

6.9 HFC-236fa	76
6.10 HFC-245fa	77
6.11 SO ₂ F ₂	78
6.12 CH ₃ Cl	79
6.13 CH ₂ Cl ₂	80
6.14 CHCl ₃ (chloroform)	81
6.15 CCl ₄ (carbon tetrachloride)	82
6.16 CH ₃ CCl ₃ (methyl chloroform).....	83
6.17 CCl ₂ CCl ₂	84
6.18 Methyl bromide (CH ₃ Br)	85
6.19 Halon-1211	86
6.20 Halon-1301	87
6.21 Halon-2402	88
6.22 Carbon monoxide (CO)	89
6.23 Ozone (O ₃)	90
6.24 Hydrogen	91
7 Results from the European InGOS project	92
7.1 Introduction	92
7.2 Halogenated species emissions estimates	92
7.3 Methane and nitrous oxide emission estimates	94
8 Appendix – Additional Site Information.....	97
8.1 Mace Head (MHD)	97
8.1.1 Medusa-GCMS.....	97
8.1.2 GC-MD	97
8.2 Ridge Hill (RGL)	97
8.2.1 GC-ECD	97
8.2.2 CRDS	97
8.3 Tacolneston (TAC)	98
8.3.1 Medusa-GCMS.....	98
8.3.2 GC-MD	98
8.3.3 CRDS	98
8.4 Angus (TTA).....	99
8.4.1 CRDS	99

1 Executive Summary

1.1 Project Summary

Monitoring the atmospheric concentrations of gases is important in assessing the impact of international policies related to the atmospheric environment. The effects of control measures on chlorofluorocarbons (CFCs), halons and HCFCs (hydrochlorofluorocarbons) introduced under the 'Montreal Protocol of Substances that Deplete the Ozone Layer' are now being observed. Continued monitoring is required to assess the overall success of the Protocol and the implication for atmospheric levels of replacement compounds such as hydrofluorocarbons (HFCs). Similar analysis of gases regulated by the Kyoto Protocol on greenhouse gases will likewise assist policy makers.

Since 1987, high frequency, real time measurements of the principal halocarbons and radiatively active trace gases have been made as part of the Global Atmospheric Gases Experiment (GAGE) and Advanced Global Atmospheric Gases Experiment (AGAGE) at Mace Head, County Galway, Ireland. For much of the time, the measurement station, which is situated on the Atlantic coast, monitors clean westerly air that has travelled across the North Atlantic Ocean. However, when the winds are easterly, Mace Head receives substantial regional scale pollution in air that has travelled from the industrial regions of Europe. The site is therefore uniquely situated to record trace gas concentrations associated with both the Northern Hemisphere background levels and with the more polluted air arising from European emissions.

An observation network for the UK (UK DECC network) has been created, along with Mace Head, consisting of three tall tower stations: Ridge Hill near Hereford; Tacolneston near Norwich; and

Angus near Dundee. Ridge Hill became operational in February 2012, Tackleton in July 2012 and Angus began operating for the network in May 2013. The expanded network makes it possible to resolve emissions on a higher resolution across the UK, to Devolved Administration (DA) level.

This project has two principle aims:

- Estimate the background atmospheric concentrations of the principle greenhouse and ozone-depleting gases from DECC network observations.
- Estimate the UK and North-West European emissions of the principle greenhouse gases using the DECC network observations and compare these to the compiled inventory.

The atmospheric measurements and emission estimates of greenhouse gases provide an important independent cross-check for the national greenhouse gas inventories (GHGI) of emissions submitted annually to the United Nations Framework Convention on Climate Change (UNFCCC). The GHGI are estimated through in-country submissions of Activity Data and Emission Factors that are, in some cases, very uncertain. Independent emissions verification is considered good practice by the Intergovernmental Panel on Climate Change (IPCC).

1.2 Background atmospheric trends

The Met Office particle transport model, NAME (Numerical Atmospheric dispersion Modelling Environment), is run in backward-running mode to estimate the dilution of emissions from recent (within 30-days) surface releases to a concentration at the observing station, Mace Head on the west coast of Ireland. These so called 'air history maps' have been produced for each 2-hour period from 1989 until present day. NAME is 3-dimensional and therefore it is not just surface transport that is modelled, an air parcel can travel from the surface to a high altitude and then back to the surface but only those times when the air parcel is within the lowest 40 m above the ground will it be recorded in the surface air history maps. The impact of air from higher altitudes arriving at the surface at Mace Head is also separately recorded. The model domain covers North America to Russia and North Africa to the Arctic Circle and extends to more than 10 km vertically. No chemical or deposition processes were modelled; this is realistic given the long atmospheric lifetimes of the gases considered.

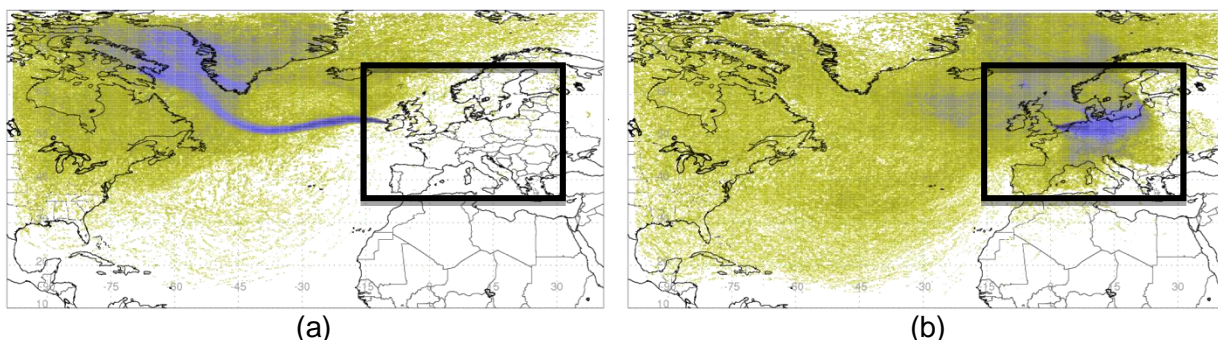


Figure 1: Examples of 2-hour air history surface maps derived from NAME (a) baseline period (b) regionally polluted period. The maps describe which surface areas (defined as within 40 m of the surface) in the previous 30-days impact the observation point at a particular time.

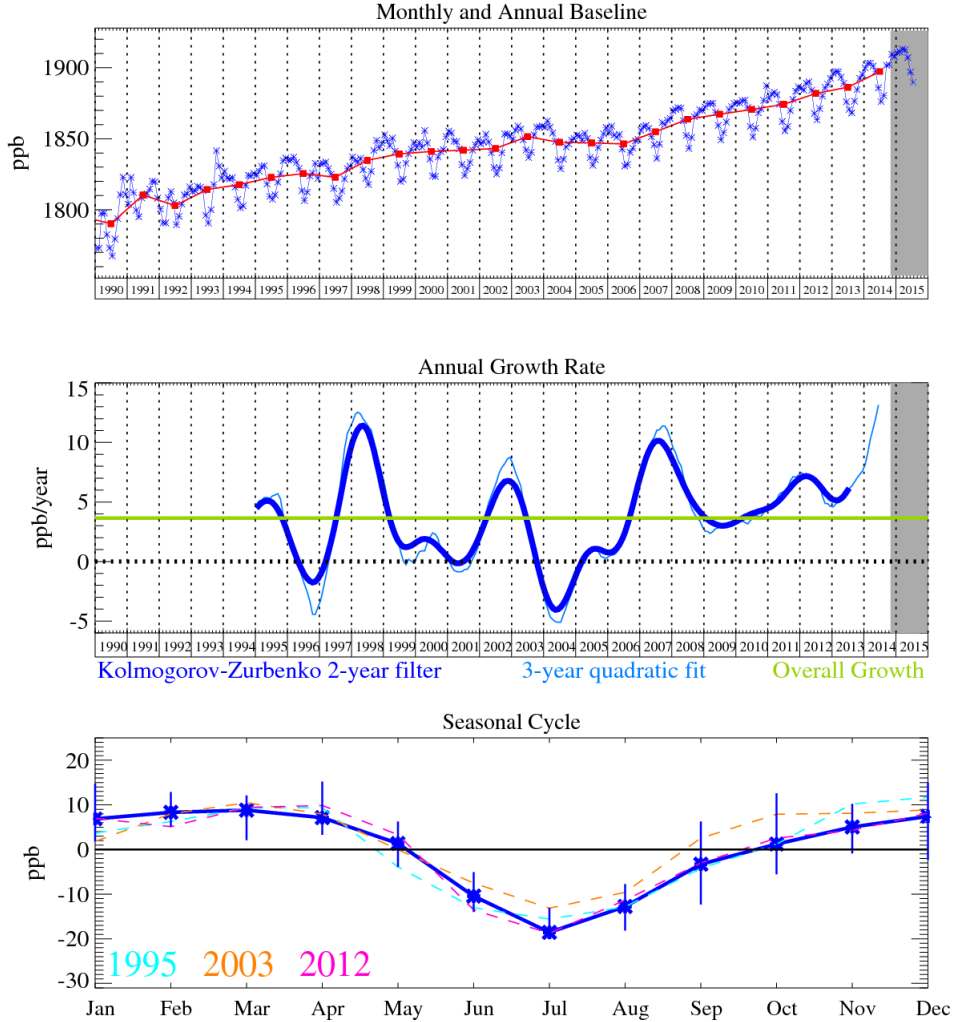


Figure 2: Methane: Monthly (blue) and annual (red) baseline mole fractions (top plot); Annual (blue) and overall average growth rate (green) (middle plot); Seasonal cycle (de-trended) with year-to-year variability (lower plot). Grey area covers un-ratified and therefore provisional data.

The first step is to estimate the Northern Hemisphere (NH) atmospheric background concentration (referred to as the baseline) of each gas measured at Mace Head; their long-term baseline trends and growth rates and their seasonal cycle. Baseline concentration times are defined here as those times when the air mass arriving at Mace Head has not been influenced by significant emissions within the previous few weeks (varying depending on how quickly the winds move the air from the edge of the defined model domain to Mace Head), i.e. those times when the air is well mixed and is representative of the NH background concentration. Figure 1 shows two example air history maps, the one on the left shows a 2-hour period when the air mass will be considered baseline, the one on the right, when the air mass is not considered baseline because of the recent influence of Europe, a source region. Times when the air has rapidly descended to Mace Head from the upper troposphere (defined here as above 9 km) are also not considered baseline because many gases have a strong vertical gradient, usually decreasing concentration with height.

By fitting a time-varying line through just those Mace Head observations recorded within the 2-hour time periods when the air masses are representative of the NH baseline it is possible to extract from the observational data an estimate of the hourly baseline across the entire measurement record. The hourly baseline can then be further interrogated to estimate monthly and annual values, reveal whether the NH atmospheric mole fraction is growing or declining and the strength of the baseline seasonal cycle. Figure 2 shows the results for methane.

1.3 Estimates of regional emissions

By removing the time-varying baseline concentrations from the raw measurement data, a time-series of excursions from the baseline, averaged over each 2-hour period, for each observed gas has been generated. The perturbations above baselines, observed across the UK DECC network,

are driven by emissions on regional scales that have yet to be fully mixed on the hemisphere scale and are the principle tool used to estimate surface emissions across north-west Europe. A method for estimating emissions from observations, referred to as ‘Inversion Technique for Emission Modelling’ (InTEM), has been developed over many years and is used here to estimate UK and North-West European (NWEU = UK + Ireland + France + Germany + Denmark + the Netherlands + Belgium + Luxembourg) emissions using the observations from the UK DECC network.

InTEM links the observation time-series with the NAME air history estimates of how surface emissions dilute as they travel to the observation stations. An estimated emission distribution when combined with the NAME output can be transformed into a modelled time-series at each of the measurement stations. The modelled and the observed time-series can be compared using a single or a range of statistics (referred to as a cost function) to produce a skill score for that particular emission distribution. InTEM uses a well known best-fit technique, simulated annealing, to search for the emission distribution that produces a modelled times-series that has the best statistical match to the observations. InTEM can either start from a random emission distribution or from an inventory-defined distribution.

In order for InTEM to provide robust solutions for every area within the modelled domain, each region needs to significantly contribute to the air concentrations at the UK DECC network sites for a reasonable number of time periods. If the signal from an area is only rarely or poorly seen by the network, then its impact on the cost function is minimal and the inversion method will have little skill at determining its true emission. The contributions that different grid boxes make to the observed air concentration varies from grid to grid. Grid boxes that are distant from the observation site contribute little to the observation, whereas those that are close have a large impact. In order to balance the contribution from different grid boxes, those that are more distant are grouped together into increasingly larger regions. The grouping cannot extend beyond country (or DA) boundaries. The country boundaries extend into the surrounding seas to reflect both emissions from shipping, off-shore installations and river runoff but also because the inversion has geographical uncertainty.

There is significant uncertainty in the emissions that are estimated. Uncertainty arises from many factors: errors in the baseline estimate; emissions that vary over time-scales shorter than the inversion time-period e.g. diurnal, seasonal or intermittent; heterogeneous emissions i.e. emissions that vary within the regions solved for; errors in the transport model (NAME) or the underpinning 3-dimensional meteorology; errors in the observations themselves. The potential magnitudes of these uncertainties have been estimated and are incorporated within InTEM to inform the uncertainty of the modelled results.

1.4 Summary of the main findings

- The Northern Hemisphere atmospheric concentrations of ALL Kyoto gases except HFC-152a are increasing.
- Carbon dioxide (CO_2): The anthropogenic component of CO_2 is very difficult to assess because of the very significant, temporally and spatially varying biogenic sink/source terms. In the previous annual report the correlation between anthropogenic CO_2 and carbon monoxide (CO) was exploited to estimate the UK anthropogenic component. The agreement between the GHGI and InTEM estimates is fair but the uncertainty in the InTEM estimates are considerably larger than those reported for the GHGI. Other gases such as ethane and propane could be used together with the CO as surrogates for CO_2 anthropogenic emissions. Isotopes could also play a significant role in disentangling the CO_2 observations into their anthropogenic and biogenic components.
- The inclusion of the extended DECC network observations allows the InTEM time frame to be reduced from 3-year to 1-year, and agreement is maintained within the uncertainty estimates.
- Methane (CH_4 ; 8-11% of total UK GHG emissions): The UK InTEM estimates are lower than the Greenhouse Gas Inventory (GHGI) estimates (as published by DECC in 2015) in the 1990s but there is good agreement from 2000s onwards.
- Nitrous oxide (N_2O ; 4-9% of total UK GHG emissions): The UK GHGI and InTEM estimates are broadly in agreement. The 3-year Mace Head (MHD) only InTEM estimates are showing a positive trend in the latter period unlike the GHGI. The UK DECC network 1-year estimates are higher than the GHGI and the MHD-only estimates although the uncertainties overlap. The difference between the MHD-only and the DECC network results show the value of moving to a higher temporal resolution. The impact of the extended network on the emissions trend cannot yet be understood given the short timeseries available.
- HFC-134a (0.6-0.9% of total UK GHG emissions): The UK GHGI is approximately double that estimated by InTEM and the uncertainty estimates for the two methods do not overlap. The inventory emission factors used by countries across NWEU vary significantly yet reasons for such large discrepancies are not clear. Factors used by the UK inventory, therefore, could be inaccurate and be a reason for the disagreement with the InTEM estimates.
- HFC-125 (0.4-0.6% of total UK GHG emissions) and HFC-32 (of total UK GHG emissions): The UK GHGI estimates for these gases (used in refrigerant blends) are increasing. UK InTEM estimates agree with the GHGI up until 2009 after which time InTEM emission estimates level off. For NWEU, both the InTEM and GHGI estimates are increasing. It is possible the balance between UK and non-UK NWEU usage of these gases is changing over time.
- For HFC-143a (0.4-0.6% of total UK GHG emissions): UK InTEM is around 20% higher than the GHGI, though UK InTEM estimates are now falling whereas GHGI estimates are growing.
- Sulphur hexafluoride (SF_6 ; 0.1-0.2% of total UK GHG emissions): The UK InTEM estimates are consistently elevated compared to the GHGI, however the InTEM uncertainty ranges do encompass the inventory estimates. The NWEU InTEM estimates are higher than the inventory until 2010 after which the agreement is good.
- Nitrogen trifluoride (NF_3) has been added to the list of compounds being measured by the Medusa GC-MS at Mace Head and is amongst the first *in situ* measurements made of this potent greenhouse gas. The UK emissions of the gas are very small.

1.5 Summary of headline progress

Major progress has been made during the last 18 months of the contract period. Full descriptions are provided in the Interim reports (Oct 2014 and May 2015). There have been improvements to how the baseline is estimated, how uncertainty in the inversion process is represented and its individual constituent components, UK emissions of NF₃ have been estimated for the first time and the inventory Refrigeration and Air Conditioning (RAC) model has been investigated.

- **All the UK DECC Network sites are working well.** The compounds measured at each site are shown in Interim reports (Oct 2014 and May 2015). This is the first network of its kind in the UK (and Europe) and has been a major achievement of this contract.
- **Mace Head** continues to be a baseline station at the forefront of global atmospheric research. This is evident through the high volume of peer-reviewed publications related to work using the Mace Head observational record. The recent publications related to this contract are detailed in the publication section of this report. In addition, the inclusion of Mace Head in many EU funded atmospheric research programmes, such as ICOS, InGOS, ACTRIS, and continued support from other global programmes such as AGAGE and NOAA-ESRL indicates its international significance.
- **Mid-latitude Northern Hemisphere baseline trends are updated on website.** The trends are also presented in this report and have been extended up to and including July 2015.
- **UK emission estimates.** Inversion emission estimates for the UK and North West Europe are reported up to and including 2014 and have been compared to the 2015-reported GHGI UK inventory (the 2015 GHGI submission covers emissions up to and including 2013).
- **UNFCCC verification appendix chapter** for the UK National Inventory Report (NIR) submission was delivered (March 2015).
- **Investigating uncertainties in InTEM and the impact of using the different measurement stations.** The inversion system (InTEM) uses uncertainty estimates from several sources: (a) Atmospheric baseline uncertainty; (b) Degree of influence of the surface area local to the observation point; (c) Repeatability uncertainty of the observation; and (d) Variability uncertainty of the observation within a 2-hour window. Uncertainty elements (a) and (b) are classed as model uncertainty as they relate to the ability of the model to correctly model the airflow to the observation point. Uncertainty elements (c) and (d) are classed as observation uncertainty as they relate to the uncertainty of the observation within a 2-hour window. The relative strengths of the model and observation uncertainties were reported (Nov 2014) for each year and station for the Kyoto basket of gases. The impact on uncertainty reduction on emission estimates of methane for the different Devolved Administrations (DAs) within the UK using different combinations of stations within the UK DECC network and also the two Greenhouse gAs UK and Global Emissions (GAUGE) tall towers were investigated and reported in Nov 2014.
- **Direction specific baselines developed within InTEM.** The concept of direction specific baselines has been developed within InTEM. 11 additional direction and height specific variables are solved for within the inversion. The prior baseline used is from the standard baseline estimation method for Mace Head. After the inversion each station has a specific and unique baseline that depends on where the air enters the model domain arriving at that particular station. The results of this work are presented in the May 2015 report.
- **Reporting a new Kyoto basket gas.** Nitrogen trifluoride (NF₃) inversions have been performed for the first time and were reported (Nov 2014). The emissions of NF₃ from the UK are not significant relative to the magnitude of the uncertainties. Nitrogen trifluoride inversions were also performed for the first time across East Asia and were reported in the

May 2015 report. The emissions estimates of NF₃ from South Korea are significant relative to the magnitude of the uncertainties.

- **Investigating the sensitivities in the inventory model for estimating HFC-134a emissions.** The inventory refrigerant model (RAC) was provided for investigation by DECC. The sensitivities of the model to the input parameters were considered for the gas HFC-134a, the principle gas used as a mobile air conditioner, e.g. in cars. The results of this on-going analysis were presented in the May 2015 report.

2 Introduction

2.1 Objectives

This project has two principle aims:

- **Estimate the background atmospheric concentrations of the principle greenhouse and ozone-depleting gases from the DECC network observations.**
- **Estimate the UK and North-West European emissions of the principle greenhouse and ozone-depleting gases using the DECC network observations and compare these to the compiled inventory.**

For the measurement section of the project the objectives are:

- To either, lease, purchase or otherwise provide, and maintain instrumentation to obtain measurements of the gases listed in the contract and to run the atmospheric observation site at Mace Head, Ireland.
- To continue high quality real-time measurements of the gases listed in Annex 1 at Mace Head, Ireland, including routine in situ GC-MS measurements of hydrofluorocarbons (HFCs), perfluorocarbons (PFCs), hydrochlorofluorocarbons (HCFCs), methyl bromide, halons and other halogenated gases relevant to stratospheric ozone depletion and climate change.
- To either lease, purchase or otherwise provide, and maintain instrumentation to obtain measurements of the major Kyoto gases (CO_2 , CH_4 , and N_2O) and to run atmospheric observation sites at any proposed additional site/s across the UK.
- To make high-quality real time measurements of the major Kyoto gases at any additional observation site(s), consistent with the requirements set out above.
- To continue international collaboration and data exchange within the global Advanced Global Atmospheric Gases Experiment (AGAGE) project. This will include, *inter alia*, the determination of global magnitude and latitudinal distribution of the surface sources of greenhouse gases
- To provide data to help study the atmospheric behaviour of trace gases, to estimate source gas strengths in the UK and NW Europe and to study the concentrations and trends in the total chlorine/bromine content of the atmosphere and the oxidising capacity of the atmosphere
- To maintain an up-to-date calibrated database of any of the trace gases measured under contract to DECC at Mace Head and any additional site/s, and to maintain a secondary database of any measurements made as part of the AGAGE global network.
- To continue technical development of measurement methodologies to improve reliability and accuracy wherever possible.

For the interpretation part of the project the objectives are:

- To quantify anthropogenic emissions (by source gas) of halocarbons, and anthropogenic emissions (by source gas, also source gas removal by sinks) of greenhouse gases, at the North West European, UK and Devolved Administrations (DA) levels and to use these for inventory verification.

- To identify new substances with ozone depleting or radiative forcing properties, and quantify these where necessary.
- To assess trends in emissions and concentrations of greenhouse gases and halocarbons and identify departure from expected trends, and the causes of any noted departure.
- To identify additional sources of data for assessing compliance and verification of emissions inventories, particularly work initiated under the auspices of Working Group 1 of the EU Monitoring Mechanism and other EU programmes currently underway and report on these to DECC, with forewarning of upcoming meetings and their objectives.

2.2 Detail on Specific Work Programme Items

- Assess and report concentrations of direct and indirect greenhouse gases measured at Mace Head and any additional site/s.

Mole fraction data from Mace Head are submitted to the Carbon Dioxide Information Analysis Center (CDIAC, <http://cdiac.ornl.gov>) every six months. CDIAC is the primary climate-change data and information analysis centre of the U.S. Department of Energy. CDIAC data are automatically reformatted and sent to the World Data Centre (WDC) for Greenhouse Gases (WDCGG, <http://ds.data.jma.go.jp/gmd/wdcgg/>) which is one of the WDCs under the WMO (World Meteorological Organisation) GAW (Global Atmospheric Watch) programme that serve to gather, archive and provide data on greenhouse gases and other related gases in the atmosphere and ocean. As part of the European InGOS project, the Mace Head data submitted to CDIAC data are also submitted to the EBAS database (<http://ebas.nilu.no/>). The observations from the UK DECC network are submitted directly to EBAS every six months.

The reported baseline concentrations (mole fractions), annual growth rates and seasonal cycles along with instrumentation and calibration details are presented in the “UK DECC Network” website (<http://www.metoffice.gov.uk/atmospheric-trends/>). Note that the information in this website is due to move to a .gov.uk domain in the near future.

- Analyse and update annual global baseline atmospheric concentration trends and European emissions of the gases in Annex 1. Comparisons should be made with inventory data, and if relevant production and consumption figures provided by industry to the EU.

For each gas, baseline atmospheric concentration trends for the mid-latitude northern hemisphere have been reported quarterly through the website and are reported in Chapter 5.

For each gas measured by the UK DECC network, an estimate of the UK and North West European (NWEU) (comprising of Ireland, UK, France, Belgium, the Netherlands, Luxembourg, Germany, Denmark) annual emissions have been made using the InTEM system (Chapter 5). Where available the InTEM results have been compared against GHG inventory data.

- Identify departure from expected trends in concentration and emissions of gases listed in Annex 1 and identify causes of these variations. Identify and assess the reasons for any departure from expected trends in concentration.

The trends in the mid-latitude northern hemisphere baseline concentrations of each gas are discussed in Chapter 5. The UK emission trends of each gas are discussed and any departures from the expected have been highlighted.

- Identify any additional sources of data for monitoring gases listed in Annex 1.

The data from the additional UK DECC network stations, Ridge Hill, Tacolneston and Angus are used where available (for more details on the sites see the Appendix, and the website www.metoffice.gov.uk/atmospheric-trends).

Relevant observations from the wider GAUGE network (Heathfield and Bilsdale towers) have been incorporated within the InTEM analysis and presented in an Interim report (May 2015).

CH₄ and N₂O observations from the InGOS European network have been incorporated within InTEM and are presented in Chapter 7. This work has been facilitated through collaborations within the EU InGOS project.

- Make and update annual estimates of European and UK emissions of direct and indirect GHG and provide comparisons with the UKGHGI, EMEP and the EEA emissions inventories. Any discrepancies with emissions inventories should be highlighted and discussed.

InTEM has been applied to the direct and indirect greenhouse gases measured by the UK DECC network. Annual UK and NW European emission estimates using Mace Head (MHD) observations are reported in Chapter 5. The observations from Ridge Hill (RGL), Tacolneston (TAC) and Angus (TTA) have been incorporated within InTEM to estimate UK emissions from 2012 onwards.

Where data are available these estimates have been compared to those reported elsewhere, most notably those reported through the UNFCCC programme, and the discrepancies are discussed. Due to the significant biogenic emissions and sinks of CO₂, estimating the anthropogenic emissions of CO₂ is very difficult and was discussed at length in a previous annual report (May 2014).

- Identify new ozone depleting or global warming substances of potential policy interest, and provide details to DECC. Investigate the potential and feasibility for further expanding the policy relevance of Mace Head or any other sites' data, by considering other classes of atmospheric trace gases such as hydrocarbons, oxygenated species, perfluorocarbons, very long lived molecules, and oxygen concentrations.

It is a primary aim of the AGAGE programme and UK DECC Network to identify new ozone depleting or global warming substances and where possible add these compounds to the ever increasing number of substances measured using the Medusa GC-MS at Mace Head, and more recently at Tacolneston. However, with this type of activity there will always be a compromise between the number of substances measured and the precision of the measurement that can be achieved. For this reason, it normally takes a reasonable amount of time between identification of a new compound, assessment of the implication of adding the compound to the analysis list (i.e. degradation of measurement performance for existing compounds) and agreeing that the importance of the scientific questions that can be answered from the addition of the compound, warrant its inclusion. This process has taken place for two sets of compounds over the last few years: NF₃; and the higher molecular weight perfluorocarbons (PFCs). A discussion of potential new compounds was presented in a previous report (May 2014).

- Identify any gaps in existing data from Mace Head and any additional site/s that could potentially be of policy relevance.

Isotope measurements of CO₂, CH₄ and N₂O have the potential to add further constraints to the inversion system, for example by providing additional information on the emissions from different source sector categories. The scope and challenges of isotope observations are significant but are being investigated by the NERC GAUGE programme that is undertaking a measurement campaign of some of the principle isotopes of CO₂, CH₄ and N₂O.

- Liaise with Hadley Centre over 3D atmospheric chemistry modelling being carried out at the Hadley Centre and provide data for model validation purposes, if required.

The monthly time-series of baseline concentrations and average seasonal cycles of all of the gases measured at Mace Head are provided to the Hadley Centre (part of the Met Office). Currently the data provided, although of direct relevance, are not widely used. To facilitate raising awareness of

this useful source of data, the Met Office staff directly involved in this contract are now part of the Hadley Centre Earth System and Mitigation Science group.

- Investigate the use that could be made of new or additional sources of data such as isotope measurements or flux data, in conjunction with data from Mace Head and the additional site/s, or from any other sites that could potentially be of policy relevance, for verifying GHG emissions.

Through the NERC funded GAUGE programme, new sources of data are becoming available. These include inter-calibrated information from ground-based, airborne, ferry-borne, balloon-borne, and space-borne sensors, including new sensor technology and isotope measurements. (<http://www.greenhouse-gases.org.uk/>). Professor Simon O'Doherty and Dr Alistair Manning are also partners in this programme and have presented some results from the use of these new data sources in a previous report (May 2015). As discussed above, use will also be made of relevant and available non-UK ICOS observations e.g. through the EU InGOS programme, which are presented in Chapter 7. There are some isotope measurements made at Mace Head ($\Delta^{14}\text{CO}_2$ by University of Heidelberg and $\delta^{13}\text{CO}_2$ by NOAA) although, in isolation, these measurements do not provide a great deal of useful information about UK anthropogenic/biogenic emissions. As part of the NERC GAUGE programme the existing "baseline" measurements at Mace Head have been extended and measurements are now also made at Tacolneston where the measurements contain more information on UK pollution. In future work this information may prove to be useful in policy relevant work for verifying GHG emissions.

- Provide advice, as requested by DECC, on the relative roles of radiatively active trace gases in forcing climate change and, where possible, compute global warming potentials (GWPs) for any new substances identified.

This has taken place for the higher molecular weight perfluorocarbons (PFCs) and also in consideration of new gases of potential policy interest, see previous report (May 2014).

- Report on developments in the understanding of anthropogenic and natural sources and sinks of carbon dioxide, methane and nitrous oxide, using seasonal trends in emissions and analysis of annual trends

Annual UK and North West European emission estimates, through the use of inversion modelling, of methane (CH_4) and nitrous oxide (N_2O) are reported in Chapter 5. The agreement between the anthropogenic inventory and the InTEM results for CH_4 and N_2O is good. For CH_4 the UK InTEM results are consistently lower than the inventory pre-2000 estimates but agree, within the uncertainty, post-2002. The magnitude of the uncertainties in the InTEM CH_4 estimates is comparable to those reported for the inventory. For N_2O and CH_4 it has been assumed that on the NWEU scale the biogenic emissions are small compared to the anthropogenic contribution. For CO_2 the same assumption is not plausible and so an alternative route through the ratio to anthropogenic carbon monoxide was used to estimate UK anthropogenic CO_2 emissions. The InTEM CO_2 estimates calculated through this method have very significant uncertainties compared to the reported inventory uncertainties (see report May 2014).

Isotopic measurements may also aid our understanding of this split, but the paucity of observations will make this very challenging. The scope and challenges of isotope observations is discussed above.

- Compare data from Mace Head and any additional site/s with data from other national and international studies, where appropriate.

The consortium is part of the AGAGE community and regularly compares analyses where appropriate. CSIRO (Australia) conducts comprehensive comparisons between all of the data measured by AGAGE (including Mace Head) and other global sites around the world. This comparison data set is reviewed together with the international AGAGE team at biannual meetings.

- Provide assistance and as requested by DECC, on validation of European and national-level trace gas emission inventories, and on monitoring compliance with international protocols and agreements or other research conducted for the contract.

Each year a verification annex has been prepared under this contract and has been included in the UK National Inventory Report submission to the UNFCCC.

- Ensure information-exchange and coordination with complementary European Union projects on verification of greenhouse gas emissions, for example CarboEurope, NitroEurope, IPCC reports, guidelines or studies, and attend inverse-modelling workshops arranged under the auspices of the EU Monitoring Mechanism.

The contractors are active members and share information with the AGAGE, NOAA, ICOS, InGOS and GAUGE programmes and are available to contribute to IPCC reports, WMO Ozone Assessments, guidelines and studies, SPARC assessments, and attend appropriate workshops as required. InGOS meetings (Florence, Italy, Oct 2014; Utrecht, the Netherlands, Sept 2015), AGAGE meetings (Ascona, Switzerland, April 2014; La Jolla, California, Dec 2014), a GAUGE meeting (Manchester, Oct 2014), UK ICOS meetings (Southampton, Jan 2015; London March 2015) and a JPI European meeting (Dublin, Ireland, Jul 2015) were attended.

- Advise on developments in remote sensing techniques in general as applied to measurement of atmospheric trace gases and inventory verification.

Through the NERC GAUGE programme specific use will be made of the GOSAT satellite methane data. The contractors will liaise with Dr. Hartmut Bosch of the University of Leicester who is leading this GAUGE work package. Satellite information will be used within the global inversion studies, the success of these efforts will be reported to DECC as they come to fruition.

- Make provision for up to 5 days' ad-hoc policy support per year to DECC's Science team.

Over the last 18 months nothing specific has been done under this work item.

- Provide quarterly project updates, annual project reports, and an end of contract project report.

Interim and annual contract reports have been produced as specified in the milestone plan. These reports, in addition to being delivered to DECC, have also been made available (when released by DECC) through the contract website (<http://www.metoffice.gov.uk/atmospheric-trends>).

- Host a website containing information about Mace Head and any other observation sites. The website should contain up to date project reports, the interpreted and ratified observations data, and be updated at least once every three months.

A website (<http://www.metoffice.gov.uk/atmospheric-trends>) containing all relevant information relating to this work has been further developed (note that the information available here will soon move to a .gov.uk domain). Each observation site is described in detail, including geographical location, photographs and the gases measured. The record of monthly and annual baseline mole fractions, the growth rates and the seasonal cycles for each gas are presented, together with relevant information about each gas, and updated quarterly. All contract reports, containing information on baseline trends and emission estimates, are available through the website. The comparison of the UK InTEM emission estimates with the GHGI are reported through the Interim and annual reports.

2.3 Recent Publications

- Arnold, T., D. J. Ivy, C. M. Harth, M. K. Vollmer, J. Mühlé, P. K. Salameh, L. P. Steele, P. B. Krummel, R. H. J. Wang, D. Young, C. R. Lunder, O. Hermansen, T. S. Rhee, J. Kim, S. Reimann, S. O'Doherty, P. J. Fraser, P. G. Simmonds, R. G. Prinn, and R. F. Weiss, HFC-43-10mee atmospheric abundances and global emission estimates, *Geophysical Research Letters*, doi:10.1002/2013GL059143, 2014.**
- Arnold, T., C.M. Harth, J. Mühlé, A.J. Manning, P.K. Salameh, J. Kim, D.J. Ivy, L.P. Steele, V.V. Petrenko, J.P. Severinghaus, D. Baggenstos, and R.F. Weiss, Nitrogen trifluoride global emissions estimated from updated atmospheric measurements, *PNAS* 2013 110 (6) 2029-2034, 2013, doi:10.1073/pnas.1212346110.**
- Bergamaschi, P., M. Corazza, U. Karstens, M. Athanassiadou, R. L. Thompson, I. Pison, **A. J. Manning**, P. Bousquet, A. Segers, A. T. Vermeulen, G. Janssens-Maenhout, M. Schmidt, M. Ramonet, F. Meinhardt, T. Aalto, L. Haszpra, J. Moncrieff, M. E. Popa, D. Lowry, M. Steinbacher, A. Jordan, **S. O'Doherty**, S. Piacentino, and E. Dlugokencky, Top-down estimates of European CH₄ and N₂O emissions based on four different inverse models, *Atmospheric Chemistry & Physics*, 15, 715-736, 2015, doi:10.5194/acp-15-715-2015
- Derwent, R. G., P. G. Simmonds, S. O'Doherty, A. Grant, D. Young, M. C. Cooke, A. J. Manning, S. R. Utetbe, M. E. Jenkin, and D. E. Shallcross, Seasonal cycles in short-lived hydrocarbons in baseline air masses arriving at Mace Head, Ireland, *Atmospheric Environment*, 62, 89–96, doi:10.1016/j.atmosenv.2012.08.023, 2012.**
- Fraser, A., P. I. Palmer, L. Feng, H. Boesch, A. Cogan, R. Parker, E. J. Dlugokencky, P. J. Fraser, P. B. Krummel, R. L. Langenfelds, **S. O'Doherty**, R. G. Prinn, L. P. Steele, M. van der Schoot, and R. F. Weiss, Estimating regional methane surface fluxes: the relative importance of surface and GOSAT mole fraction measurements, *Atmospheric Chemistry & Physics*, 13(11), 5697–5713, doi:10.5194/acp-13-5697-2013, 2013.
- Fraser, P. J., B. L. Dunse, **A. J. Manning**, S. Walsh, R. H. J. Wang, P. B. Krummel, L. P. Steele, L. W. Porter, C. Allison, **S. O'Doherty**, P. G. Simmonds, J. Mühlé, R. F. Weiss, and R. G. Prinn, Australian carbon tetrachloride emissions in a global context, *Environmental Chemistry*, 11(1), 77, doi:10.1071/EN13171, 2014.
- Fraser, A., P. I. Palmer, L. Feng, H. Boesch, A. Cogan, R. Parker, E. J. Dlugokencky, P. J. Fraser, P. B. Krummel, R. L. Langenfelds, **S. O'Doherty**, R. G. Prinn, L. P. Steele, M. van der Schoot, and R. F. Weiss, Estimating regional methane surface fluxes: the relative importance of surface and GOSAT mole fraction measurements, *Atmospheric Chemistry & Physics*, 13(11), 5697–5713, doi:10.5194/acp-13-5697-2013, 2013.
- Ganesan, A. L., A. Chatterjee, R. G. Prinn, C. M. Harth, P. K. Salameh, A. J. Manning, B. D. Hall, J. Mühlé, L. K. Meredith, R. F. Weiss, S. O'Doherty, and D. Young, The variability of methane, nitrous oxide and sulfur hexafluoride in Northeast India, *Atmospheric Chemistry & Physics*, 13(21), 10633–10644, doi:10.5194/acp-13-10633-2013, 2013.**
- Ganesan, A. L., Rigby, M., Zammit-Mangion, A., Manning, A. J., Prinn, R. G., Fraser, P. J., Harth, C. M., Kim, K.-R., Krummel, P. B., Li, S., Mühlé, J., O'Doherty, S. J., Park, S., Salameh, P. K., Steele, L. P., and Weiss, R. F.: Characterization of uncertainties in atmospheric trace gas inversions using hierarchical Bayesian methods, *Atmos. Chem. Phys.*, 14, 3855-3864, doi:10.5194/acp-14-3855-2014, 2014.**
- Ganesan, A. L., A. J. Manning, A. Grant, D. Young, D. E. Oram, W. T. Sturges, J. B. Moncrieff, S. O'Doherty, Quantifying methane and nitrous oxide emissions from the UK and Ireland using a national-scale monitoring network. *Atmos. Chem. Phys.*, 15, 6393-6406, 2015, doi:10.5194/acp-15-6393-2015**
- Giostra, U., F. Furlani, J. Arduini, D. Cava, **A. J. Manning**, **S. J. O'Doherty**, S. Reimann, and M. Maione, The determination of a “regional” atmospheric background mixing ratio for anthropogenic greenhouse gases: A comparison of two independent methods, *Atmospheric Environment*, 45(39), 7396–7405, doi:10.1016/j.atmosenv.2011.06.076, 2011.
- Grant, A., C. S. Witham, P. G. Simmonds, A. J. Manning, and S. O'Doherty, A 15 year record of high-frequency, in situ measurements of hydrogen at Mace Head, Ireland, *Atmospheric Chemistry & Physics*, 10(3), 1203–1214, doi:10.5194/acp-10-1203-2010, 2010.**
- Grant, A., E. L. Yates, P. G. Simmonds, R. G. Derwent, A. J. Manning, D. Young, D. E. Shallcross, and S. O'Doherty, A five year record of high-frequency in situ measurements of non-methane hydrocarbons at Mace Head, Ireland, *Atmospheric Measurement Techniques*, 4, 913–937, doi:10.5194/amt-4-955-2011, 2011.**
- Hall, B. D., Engel, A., Mühlé, J., Elkins, J. W., Artuso, F., Atlas, E., Aydin, M., Blake, D., Brunke, E.-G., Chiavarini, S., Fraser, P. J., Happell, J., Krummel, P. B., Levin, I., Loewenstein, M., Maione, M., Montzka, S. A., **O'Doherty, S.**, Reimann, S., Rhoderick, G., Saltzman, E. S., Scheel, H. E., Steele, L. P., Vollmer, M. K., Weiss, R. F., Worthy, D., and Yokouchi, Y.: Results from the International Halocarbons in Air Comparison Experiment (IHALACE), *Atmos. Meas. Tech.*, 7, 469-490, doi:10.5194/amt-7-469-2014, 2014.
- Henne, S., D.E. Shallcross, S. Reimann, P. Xiao, D. Brunner, S. O'Doherty, B. Buchmann, Future emissions and atmospheric fate of HFC-1234yf from mobile air conditioners in Europe, *Environ. Sci. Technol.*, 46, 3, 1650-1658, 2012. DOI: 10.1021/es2034608
- Hossaini, R., M. P. Chipperfield, A. Saiz-Lopez, J. J. Harrison, R. von Glasow, R. Sommariva, E. Atlas, M. Navarro, S. A. Montzka, W. Feng, S. Dhomse, C. Harth, J. Mühlé, C. Lunder, **S. O'Doherty, D. Young**, S. Reimann, M. K.

Vollmer, P. B. Krummel, and P. F. Bernath, Growth in stratospheric chlorine from short-lived chemicals not controlled by the Montreal Protocol, *Geophysical Research Letters*, 2015GL063783, doi:10.1002/2015GL063783, 2015.

Khan, M. A. H., M. C. Cooke, S. R. Utembe, A. T. Archibald, P. Maxwell, W. C. Morris, P. Xiao, R. G. Derwent, M. E. Jenkin, C. J. Percival, R. C. Walsh, **T. D. S. Young, P. G. Simmonds**, G. Nickless, **S. O'Doherty**, and D. E. Shallcross, A study of global atmospheric budget and distribution of acetone using global atmospheric model STOCHEM-CRI, *Atmospheric Environment*, 112, 269–277, doi:10.1016/j.atmosenv.2015.04.056, 2015.

Lunt, M.F., M. Rigby, **A.L. Ganesan, A. J. Manning**, R.G. Prinn, **S. O'Doherty**, J. Mühlé, C.M. Harth, P.K. Salameh, **T. Arnold**, R.F. Weiss, T. Saito, Y. Yokouchi, P.B. Krummel, L. P. Steele, P.J. Fraser, S. Li, S. Park, S. Reimann, M. K. Vollmer, C. Lunder, O. Hermansen, N. Schmidbauer, M. Maione, **D. Young**, and **P.G. Simmonds** (2015): Aggregated HFC emissions reports – right for the wrong reasons. *PNAS.*, in Press.

Keller, C. A., M. Hill, M. K. Vollmer, S. Henne, D. Brunner, S. Reimann, **S. O'Doherty**, J. Arduini, M. Maione, Z. Ferenczi, L. Haszpra, **A. J. Manning**, and T. Peter, European Emissions of Halogenated Greenhouse Gases Inferred from Atmospheric Measurements, *Environmental Science & Technology*, 46(1), 217–225, doi:10.1021/es202453j, 2012.

Kirschke, S., P. Bousquet, P. Ciais, M. Saunois, J. G. Canadell, E. J. Dlugokencky, P. Bergamaschi, D. Bergmann, D. R. Blake, L. Bruhwiler, P. Cameron-Smith, S. Castaldi, F. Chevallier, L. Feng, A. Fraser, M. Heimann, E. L. Hodson, S. Houweling, B. Josse, P. J. Fraser, P. B. Krummel, J.-F. Lamarque, R. L. Langenfelds, C. Le Quéré, V. Naik, S. **O'Doherty**, P. I. Palmer, I. Pison, D. Plummer, B. Poulter, R. G. Prinn, M. Rigby, B. Ringeval, M. Santini, M. Schmidt, D. T. Shindell, I. J. Simpson, R. Spahni, L. P. Steele, S. A. Strode, K. Sudo, S. Szopa, G. R. van der Werf, A. Voulgarakis, M. van Weele, R. F. Weiss, J. E. Williams, and G. Zeng, Three decades of global methane sources and sinks, *Nature Geoscience*, 6(10), 813–823, doi:10.1038/ngeo1955, 2013.

Logan, J.A., Staehelin, J., Megretskiaia, I.A., Cammas, J.-P., Thouret, V., Claude, H., De Backer, H., Steinbacher, M., Scheel, H.-E., Stubi, R., Frohlich, M., and **Derwent**, R. Changes in ozone over Europe: Analysis of ozone measurements from sondes, regular aircraft (MOZAIC) and alpine surface sites. *Journal of Geophys.Res.*, 117,D09301,doi:10.1029/2011JD016952, 2011.

Manning, A. J., S. O'Doherty, A. R. Jones, P. G. Simmonds, and R. G. Derwent, Estimating UK methane and nitrous oxide emissions from 1990 to 2007 using an inversion modeling approach, *Journal of Geophysical Research: Atmospheres*, 116(D2), n/a–n/a, doi:10.1029/2010JD014763, 2011.

Manning, A.J., The challenge of estimating regional trace gas emissions from atmospheric observations. *Phil. Trans. R. Soc. A*, 369, 1943–1954. doi: 10.1098/rsta.2010.0321, 2011

O'Doherty, S., Rigby, M., Mühlé, J., Ivy, D. J., Miller, B. R., Young, D., **Simmonds, P. G.**, Reimann, S., Vollmer, M. K., Krummel, P. B., Fraser, P. J., Steele, L. P., Dunse, B., Salameh, P. K., Harth, C. M., **Arnold, T.**, Weiss, R. F., Kim, J., Park, S., Li, S., Lunder, C., Hermansen, O., Schmidbauer, N., Zhou, L. X., Yao, B., Wang, R. H. J., **Manning, A.**, and Prinn, R. G.: Global emissions of HFC-143a (CH₃CF₃) and HFC-32 (CH₂F₂) from in situ and air archive atmospheric observations, *Atmos. Chem. Phys. Discuss.*, 14, 6471–6500, doi:10.5194/acpd-14-6471-2014, 2014.

Parrish, D.D., Law, K.S., Staehelin, J., **Derwent, R.**, Cooper, O.R., Tanimotot, H., Volz-Thomas, A., Gilge, S., Scheel, H.-E., Steinbacher, M., and Chan, E. Long-term changes in lower tropospheric baseline ozone concentrations at northern mid-latitudes. *Atmos. Chem. Phys.*, 12, 11485–11504, 2012.

Parrish, D.D., Law, K.S., Staehelin, J., **Derwent, R.**, Cooper, O.R., Tanimotot, H., Volz-Thomas, A., Gilge, S., Scheel, H.-E., Steinbacher, M., and Chan, E. Lower tropospheric ozone at northern mid-latitudes: Changing seasonal cycle. *Geophys. Res. Letters*, 40, 1–6, 2013, DOI: 10.1002/grl.50303, 2013.

Patra, P. K., Krol, M. C., Montzka, S. A., Arnold, T., Atlas, E. L., Lintner, B. R., Stephens, B. B., Xiang, B., Elkins, J. W., Fraser, P. J., Ghosh, A., Hintsa, E. J., Hurst, D. F., Ishijima, K., Krummel, P. B., Miller, B. R., Miyazaki, K., Moore, F. L., Muhle, J., **O'Doherty, S.**, Prinn, R. G., Steele, L. P., Takigawa, M., Wang, H. J., Weiss, R. F., Wofsy, S. C. and **Young, D.**: Observational evidence for interhemispheric hydroxyl-radical parity, *Nature*, 513(7517), 219–223 [online] Available from: <http://dx.doi.org/10.1038/nature13721>, 2014.

Pieterse, G., M. C. Krol, A. M. Batenburg, C. A. M. Breninkmeijer, M. E. Popa, **S. O'Doherty, A. Grant**, L. P. Steele, P. B. Krummel, R. L. Langenfelds, H. J. Wang, A. T. Vermeulen, M. Schmidt, C. Yver, A. Jordan, A. Engel, R. E. Fisher, D. Lowry, E. G. Nisbet, S. Reimann, M. K. Vollmer, M. Steinbacher, S. Hammer, G. Forster, W. T. Sturges, and T. Röckmann, Reassessing the variability in atmospheric H₂ using the two-way nested TM5 model, *Journal of Geophysical Research: Atmospheres*, 118(9), 3764–3780, doi:10.1002/jgrd.50204, 2013.

Rigby, M., R. G. Prinn, **S. O'Doherty**, S. A. Montzka, A. McCulloch, C. M. Harth, J. Mühlé, P. K. Salameh, R. F. Weiss, D. **Young**, P. G. **Simmonds**, B. D. Hall, G. S. Dutton, D. Nance, D. J. Mondeel, J. W. Elkins, P. B. Krummel, L. P. Steele, and P. J. Fraser, Re-evaluation of the lifetimes of the major CFCs and CH₃CCl₃ using atmospheric trends, *Atmospheric Chemistry & Physics*, 13(5), 2691–2702, doi:10.5194/acp-13-2691-2013, 2013.

- Rigby, M., R. G. Prinn, **S. O'Doherty**, B. R. Miller, D. Ivy, J. Mühle, C. M. Harth, P. K. Salameh, **T. Arnold**, R. F. Weiss, P. B. Krummel, L. P. Steele, P. J. Fraser, **D. Young**, and P. G. Simmonds, Recent and future trends in synthetic greenhouse gas radiative forcing, *Geophysical Research Letters*, doi:10.1002/2013GL059099, 2014.
- Rigby, M., **A.J. Manning**, R. Prinn, The value of high-frequency, high-precision methane isotopologue measurements for source and sink estimation, *J. Geophys. Res.*, 117, D12, Doi:10.1029/2011JD017384, 2012
- Simmonds, P. G., R. G. Derwent, A. J. Manning, S. O'Doherty, and G. Spain**, Natural chloroform emissions from the blanket peat bogs in the vicinity of Mace Head, Ireland over a 14-year period, *Atmospheric Environment*, 44(10), 1284–1291, doi:10.1016/j.atmosenv.2009.12.027, 2010.
- Simmonds, P. G., R. G. Derwent, A. J. Manning, A. Grant, S. O'Doherty, and T. G. Spain**, Estimation of hydrogen deposition velocities from 1995–2008 at Mace Head, Ireland using a simple box model and concurrent ozone depositions, *Tellus B*, 63(1), 40–51, doi:10.1111/j.1600-0889.2010.00518.x, 2011.
- Simmonds, P. G., A. J. Manning**, M. Athanassiadou, A. A. Scaife, **R. G. Derwent, S. O'Doherty**, C. M. Harth, R. F. Weiss, G. S. Dutton, B. D. Hall, C. Sweeney, and J. W. Elkins, Interannual fluctuations in the seasonal cycle of nitrous oxide and chlorofluorocarbons due to the Brewer-Dobson circulation, *Journal of Geophysical Research: Atmospheres*, 118(19), 10,694–10,706, doi:10.1002/jgrd.50832, 2013.
- Simmonds, P. G., R. G. Derwent, A. J. Manning**, A. McCulloch, and **S. O'Doherty**: USA emissions estimates of CH₃CHF₂, CH₂FCF₃, CH₃CF₃, and CH₂F₂ based on in situ observations at Mace Head, *Atmospheric Environment*, 104, 27-38, doi:10.1016/j.atmosenv.2015.01/010, 2015.
- Thompson, R. L., F. Chevallier, A. M. Crotwell, G. Dutton, R. L. Langenfelds, R. G. Prinn, R. F. Weiss, Y. Tohjima, T. Nakazawa, P. B. Krummel, L. P. Steele, P. Fraser, **S. O'Doherty**, K. Ishijima, and S. Aoki, Nitrous oxide emissions 1999 to 2009 from a global atmospheric inversion, *Atmospheric Chemistry & Physics*, 14(4), 1801–1817, doi:10.5194/acp-14-1801-2014, 2014.
- Thompson, R. L., A. Stohl, L. X. Zhou, E. Dlugokencky, Y. Fukuyama, Y. Tohjima, S.-Y. Kim, H. Lee, E. G. Nisbet, R. E. Fisher, D. Lowry, R. F. Weiss, R. G. Prinn, **S. O'Doherty, D. Young**, and J. W. C. White, Methane emissions in East Asia for 2000–2011 estimated using an atmospheric Bayesian inversion, *Journal of Geophysical Research: Atmospheres*, 120(9), 4352–4369, doi:10.1002/2014JD022394, 2015.
- Thompson, R. L., Patra, P. K., Ishijima, K., Saikawa, E., Corazza, M., Karstens, U., Wilson, C., Bergamaschi, P., Dlugokencky, E., Sweeney, C., Prinn, R. G., Weiss, R. F., **O'Doherty, S.**, Fraser, P. J., Steele, L. P., Krummel, P. B., Saunois, M., Chipperfield, M., and Bousquet, P.: TransCom N₂O model inter-comparison – Part 1: Assessing the influence of transport and surface fluxes on tropospheric N₂O variability, *Atmos. Chem. Phys.*, 14, 4349–4368, doi:10.5194/acp-14-4349-2014, 2014.
- Thompson, R. L., Ishijima, K., Saikawa, E., Corazza, M., Karstens, U., Patra, P. K., Bergamaschi, P., Chevallier, F., Dlugokencky, E., Prinn, R. G., Weiss, R. F., **O'Doherty, S.**, Fraser, P. J., Steele, L. P., Krummel, P. B., Vermeulen, A., Tohjima, Y., Jordan, A., Haszpra, L., Steinbacher, M., **Van der Laan, S.**, Aalto, T., Meinhardt, F., Popa, M. E., Moncrieff, J., and Bousquet, P.: TransCom N₂O model inter-comparison – Part 2: Atmospheric inversion estimates of N₂O emissions, *Atmos. Chem. Phys.*, 14, 6177–6194, doi:10.5194/acp-14-6177-2014, 2014.
- Vardag, S. N., Hammer, S., **O'Doherty, S.**, Spain, T. G., Wastine, B., Jordan, A., and Levin, I.: Comparisons of continuous atmospheric CH₄, CO₂ and N₂O measurements – results of InGOS travelling instrument campaign at Mace Head, *Atmos. Chem. Phys.*, 14, 8403–8418, doi:10.5194/acp-14-8403-2014, 2014.

2.4 Related information

Project website: www.metoffice.gov.uk/atmospheric-trends

3 Instrumentation

3.1 Sites

A brief summary of site operations is presented below and in Table 1; a more detailed account of operations over the past year is presented in the Appendices. In addition, more detailed description of the instrumentation is detailed on the website (<http://www.metoffice.gov.uk/atmospheric-trends/instrumentation>).

3.1.1 Mace Head (MHD)

- Medusa GC-MS: Overall, the Medusa worked well over the past 16 months. An issue with HFC-125 and HFC-32 contamination occurred after the installation of a new trap in May 2014; however, this was rectified in the short-term by flushing the complete sample pump module with ambient air. Switching pump or air conditioning unit are currently being explored as a long-term solution to the problem. A computing issue in June 2015 resulted in 10 days data loss.
- GC-MD: The MD performed well for the reporting period. Most of the data loss (11 days) resulted from ancillary equipment failure or a computing issue.

3.1.2 Ridge Hill (RGL)

- Ridge Hill began operation in February 2012 and has collected 43 months of data from two sample inlets at 45 m and 90 m. The GC-ECD samples from the 90 m inlet, whilst the CRDS samples sequentially from both 45 and 90 m inlets.
- GC-ECD: The ECD instrument has undergone a trouble free year.
- CRDS: The CRDS has been running well over the last 16 months.
- An inter-comparison exercise with the UK GAUGE project was conducted in November 2014.
- The Nafion drying system was removed from the CRDS in June 2015. H₂O correction coefficients were established using a H₂O droplet test and coefficients implemented in the post-processing of the data.

3.1.3 Tacolneston (TAC)

- Tacolneston began operation in July 2012 and has collected 38 months of data. The Medusa GC-MS and GC-MD sample from the 100 m inlet, whilst the CRDS samples sequentially from inlets at heights of 54, 100 and 185 m.
- Medusa GC-MS: The Medusa has generally performed well since it was installed. A problem with the Cryotiger cooling system resulted in a two days loss of data between 26th and 28th June 2014. A problem with the air conditioning unit resulted in the Medusa being switched off from 6th January to 17th February 2015.
- GC-MD: The MD has operated well since it was installed. A problem with the air conditioning unit resulted in no data acquisition between 9th and 28th January 2015, as the MD was shutdown.
- CRDS: The CRDS has been running well over the past 16 months.
- An inter-comparison exercise with the UK GAUGE project was conducted in January 2015.
- The Nafion drying system was removed from the CRDS in June 2015. H₂O correction coefficients were established using a H₂O droplet test and coefficients implemented in the post-processing of the data.

3.1.4 Angus (TTA)

- The University of Bristol (UoB) took over routine operation of Angus in January 2013 and has collected 32 months of data since this transition, sampling from an inlet at 222 m.
- CRDS: The CRDS has operated well during the past 16 months, and is visited by a local site operator on a monthly basis to carry out routine maintenance and repairs. A power failure in January 2015 resulted in 4 days loss of data until a hard reboot of the system was done.

- An inter-comparison exercise with the Cucumber Intercomparison Programme was conducted in April 2015 (This InGOS funded project consists of 7 fast-rotating loops, each loop consisting of 3 ‘cucumbers’ – a cylinder filled with natural air - spanning a range of CO₂ concentrations from about 360 to 400 ppm). Within each loop the cucumbers cycle perpetually between several field stations or laboratories, and are analysed at each, according to common procedures.

Sites -> Species	Mace Head MHD	Tacolneston TAC	Ridge Hill RGL	Angus TTA
CO ₂	Picarro 2301(1)	Picarro 2301(1)	Picarro 2301(1)	Picarro 2301(1)
CH ₄	Picarro 2301(1), GC-FID(40)	Picarro 2301(1)	Picarro 2301(1)	Picarro 2301(1)
N ₂ O	GC-ECD(40)	GC-ECD(20)	GC-ECD(20)	-
SF ₆	Medusa(120)	GC-ECD(20), Medusa(120)	GC-ECD(20)	-
NF ₃	Medusa(120)			
H ₂	GC-RGA(40)	GC-RGA(20)	-	-
CO	GC-RGA(40)	GC-RGA(20)	-	-
CF ₄	Medusa(120)	Medusa(130)	-	-
C ₂ F ₆	Medusa(120)	Medusa(130)	-	-
C ₃ F ₈	Medusa(120)	Medusa(130)	-	-
c-C ₄ F ₈	Medusa(120)	Medusa(130)	-	-
HFC-23	Medusa(120)	Medusa(130)	-	-
HFC-32	Medusa(120)	Medusa(130)	-	-
HFC-134a	Medusa(120)	Medusa(120)	-	-
HFC-152a	Medusa(120)	Medusa(130)	-	-
HFC-125	Medusa(120)	Medusa(130)	-	-
HFC-143a	Medusa(120)	Medusa(130)	-	-
HFC-227ea	Medusa(120)	Medusa(130)	-	-
HFC-236fa	Medusa(120)	Medusa(130)	-	-
HFC-43-10mee	Medusa(120)	Medusa(130)	-	-
HFC-365mfc	Medusa(120)	Medusa(130)	-	-
HFC-245fa	Medusa(120)	Medusa(130)	-	-
HCFC-22	Medusa(120)	Medusa(130)	-	-
HCFC-141b	Medusa(120)	Medusa(130)	-	-
HCFC-142b	Medusa(120)	Medusa(130)	-	-
HCFC-124	Medusa(120)	Medusa(130)	-	-
CFC-11	Medusa(120)	Medusa(130)	-	-
CFC-12	Medusa(120)	Medusa(130)	-	-
CFC-13	Medusa(120)	Medusa(130)	-	-
CFC-113	Medusa(120)	Medusa(130)	-	-
CFC-114	Medusa(120)	Medusa(130)	-	-
CFC-115	Medusa(120)	Medusa(130)	-	-
H-1211	Medusa(120)	Medusa(130)	-	-
H-1301	Medusa(120)	Medusa(130)	-	-
H-2402	Medusa(120)	Medusa(130)	-	-
CH ₃ Cl	Medusa(120)	Medusa(130)	-	-
CH ₃ Br	Medusa(120)	Medusa(130)	-	-
CH ₃ I	Medusa(120)	Medusa(130)	-	-
CH ₂ Cl ₂	Medusa(120)	Medusa(130)	-	-
CH ₂ Br ₂	Medusa(120)	Medusa(130)	-	-
CHCl ₃	Medusa(120)	Medusa(130)	-	-
CHBr ₃	Medusa(120)	Medusa(130)	-	-
CCl ₄	Medusa(120)	Medusa(130)	-	-
CH ₃ CCl ₃	Medusa(120)	Medusa(130)	-	-
CHCl=CCl ₂	Medusa(120)	Medusa(130)	-	-
CCl ₂ =CCl ₂	Medusa(120)	Medusa(130)	-	-

Table 1: Operational sites, instrumentation and observed species. Number in brackets indicates frequency of calibrated air measurement in minutes.

4 Description of data analysis methods

4.1 Introduction

This chapter discusses the methods used to analyse the observations from the UK DECC network. The following chapter presents the results for the key GHGs that are reported through the UNFCCC process and then, following that, the analysis of the remaining gases observed by the UK DECC Network.

The first section describes the method for estimating the long-term Northern Hemisphere atmospheric baseline trend, the growth rate and the seasonal cycle of each gas measured at Mace Head given knowledge of the recent history of the air as it travels to the station.

The subsequent section presents the InTEM (Inversion Technique for Emission Modelling) inversion system. This is the tool that is used to estimate the UK and North West European (NWEU) (UK + Ireland + France + Germany + Belgium + the Netherlands + Luxembourg + Denmark) emissions of each gas for each year from 1990 or from when the observations started.

4.2 Northern Hemisphere Atmospheric Baseline Trend Analysis

4.2.1 Summary

The aim is to estimate the Northern Hemisphere atmospheric background mole fraction (referred to as the baseline) of each gas measured at Mace Head; their long-term baseline trends and growth rates and their seasonal cycle. Baseline concentration times are defined as those times when the air mass arriving at Mace Head has not been influenced by significant emissions within the previous few weeks or unduly influenced by local effects i.e. those times when the air is well mixed and is representative of the Northern Hemisphere background concentration. Figure 3 shows two example air history maps, the one on the left shows a 2-hour period when the air mass will be considered baseline, the one on the right, when the air mass is not considered baseline because of the recent influence of Europe, a source region. Times when the air has rapidly descended to Mace Head from the upper troposphere (defined here as above 9 km) are also not considered baseline because many gases have a strong vertical gradient, usually decreasing concentration with height.

By fitting a time-varying line through just those Mace Head observations recorded when the air masses are representative of the Northern Hemisphere baseline it is possible to extract from the observational data an estimate of the hourly baseline across the entire measurement record. The hourly baseline can then be further interrogated to estimate monthly and annual values, reveal whether the Northern Hemisphere atmospheric concentration is growing or declining and the strength of the baseline seasonal cycle. Figure 9 shows the results for methane.

4.2.2 Introduction

This section describes the method behind the analysis of the baseline concentrations of the Mace Head observations from Feb 1989 – Jun 2015 inclusive.

The principle tool used to estimate the baseline concentrations is the NAME dispersion model. The methodology used is presented first, followed by the analysis of each individual gas. The analysis considers the long-term trend of the monthly and annual baseline concentrations, their rate of growth and their seasonal cycle.

4.2.3 Methodology

The NAME model is run in backwards mode to estimate the recent history (30 days) of the air on route to Mace Head. Air history maps, such as those shown in Figure 3, have been calculated for each 2-hour period from Jan 2003 until April 2015 using Met Office Unified Model (UM) meteorology and from 1989-2002 using ECMWF ERA-Interim (European Centre for Medium-Range Weather Forecasts Re-Analysis Interim) meteorology, amounting to more than 100,000 maps. The model output estimates the 30-day time-integrated air concentration (dosage) at each grid box (25 km horizontal resolution and 0-40 m above ground level) from a release of 1 g/s at Mace Head (the

receptor). The model is 3-dimensional and therefore it is not just surface transport that is modelled, an air parcel can travel from the surface to a high altitude and then back to the surface but only those times when the air parcel is within the lowest 40 m above the ground will it be recorded in the surface maps. The impact of air from higher altitudes arriving at the surface at Mace Head is also, separately, recorded. The computational domain covers -98° W to 40° E longitude (North America to Russia) and 11° N to 79° N (North Africa to Arctic Circle) latitude and extends to more than 16 km vertically (actual height varies depending on version of meteorology used). For each 2-hour period 40,000 inert model particles were used to describe the dispersion. No chemical or deposition processes were modelled; this is realistic given the long atmospheric lifetimes of the vast majority of gases considered.

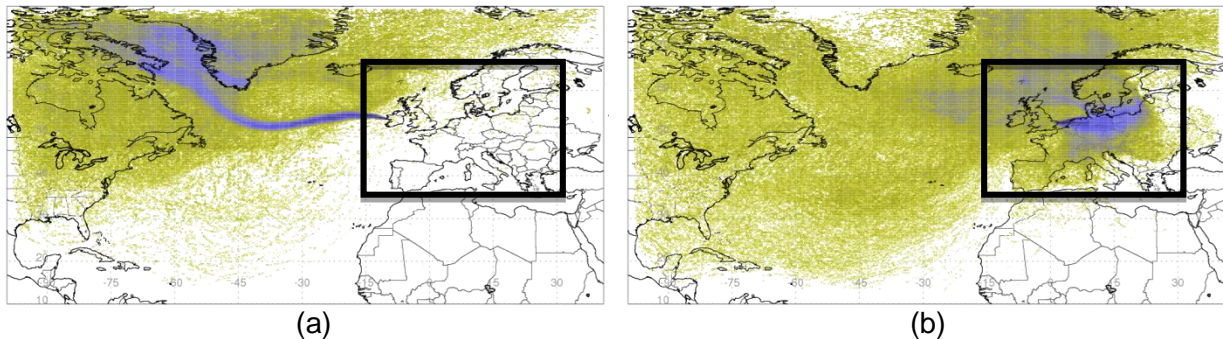


Figure 3: Examples of 2-hour air history surface maps derived from NAME (a) baseline period (b) regionally polluted period. The air-history surface maps describe which surface areas (defined as within 40 m of the surface) in the previous 30-days impact the observation point at a particular time.

By dividing the dosage (g s/m^3) by the total mass emitted ($3600 \text{ s/hr} \times 2\text{hr} \times 1 \text{ g/s}$) and multiplying by the geographical area of each grid box (m^2), the model output is converted into a dilution matrix (s/m). Each element of this matrix D dilutes a continuous emission (e) of $1 \text{ g/m}^2\text{s}$ from a given grid box over the previous 30 days to an air concentration (g/m^3) at the receptor (o) during a 2-hour period.

$$D e = o \quad \dots \text{Equation 1}$$

Baseline concentrations are defined as those that have not been influenced by significant emissions or local effects within the previous 30-days of travel on route to Mace Head, i.e. those that are well mixed and are representative of the mid-latitude Northern Hemisphere background concentrations.

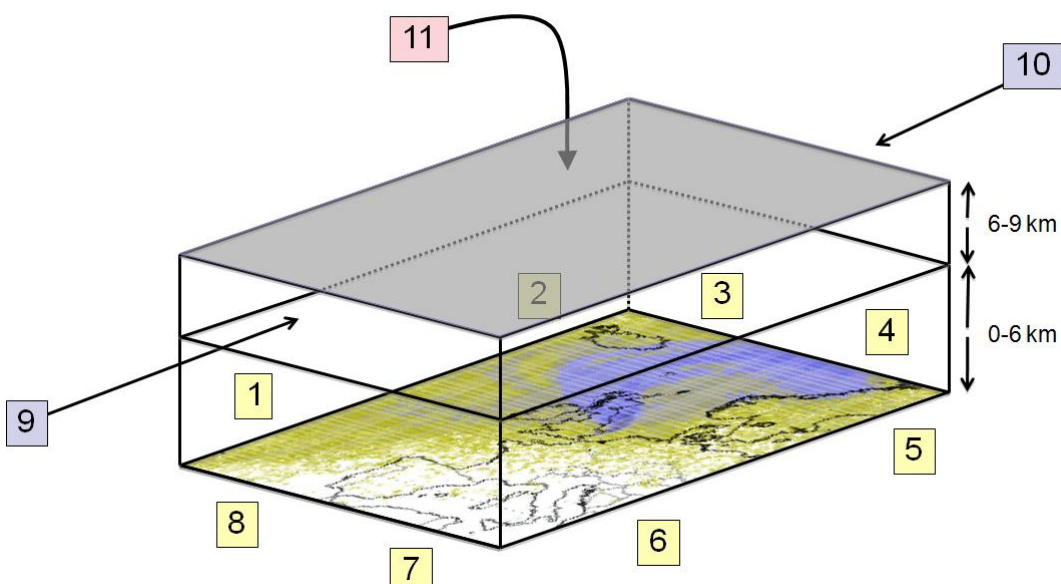


Figure 4: The eleven directions classified for each air history map. The dominant baseline edges are 1-4.

A 2-hour period is classed as ‘baseline’ if it meets the following criteria:

- The total air concentration from the nine grid boxes centred on and surrounding Mace Head is less than a low (arbitrary) limit. The limit is set so that it is clear that local emissions do not significantly contribute.
- The total contribution from populated areas is less than a low (arbitrary) limit. The limit is set so that it is clear that populated regions have not significantly contributed.
- The percentage of air entering from the north (directions 3 and 4 in Figure 4) and west (directions 1 and 2) edges dominates (>90%) (Figure 4).
- Less than 4% of the air entering the domain has come from higher than 9km, i.e. from the upper troposphere.

The limits chosen attempt to define a threshold below which any emission sources would generate a concentration at Mace Head that would not be discernible above the baseline noise. The same limit value is used for all of the gases analysed. The chosen limit is arbitrary but the impact of doubling it is small.

Figure 5 shows a three-month extract of the HFC-134a observations measured at Mace Head. The observations have been colour coded to indicate whether, using the above classification, the air mass they were sampled from was considered baseline. For the baseline analysis all non-baseline observations are removed.

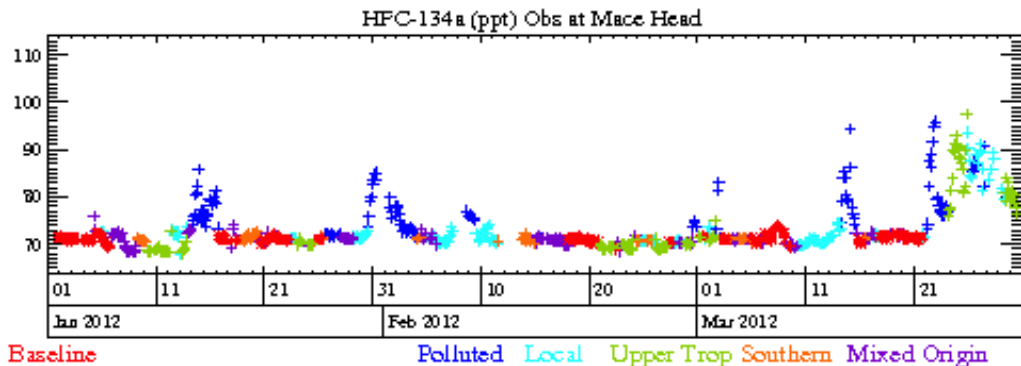


Figure 5: Three-month time-series of Mace Head HFC-134a observations showing the impact of the baseline and non-baseline classification. The baseline observations are shown in red.

The points defined as baseline using the above methodology still have a certain level of noise. The principle reasons for this are: unexpected short-lived emissions e.g. forest fires in Canada or from shipping, local effects that are not identified, incorrectly modelled meteorology or transport, i.e. European or southerly or upper troposphere air defined as baseline by error.

Irrespective of the methodology used to identify these events some will inevitably be classed as baseline when it is inappropriate to do so. To capture such events the baseline data are statistically filtered to isolate and remove these non-baseline observations. For each baseline point in turn, the baseline points in a 40-day window surrounding this central value are considered and, provided that there are sufficient points (>11 with at least 4 in each third of the time window or more than 18 in two thirds of the time window), a quadratic is fitted to these values. The standard deviation of the actual points and the fitted curve is calculated (std) and if the current baseline value is more than $x std$ away from the fitted value it is marked for exclusion from the baseline observations. After all baseline points have been considered, those to be excluded are removed. The process is repeated nine times, each time the value for x is gradually reduced from 6 to 2, thus ensuring that those points statistically far from the fitted baseline do not unduly affect the points to be excluded by skewing the fitted curve. If there are insufficient baseline points in a 40-day window the values are only included if the spread in the points is small and there are at least 5 data points.

For each hour in the time-series the baseline points in a running 40-day window are fitted using a quadratic function and the value extracted for the current hour in question. The process is then advanced by an hour and repeated. If there are insufficient baseline points well spaced within the window (at least 3 in each quarter) it is gradually extended up to 150 days.

For each hour within the observation time record a smoothed baseline concentration is estimated by taking the median of all fitted baseline values within a 20-day time window. If there are fewer than 72 baseline values in the time window then the window is steadily increased up to a maximum of 40 days. If there are still insufficient points then no smoothed baseline concentration is estimated for that hour.

The noise or potential error in the smoothed baseline concentration is estimated to be the standard deviation of the difference between the observations classed as baseline and the smoothed baseline concentrations at the corresponding times. Figure 6 shows, on a much-expanded y-axis compared to Figure 5, the typical spread of baseline observations about the smoothed continuous baseline estimate.

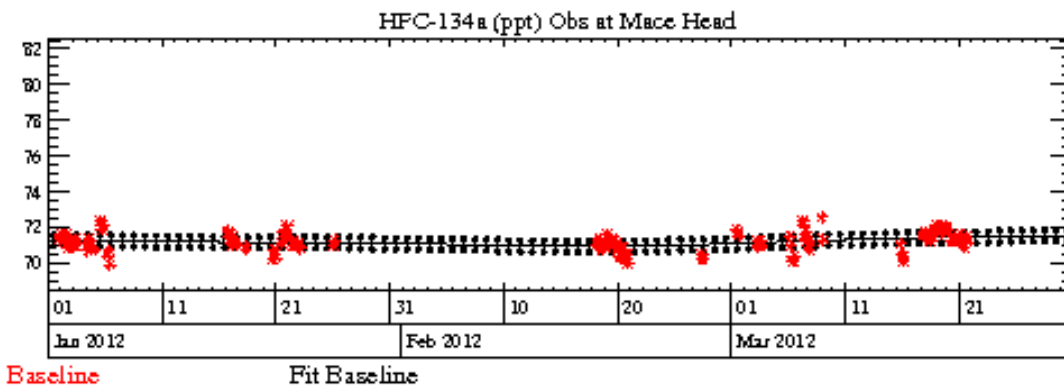


Figure 6: Observations of HFC-134a at Mace Head within a 3-month period classed as baseline (red) with the estimated daily baseline mole fractions with uncertainty for the same period (black). Note: the y-axis has been expanded compared to Figure 5.

The hourly baseline concentrations are split into two components, a long-term trend and a residual component (seasonal cycle). Two methods have been used; the Kolmogorov-Zurbenko (KZ) method and a 3-year quadratic (3Q) method, both are shown on the growth rate plots.

- **Kolmogorov–Zurbenko method**

A Kolmogorov–Zurbenko (KZ) filter involves k time iterations of a moving average of a given time duration and is ideally suited to this type of problem. For this application, the length of the moving average window was set to one year and the number of iterations was set to four. With these parameters a 12-month moving average was applied to the data four times, thereby approximately removing wavelengths smaller than 2-years. At each hour in the time-series the 12-month average of the baseline mass mixing ratios centred on this hour is calculated. This is the long-term trend component, subtracting this from the actual hourly baseline estimate at this time gives the residual.

- **3-year quadratic method**

At each hour calculate the 12-month average centred on this hour (y_a). For the three-year period centred on this hour calculate the quadratic line using standard value decomposition that best fits (minimises) the difference between the computed time-series and y_a . This is the long-term trend component, subtracting this from the actual hourly baseline estimate at this time gives the residual.

The KZ approach is the preferred method, however this does not calculate values for the first two and last two years. The 3Q method extends the calculation by a year either side.

Monthly and annual baseline concentrations are estimated by averaging all of the long-term trend daily baseline values within the appropriate time window. A monthly value is estimated if there are at least 21 daily values within the month, this ensures a good representation of the whole month. An annual value is estimated if there are at least 330 daily values within the calendar year, ensuring a good representation of the whole year.

The annual growth rate on a particular day is defined as the local slope of the long-term trend on that day. The local slope is estimated by linearly fitting a best-fit line through the trend concentration

values for the day before, current day and day after. Monthly averages of these growth rates are shown for each gas.

The daily residual concentration values are averaged for each month over the data period studied to produce a seasonal cycle. The mean seasonal cycles for each gas are shown for each gas. The range of values for each month is also shown, along with the first, middle and last individual year seasonal cycles.

4.2.4 Baseline Mole Fractions

For each gas observed at Mace Head a baseline analysis has been performed. ECMWF meteorology is used from 1989 – 2002 inclusive and Met Office meteorology from 2003-2015 inclusive. For each gas, monthly and annual Northern Hemisphere (NH) baselines, time-varying baseline growth rates and the average seasonal cycle seen within the observations are calculated. Table 2 - Table 4 summarise the annual baseline mole fractions for each of the gases considered.

Gas	1990	1991	1992	1993	1994	1995	1996	1997	1998	1999
CFC-11	264	267	268	269	268	267	266	264	263	261
CFC-12	496	506	516	522	529	533	537	540	542	544
CFC-13										
CFC-113	75.5	81	84.2	85	84.6	84.6	84.3	83.8	83.2	82.7
HCFC-124										1.3
HCFC-141b						5.1	7.3		11.4	13.3
HCFC-142b						8	9.3	10.7		12.4
HCFC-22										145
HFC-125										1.4
HFC-134a						2.3	4.3	6.4	9.6	13.4
HFC-143a										
HFC-152a						1.2	1.2	1.4	1.8	2.2
HFC-23										
HFC-32										
HFC-227ea										
HFC-236fa										
HFC-245fa										
HFC-365mfc										
HFC-4310mee										
PFC-14										
PFC-116										
PFC-218										
PFC-318										
SF6										
SO2F2										
CH3Cl										534
CH2Cl2							36.3	35.9	32.6	31.3
CHCl3						12.5	12.7	12	12.1	11.4
CH3CCl3	151	152	150	139	125	111	95	80	66	55
CCl4			105	104	103	102	101	100	99	98
CCl2CCl2										
CH3Br										10.9
Halon-1301										2.8
Halon-1211										4.2
Halon-2402										
CH4 (ppb)	1790	1810	1803	1814	1818	1823	1825	1823	1835	1839
CO (ppb)						124	132	118	148	123
CO2 (ppm)				357	359	361	363	364	367	369
N2O (ppb)	309	310	310	311	312	312	313	314	315	315
O3 (ppb)	34.8	36.3	35	35.3	37	35.4	36.9	37.4	40.4	41.9
H2 (ppb)						507	513	506	519	520

Table 2: Annual Northern hemisphere baseline mass mixing ratios for all gases measured at Mace Head 1990-1999 (ppt unless stated).

Gas	2000	2001	2002	2003	2004	2005	2006	2007	2008	2009
CFC-11	260	259	256	255	253	250	248	246	244	243
CFC-12	546	546	546	546	545	544	543	541	539	536
CFC-13					2.8	2.8			2.9	2.9
CFC-113	82.2	81.5	80.6	79.9	79.3	78.7	77.9	77.1	76.7	76
HCFC-124	1.4	1.6	1.6	1.6	1.6	1.6	1.6	1.6	1.6	1.6
HCFC-141b	15.1	16.3	17.6	18.6	19.2	19.1	19.6	20.2	20.9	21.3
HCFC-142b	13.6	14.6	15	15.6	16.3	17	18.1	19.3	20.6	21.4
HCFC-22	151	158	164	169	174	180	187	195	204	212
HFC-125	1.8	2.3	2.7	3.3	3.9	4.6	5.4	6.3	7.4	8.6
HFC-134a	17.2	20.8	25	29.7	34.7	39.3	43.7	47.9	53.3	58
HFC-143a					5.5	6.4	7.4	8.4	9.6	10.7
HFC-152a	2.5	2.9	3.4	4.1	4.8	5.6	6.7	7.9	8.8	8.9
HFC-23									22.5	23
HFC-32					1.1	1.6	2.1	2.7	3.4	4.1
HFC-227ea								0.5	0.5	0.6
HFC-236fa								0.1	0.1	0.1
HFC-245fa								1.1	1.3	1.4
HFC-365mfc						0.3	0.4	0.5	0.6	0.6
HFC-4310mee										
PFC-14					74.9	75.5	76.2	76.9	77.7	78.1
PFC-116					3.6	3.7	3.8	3.9	4	4.1
PFC-218					0.4	0.5	0.5	0.5	0.5	0.5
PFC-318										
SF6					5.6	5.8	6.1	6.3	6.6	6.9
SO2F2						1.5	1.5	1.6	1.6	1.7
CH3Cl	520	512	510	522	520	525	520	526	533	530
CH2Cl2	30.1	28.9	28.9	30.9	30.7	30.5	32.1	34.1	35.8	36.3
CHCl3	11	11	11.1	11.3	11.3	11.2	11.3	11.2	11.5	11
CH3CCl3	46	39	32	27	23	19	16	13	11	9
CCl4	97	96	95	94	93	92	91	90	89	88
CCl2CCl2		5.2	4.8	4.8	4.4	3.9	3.8	3.6	3.4	3
CH3Br	10.5	9.8	9.1	8.9	9.5	10.3	9.5	9.1	9.2	8.6
Halon-1301	2.9	3	3	3.1	3.1	3.2	3.2	3.2	3.3	3.3
Halon-1211	4.3	4.4	4.4	4.4	4.5	4.5	4.5	4.4	4.4	4.3
Halon-2402					0.5	0.5	0.5	0.5	0.5	0.5
CH4 (ppb)	1841	1842	1843	1851	1847	1847	1846	1855	1864	1867
CO (ppb)	119	117	131	146	132	132	131	129	129	123
CO2 (ppm)	369	371	373	375	378	379	382	384	386	387
N2O (ppb)	316	317	318	318	319	320	320	321	322	323
O3 (ppb)	40.9	40	40.4	41.5	40.4	40.1	41	39.9	40.8	40.9
H2 (ppb)	512	507	508	512	508	511	514	511	513	510

Table 3: Annual Northern hemisphere baseline mass mixing ratios for all gases measured at Mace Head 2000-2009 (ppt unless stated).

Gas	2010	2011	2012	2013	2014	AvGrow	AvGr12
CFC-11	241	238	236	235	234	-1.17	-0.98
CFC-12	533	531	528	526	523	1.3	-2.19
CFC-13	2.9	3	3	3	3	0.02	0.01
CFC-113	75.2	74.5	74	73.4	72.8	-0.03	-0.62
HCFC-124	1.5	1.5	1.4	1.3	1.3	0	-0.07
HCFC-141b	22	23.1	24.1	24.9	25.3	0.86	0.45
HCFC-142b	21.9	22.7	23	23.2	23.3	0.77	0.09
HCFC-22	219	226	231	236	241	6.45	5.09
HFC-125	10	11.7	13.4	15.5		0.98	1.97
HFC-134a	63.4	68.4	73.3	78.7	84.1	4.34	5.26
HFC-143a	11.9	13.2	14.5	15.9	17.4	1.21	1.46
HFC-152a	9.4	9.9	10.1	10.1	10	0.47	-0.13
HFC-23	23.7	24.7	25.5	26.7	27.8	0.9	1.15
HFC-32	5.2	6.5	7.7	9.3		0.92	1.46
HFC-227ea	0.7	0.8	0.9	1	1.1	0.09	0.1
HFC-236fa	0.1	0.1	0.1	0.1	0.1	0.01	0.01
HFC-245fa	1.5	1.8	2	2.2	2.4	0.19	0.17
HFC-365mfc	0.7	0.8	0.9	0.9	1	0.07	0.08
HFC-4310mee			0.2	0.2	0.3	0.01	0.01
PFC-14	78.7	79.5	80.3	80.9	81.8	0.7	0.82
PFC-116	4.1	4.2	4.3	4.4	4.5	0.08	0.09
PFC-218	0.6	0.6	0.6	0.6	0.6	0.02	0.02
PFC-318		1.3	1.4	1.4	1.5	0.05	0.06
SF6	7.2	7.5	7.8	8.1	8.4	0.29	0.34
SO2F2	1.7	1.8	1.9	2	2.1	0.08	0.1
CH3Cl	530	518	526	535	531	-0.5	-1.67
CH2Cl2	39.7	39.3	41.5	50.1	49.2	0.72	0.33
CHCl3	11.8	11.6	11.6	12	13.3	0.03	1.1
CH3CCl3	8	7	5	4		-6.15	-0.92
CCl4	87	86	85	84	83	-0.99	-0.97
CCl2CCl2	3	2.7	2.5	2.4	2.4	-0.2	0
CH3Br	8.3	8.4	8.3	8	7.6	-0.22	-0.35
Halon-1301	3.3	3.3	3.3	3.4	3.4	0.04	0.03
Halon-1211	4.2	4.2	4.1	4	3.9	-0.02	-0.1
Halon-2402	0.5	0.5	0.4	0.4	0.4	-0.01	-0.01
CH4 (ppb)	1871	1874	1882	1886	1897	4.54	8.76
CO (ppb)	129	125	133	126	129	0.22	-2.06
CO2 (ppm)	390	392	394	397	398	1.98	1.9
N2O (ppb)	323	324	325	326	327	0.75	1.16
O3 (ppb)	41.2	40.4	40.4	41.3	40.3	0.23	-0.73
H2 (ppb)	510	516	517	519	517	0.51	-1.87

Table 4: Annual Northern hemisphere baseline mole fractions for all gases measured at Mace Head 2010-2014 (ppt unless stated) and Northern hemisphere baseline growth rates (ppt/yr unless stated): over all years (penultimate column) and most recent (last column).

4.3 Regional emission estimation

4.3.1 Summary

By removing the time-varying baseline concentrations from the raw measurement data, a time-series of excursions from the baseline, averaged over each 2-hour period, has been generated for each observed gas. The perturbations above baselines, observed across the UK DECC network, are driven by emissions on regional scales that have yet to be fully mixed on the hemisphere scale and are the principle tool used to estimate surface emissions across north-west Europe. A method for estimating emissions from observations, referred to as ‘Inversion Technique for Emission Modelling’ (InTEM), has been developed over many years and is used here to estimate UK and North-West European (NWEU) emissions using the observations from the UK DECC network.

InTEM links the observation time-series with the NAME air history estimates of how surface emissions dilute as they travel to the observation stations. An estimated emission distribution when combined with the NAME output can be transformed into a modelled time-series at each of the measurement stations. The modelled and the observed time-series can be compared using a single or a range of statistics (referred to as a cost function) to produce a skill score for that particular emission distribution. InTEM uses a well known best-fit technique, simulated annealing, to search for the emission distribution that produces a modelled times-series that has the best statistical match to the observations. InTEM can either start from a random emission distribution or from an inventory-defined distribution, in the estimates that follow the random start method is used.

In order for InTEM to provide robust solutions for every area within the modelled domain, each region needs to significantly contribute to the air concentrations at the UK DECC network sites on a reasonable number of time periods. If the signal from an area is only rarely or poorly seen by the network, then its impact on the cost function is minimal and the inversion method will have little skill at determining its true emission. The contributions that different grid boxes make to the observed air concentration varies from grid to grid. Grid boxes that are distant from the observation site contribute little to the observation, whereas those that are close have a large impact. In order to balance the contribution from different grid boxes, those that are more distant are grouped together into increasingly larger regions. The grouping cannot extend beyond country or Devolved Administration (DA) boundaries. The country boundaries extend into the surrounding seas to reflect both emissions from shipping, off-shore installations and river runoff but also because the inversion has geographical uncertainty.

There is significant uncertainty in the emissions that are estimated. Uncertainty arises from many factors: errors in the baseline estimate; emissions that vary over time-scales shorter than the inversion time-period e.g. diurnal, seasonal or intermittent; heterogeneous emissions i.e. emissions that vary within the regions solved for; errors in the transport model (NAME) or the underpinning 3-dimensional meteorology; errors in the observations themselves. The potential magnitudes of these uncertainties have been estimated and are incorporated within InTEM to inform the uncertainty of the modelled results.

4.3.2 InTEM (Inversion Technique for Emission Modelling)

The observation time-series, together with the NAME model output predicting the recent history of the air, was used to estimate the emission distribution of each gas over North West Europe. The iterative best-fit technique, simulated annealing [Press et al 1992], was used to optimise these regional emission estimates using a statistical skill score (cost function) comparing the observed and modelled time-series at the observational network. The technique, referred to as InTEM, starts from a set of random emission maps, it then searches for the emission map that produces a modelled time series at the observational network that most accurately mimics the observations.

The aim of InTEM is to estimate the spatial distribution of emissions across a defined geographical area (Figure 7). In order to solve Equation 1 the set of observations (o) and the dilution matrix (D) estimated using NAME, are known. The observations are in volume mixing ratios. The dilution matrix has units (s/m) and is calculated from the time-integrated air concentrations produced by the NAME model. The dilution matrix has t rows equal to the number of 2-hour periods considered and

has n columns equal to the number of grid points in the defined geographical domain. This matrix dilutes a continuous emission of 1 g/m²s over a given grid to an air concentration (g/m³) at the receptor during a 2-hour period. The NAME dilution matrices are converted from air concentration units to volume mixing ratio units using the modelled temperature and pressure at the observation point.

The inversion domain is chosen to be a smaller subset of the full domain used for the air history maps. It covers 14°W – 31°E longitude and 36°N – 66°N latitude and is shown as the black box in Figure 3. The smaller domain covers all of Europe and extends into the Atlantic and has an intrinsic horizontal resolution of 0.352° longitude by 0.234° latitude. The inversion domain needs to be smaller to ensure re-circulating air masses are fully represented but also because emission sources very distant from the UK DECC network have little discernible impact on the concentration at the stations, i.e. the signal would be too weak to be seen. The prior baseline mole fraction for all directions is assumed to be the Mace Head baseline mole fraction as estimated using the method described above. InTEM solves for a baseline adjustment for 11 specific directions / altitudes (Figure 4). This method has been described fully in a previous report (May 2015).

In order for the best-fit algorithm to provide robust solutions for every area within the domain, each region needs to significantly contribute to the air concentration at the UK DECC network on a reasonable number of time periods. If the signal from an area is only rarely or poorly seen by the network, then its impact on the cost function is minimal and the inversion method has little skill at determining its true emission.

The contribution that different grid boxes make to the observed air concentration varies from grid to grid. Grid boxes that are distant from the observation site contribute little to the observation, whereas those that are close have a large impact. In order to balance the contribution from different grid boxes, those that are more distant are grouped together into increasingly larger blocks. The grouping varies for each time period considered and between the different gases due to varying meteorology and the impact of missing observations respectively. The underlying horizontal grid resolution is approximately 25 km (0.352° longitude by 0.234° latitude) and is equal to the resolution of the NAME output. The base grid used is shown in Figure 7(a) and conforms to country (and DA) boundaries. The country boundaries extend into the surrounding seas to reflect both emissions from shipping, off-shore installations and river runoff but also because the inversion has geographical uncertainty. Each area from the base grid is then considered in turn. If the contribution (impact) from an area at the network is above a defined threshold then the area is sub-divided into two areas. This splitting process is continued until each area just falls below the threshold or the fine (25 km) grid resolution is reached. An example grid used in the inversion process when the full DECC network of observations are available is shown in Figure 7(b). The threshold used for the splitting process has been arbitrarily defined. The sensitivity of the emission results to this arbitrary choice of threshold is, through investigation, considered to be below the baseline sensitivity that is included in the inversions.

The modelled time-series at each measurement station is calculated by applying the current emission map to the dilution matrix for that station (Equation 1).

The inversion process works by iteratively choosing different emissions, varying the emission magnitudes and distributions, with the aim of minimising the mismatch between the observations and the modelled concentrations. No prior emission conditions are set. The relative skill of a derived emission map is tested by comparing the modelled and observed time-series by using a cost function.

The cost function described here uses the baseline uncertainty described in the previous section and also the observation uncertainty and the modelling uncertainty as described in a previous report (Oct 2014). This uncertainty varies from gas to gas and over time depending on how well a smooth baseline can be constructed through the ‘clean’ observations, the variability and repeatability of the observations and the degree of local influence at a particular time.

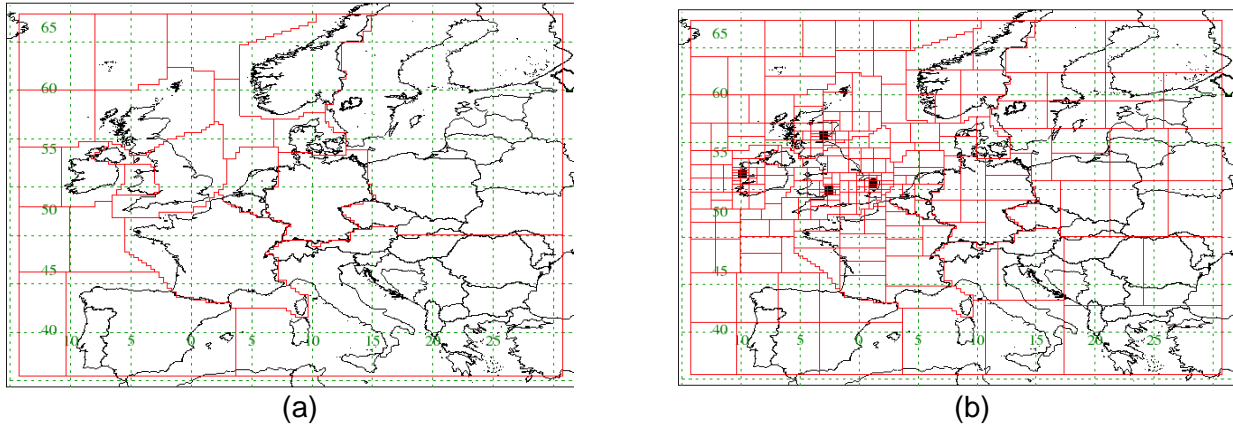


Figure 7: (a) Base regions conforming to country (and Devolved Administration) boundaries (b) Example of the distribution of the different sized regions used by InTEM to estimate regional emissions (finest scale of the grid is ~25 km) when full DECC network observations are available.

An upper (lower) time-series of observations is constructed by adding (subtracting) the baseline uncertainty to the actual observations. These two time-series enclose a range of values that are entirely plausible within the uncertainty of the baseline definition. Given a modelled emission distribution (emission map), a modelled time-series is constructed. The sum of the absolute magnitudes of the modelled minus observed values normalised by the uncertainty at each time is calculated and used as a measure of the skill of the current modelled emission map. The uncertainty at each 2-hour period is comprised of different elements:

- Observational uncertainty: The repeatability of the observation and the variability of the observations within the 2-hour window.
- Baseline uncertainty: As discussed above.
- Uncertainty of modelling local emissions: Local (sub-grid scale) emissions cannot be effectively modelled, therefore the degree of influence of the local area at each time is used to increase the uncertainty at that time.

The iteration process is repeated until the future potential improvement in skill in the emission map is estimated to be negligible.

To simulate biased uncertainties in the meteorology, dispersion and observations the inversion process is applied to three observation time-series; (a) the actual observations (b) observations minus the baseline noise and (c) observations plus the baseline noise.

The ‘local’ contribution is estimated by summing the surface contributions from the 9 grids surrounding the observation station. Times with significant local influence are typically characterised by low wind speeds and low boundary layer heights and thus poor dispersion conditions. During such times the meteorological models used, with horizontal resolutions of between 25 and 80 km, are poor at correctly resolving the local flows as they are dominated by sub-grid scale processes, e.g. land-sea breezes, hence the increased uncertainty.

For inversions when only MHD observations are available solutions are calculated for three-year periods. When observations from other stations are available the time period is reduced to one year. After solutions have been estimated for a particular time period, the time period is moved on by one month and the process repeated, e.g. Jan'95 – Dec'97, Feb'95 – Jan'98, etc.

A monthly/annual estimate of emissions is calculated by averaging all of the solutions that contain a complete month/calendar year within the solved-for time period. The range for each month/year for each geographical region is calculated from the same sample of solutions and is taken as the 5th and 95th percentile solutions.

Figure 8 is an example of the observed and modelled time series of air concentration for CH₄ for 2010 at Mace Head. The magnitudes and patterns are similar and demonstrate that the inversion process is able to derive an emission map that produces a good match to the observations.

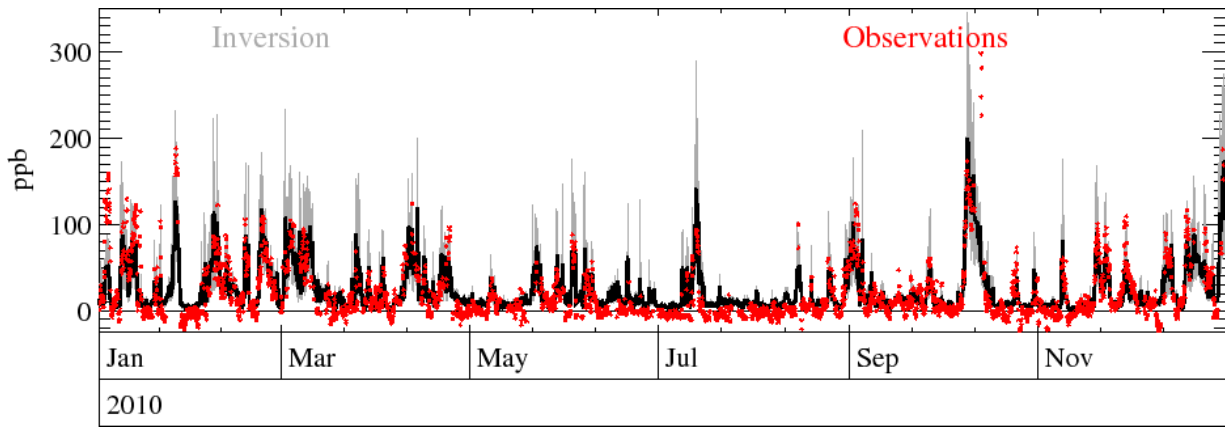


Figure 8: Time series of observed and best-fit modelled CH_4 mole fractions (deviation from baseline) at Mace Head for the first three months of 2010 (solid black line = Inversion, grey = uncertainty in inversion, red crosses = observations).

Emission totals from specific geographical areas, e.g. the UK, are calculated by summing the emissions from each 25 km grid box in that region.

All of the emissions are assumed constant in time and are geographically static within each inversion study period. This is clearly a significant simplification. A sudden, but subsequently maintained, change in emission will be picked up by solving multiple 3-year (or 1-year) periods covering slightly different time periods, e.g. by solving for a 3-year period and then advancing by one month. Enhanced emissions in any particular season, e.g. increased N_2O emissions in spring following fertilizer application, will not be resolved when the time period is one year or more.

All areas of the domain are assumed to impact reasonably equally on the measurement network. The grouping of grid cells together, so that each area contributes approximately equally to the observations, attempts to ensure this but clearly there will be some variability. Also large grid cells could have significant variability actually within the grid itself especially if there are significant orographic features within the grid, e.g. the Alps. This may lead to errors if certain parts of the grid are more frequently sampled than others. However because of the large travel distances and therefore elapsed time between emission in these large grids and measurement the impact of this will be small. Also by only reporting emissions within NWEU (i.e. areas far from the measurement sites are not considered) this issue is assumed small.

The inversion method makes no distinction between anthropogenic and natural sources and thus its estimates are for the combined total, making direct comparisons with the UNFCCC inventory difficult. For most of the gases analysed here the natural emissions are estimated to be small in comparison to the anthropogenic emissions. For example, for CH_4 the natural emissions in NWEU are estimated to be 240 Gg/yr [Bergamaschi *et al.* 2005] compared to anthropogenic emissions of ~10,000 Gg/yr as estimated by the UNFCCC.

It is also important to recognise that the release of certain gases to the atmosphere, e.g. N_2O released from agricultural practices, may occur many miles from its actual source and this therefore adds to the uncertainty of using the maps to attribute emissions to particular regions. The area considered to be the UK includes the waters directly surrounding the UK (Figure 7), so the impact of this is considered to be small for the UK. This would be problematic if the individual contributions of Belgium or the Netherlands for example were presented and is the reason why only the NWEU total is considered. The most significant region in relation to this issue is the border between Northern Ireland and Ireland, however due to the proximity to Mace Head and the corresponding high resolution of the output there the impact is assumed small.

The transport modelling and thus the inversion algorithm also assumes that the gas is inert i.e. that it is not removed by any chemical, biological or physical process. Given the atmospheric lifetimes of the vast majority of the gases studied here this is considered to be a robust assumption when calculating emissions on a regional scale.

5 Results and analysis of gases reported to the UNFCCC

5.1 Introduction

This section discusses the atmospheric trends and regional emissions of the greenhouse gases that are measured by the UK DECC network and that are reported to the UNFCCC (United Nations Framework Convention on Climate Change).

Table 5 describes the principle uses of each of the gases, their radiative efficiency, atmospheric lifetime and global warming potential in a 100-year framework (GWP₁₀₀).

Gas	Chemical Formula	Main Use	Radiative Efficiency (W m ⁻² ppb ⁻¹)	Atmos. lifetime (years)	GWP ₁₀₀
CH ₄	CH ₄	Landfill, farming, energy, wetlands	0.00037	9.8	25
N ₂ O	N ₂ O	Nylon manufacture, farming	0.00303	114	298
CO ₂	CO ₂	Combustion	0.0000138	-	1
HFC-125	CHF ₂ CF ₃	Refrigeration blend, fire suppression	0.23	28.2	3,170
HFC-134a	CH ₂ FCF ₃	Mobile air conditioner	0.16	13.5	1,370
HFC-143a	CH ₃ CF ₃	Refrigeration blend	0.13	51.4	4,470
HFC-152a	CH ₃ CHF ₂	Aerosol propellant, foam-blown agent	0.09	1.6	133
HFC-23	CHF ₃	Bi-product of manufacture of HCFC-22	0.19	228	14,200
HFC-32	CH ₂ F ₂	Refrigeration blend	0.11	5.4	716
HFC-227ea	CF ₃ CHFCF ₃	Fire suppression, inhalers, foam blowing	0.26	35.8	3,580
HFC-365mfc	C ₄ H ₅ F ₅	Foam blowing	0.21	8.6	794
HFC-43-10mee	C ₅ H ₂ F ₁₀	Electronics industry	0.4	15.9	1,640
PFC-14	CF ₄	Bi-product alum. production, electronics	0.08	>50,000	5,820
PFC-116	C ₂ F ₆	Electronics, bi-product alum. production	0.26	>10,000	12,010
PFC-218	C ₃ F ₈	Electronics, bi-product alum. production	0.26	2,600	8,690
PFC-318	C ₄ F ₈	Semiconductor and electronics industries	0.32	3,200	10,300
SF ₆	SF ₆	Circuit breaker in high voltage switchgear	0.52	3,200	22,800
NF ₃	NF ₃	Electronics manufacture	0.21	740	17,200

Table 5: The principle use, radiative efficiency, atmospheric lifetime and 100-year global warming potential of the gases measured by the UK DECC network and that are reported to the UNFCCC. Data based of the IPCC fourth Assessment Report Chapter 2.

In this chapter InTEM results are presented for each of these gases (except CO₂).

5.2 Methane (CH_4)

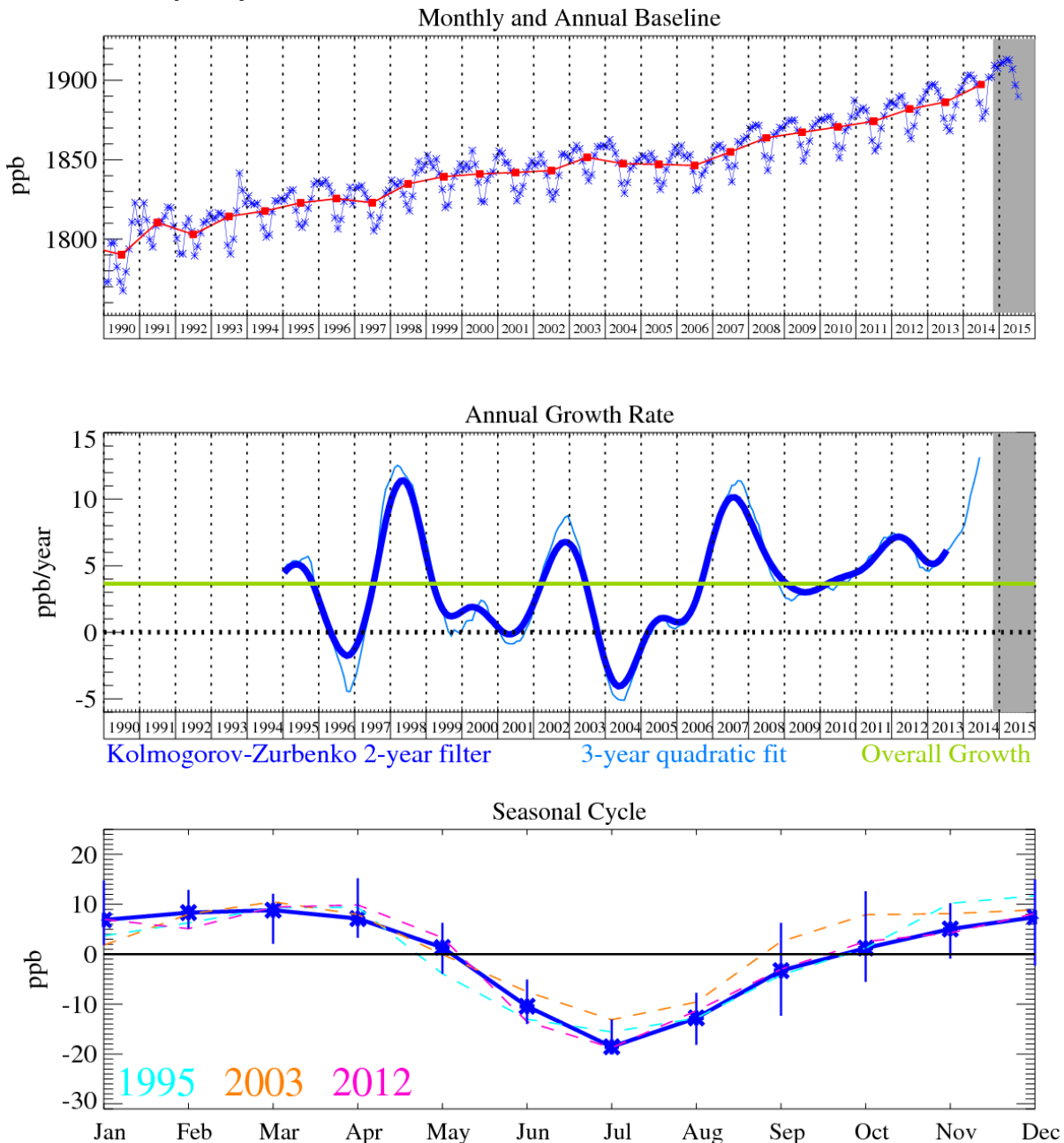


Figure 9: Methane: Monthly (blue) and annual (red) baseline mole fractions (top plot). Annual (blue) and overall average growth rate (green) (middle plot). Seasonal cycle (de-trended) with year-to-year variability (lower plot). Grey area covers un-ratified and therefore provisional data. ppb refers to 'parts per billion' dry air mole fraction

The long-term trend for CH_4 , shown in Figure 9, is of particular interest with a steep rise up to about 2000 followed by a flat period with almost no growth and then a steep rise of up to 9 ppb/yr over the period 2007-2008. Growth is estimated to be increasing again with a mole fraction of 1913 ppb in March-April 2015, its peak in the seasonal cycle.

In 2007-2008, 2010-2012 and 2014 the mole fraction of CH_4 in the atmosphere rose faster than its long-term average growth rate. Several theories are postulated:

- Increased emissions from the high latitudes in the Northern hemisphere related to wetlands and reduced permafrost/snow cover.
- Increased emissions in the tropics due to increased emissions from wetlands/rice production or biomass burning due to El Niño conditions.
- Reduced levels of hydroxyl radical (OH) in the atmosphere. Reaction with hydroxyl radical is the major sink for atmospheric CH_4 .

However each of these theories in isolation does not seem to completely fit the evidence gathered so far. For example, there is no evidence for any link to large scale biomass burning (i.e. no concomitant increase in carbon monoxide), as was the case in 1998 – driven by the largest ever El Niño drought. The inferences drawn from the observations were that the CH₄ increase is driven by wetland emissions in the boreal region (driven by a temperature anomaly) and in the tropics (possibly driven by a precipitation anomaly) with a small role for OH changes a possibility in the tropics but not statistically significant. Satellite observations have also detected an increase in global mixing ratios in recent years [Bloom *et al.*, 2010] and identified increased wetland emissions as a potential cause, consistent with *in situ* measurements. The baseline mole fractions of CH₄ reported from Mace Head (and other AGAGE stations) in 2009 indicate that the rapid rise in global average CH₄ mole fractions slowed (as shown in Figure 9). The growth calculations at the end of the time period are highly uncertain.

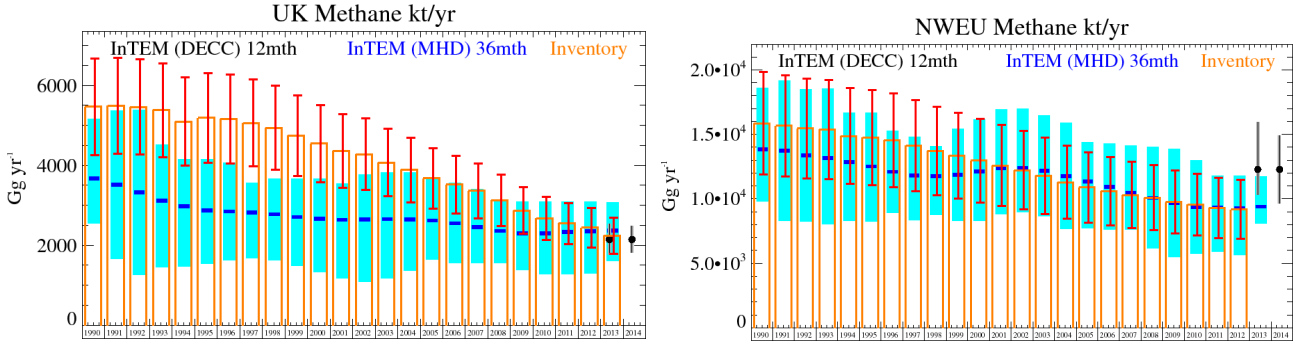


Figure 10: Emission estimates (Gg/yr – gigagrams per year) from the UNFCCC Inventory and InTEM (MHD-only and DECC network) for UK and NWEU. The uncertainty bars represent the 5th and 95th percentiles For the inversion results this uncertainty range is calculated from the solutions for a particular time period, the time period is moved on by one month and the process repeated, e.g. Jan'95 – Dec'97, Feb'95 – Jan'98, etc. An annual estimate of emission is calculated by averaging all of the solutions that contain a complete calendar year within the solved-for time period. The range for each month/year for each geographical region is calculated from the same sample of solutions and is taken as the 5th and 95th percentile solutions.

Years	InTEM (MHD) 36mth	InTEM (DECC) 12mth	Inventory
1990	3680. (2550.-5160.)		5460. (4260.-6670.)
1991	3520. (1660.-5370.)		5480. (4280.-6690.)
1992	3320. (1250.-5390.)		5460. (4270.-6650.)
1993	3120. (1450.-4520.)		5380. (4210.-6550.)
1994	2980. (1460.-4150.)		5090. (3990.-6200.)
1995	2880. (1530.-4150.)		5180. (4070.-6300.)
1996	2840. (1620.-4070.)		5160. (4050.-6260.)
1997	2820. (1690.-3560.)		5060. (3980.-6140.)
1998	2770. (1630.-3670.)		4930. (3880.-5980.)
1999	2710. (1500.-3670.)		4740. (3730.-5740.)
2000	2660. (1330.-3670.)		4540. (3580.-5500.)
2001	2640. (1170.-3550.)		4360. (3440.-5280.)
2002	2650. (1080.-3770.)		4270. (3380.-5170.)
2003	2660. (1170.-3820.)		4070. (3220.-4920.)
2004	2650. (1370.-3820.)		3890. (3080.-4690.)
2005	2620. (1650.-3660.)		3670. (2910.-4440.)
2006	2550. (1560.-3570.)		3520. (2790.-4240.)
2007	2450. (1560.-3400.)		3360. (2670.-4050.)
2008	2360. (1560.-3090.)		3120. (2490.-3760.)
2009	2300. (1390.-3090.)		2870. (2280.-3450.)
2010	2300. (1270.-3100.)		2670. (2130.-3210.)
2011	2330. (1270.-3100.)		2550. (2030.-3060.)
2012	2350. (1290.-3100.)		2440. (1950.-2930.)
2013	2370. (1610.-3080.)	2150. (1760.-2530.)	2240. (1790.-2690.)
2014		2150. (1810.-2480.)	

Table 6: Emission (Gg/yr) estimates for the UK with uncertainty (5th - 95th percentile).

The inventory and InTEM emission estimates for the UK are similar from 2000 onwards. In the early to late 1990s the InTEM estimates for the UK were markedly lower than the inventory values. For

the NWEU the two methods agree very well 1990-1999, from 2000 onwards the InTEM estimates are higher but the uncertainty bars strongly overlap throughout. The pollution events seen at Mace Head are regular and strong and the statistical match between the modelled time-series and the observations is good. The results from the DECC network InTEM inversion agree extremely well to both the MHD-only and the inventory estimates for the UK.

5.3 Nitrous oxide (N_2O)

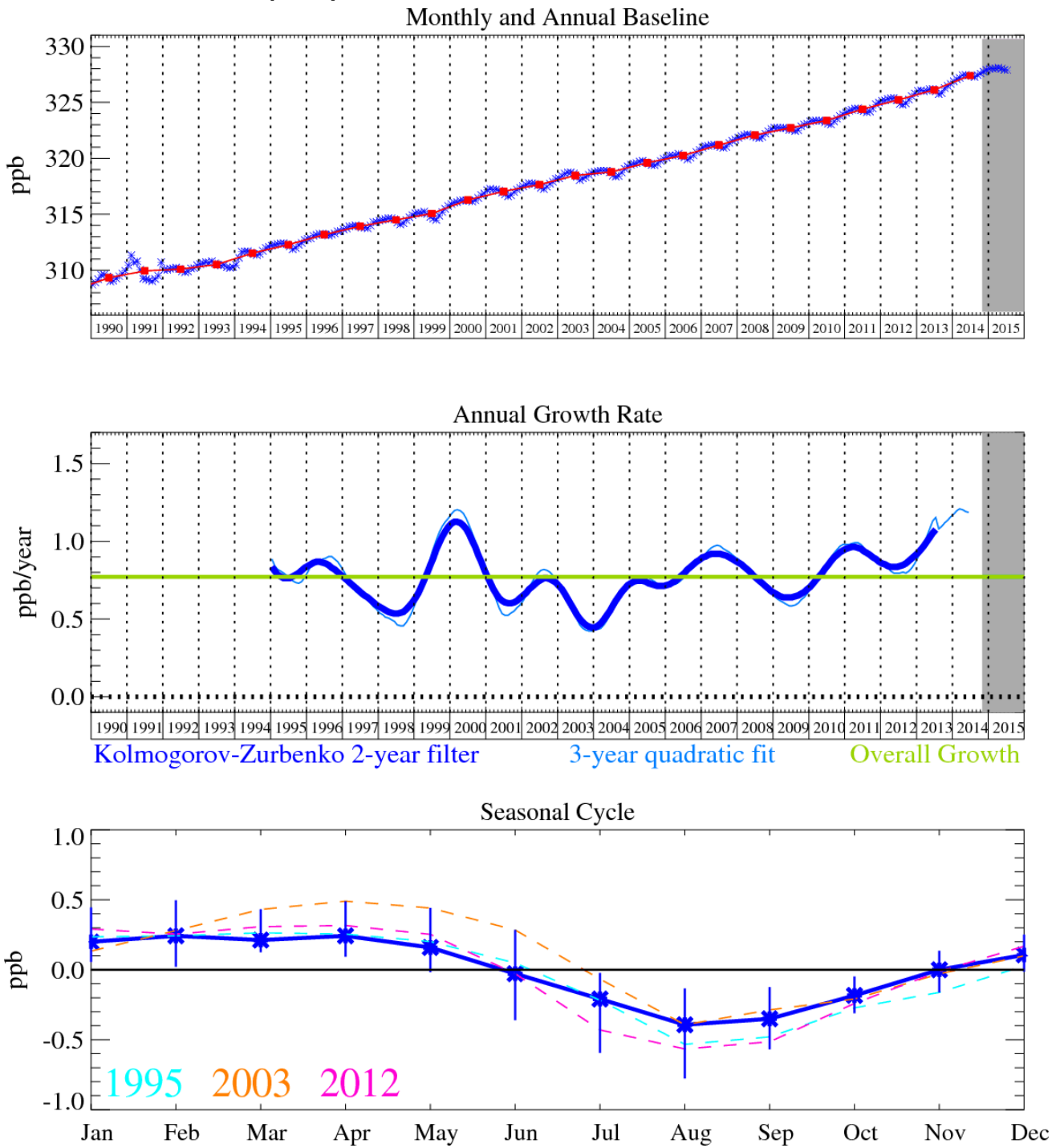


Figure 11: Nitrous oxide: Monthly (blue) and annual (red) baseline mole fractions (top). Annual (blue) and overall growth rate (green) (middle). Seasonal cycle (de-trended) with year-to-year variability (lower plot). Grey area covers un-ratified and therefore provisional data.

Figure 11 shows the baseline monthly means and trend for N_2O with an almost linear upwards average trend of 0.75 ppb/yr. The most recent growth rate is estimated to be over 1 ppb/yr. The Northern Hemisphere (NH) baseline mole fraction in July 2015 was 328 ppb. The N_2O increase is attributable to human activities, such as fertilizer use and fossil fuel burning, although it is also emitted through natural processes occurring in soils and oceans. There are large uncertainties associated with quantifying the sources of this gas. The recent global growth anomaly in N_2O is of particular interest with very substantial increases in 2010-2011 and 2013-2014. At Mace Head the average historical growth rate of about 0.75 ppb/year has increased to over 1 ppb/year. Similarly in the Southern Hemisphere at Cape Grim, Tasmania the growth rate has increased from about 0.6 ppb/year in 2003 to about 1 ppb/year in 2011. Increases in N_2O emissions may also be linked to the tropics where ‘wet and warm’ microbes in soil can produce bursts in N_2O production, although this is

contrary to reports where very saturated soils can decrease N₂O emissions, however, as noted by Prof. R. Weiss of Scripps Institution of Oceanography, there may be different spatial distributions of “wetness” with increased N₂O emissions in some regions and decreases in others. Interestingly, hydrogen has also exhibited a growth spurt in 2011. Here wet soils tend to reduce the normal H₂ deposition velocities due to a reduction in diffusivity. At this stage more global sites need to be carefully assessed to confirm these increases in the N₂O growth rate. We expect AGAGE, in collaboration with NOAA, to address these issues.

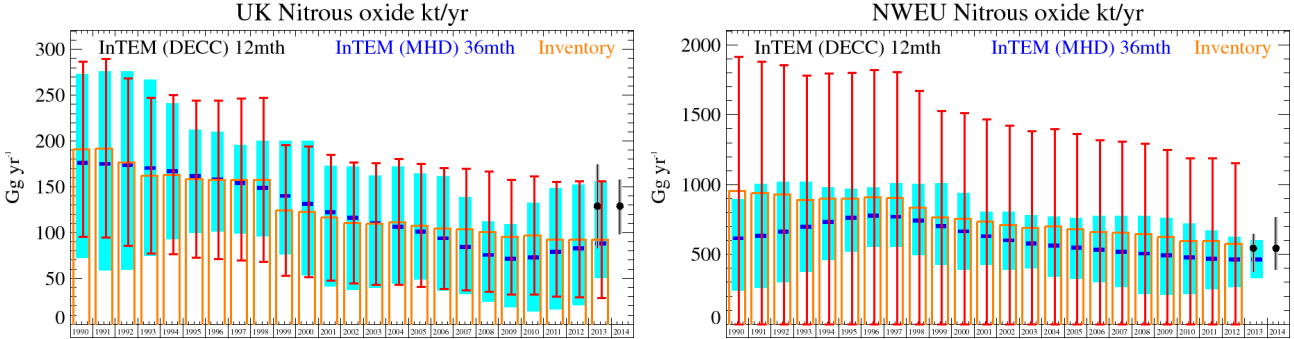


Figure 12: Emission estimates (Gg/yr) from the UNFCCC Inventory and InTEM (MHD-only and DECC network) for UK and NWEU. The uncertainty bars represent the 5th and 95th percentiles.

The UK inventory and InTEM estimates are broadly in agreement. The 3-yr Mace Head-only estimates are showing a positive trend in the latter period. The DECC network results are higher than the MHD-only estimates and the inventory estimates although the 1-sigma uncertainty bars strongly overlap.

Years	InTEM (MHD) 36mth	InTEM (DECC) 12mth	Inventory
1990	176. (72.-273.)		191. (96.-287.)
1991	175. (59.-276.)		192. (94.-289.)
1992	174. (60.-276.)		177. (85.-268.)
1993	171. (75.-267.)		162. (77.-247.)
1994	167. (93.-241.)		163. (76.-250.)
1995	162. (100-212.)		158. (73.-244.)
1996	158. (101.-210.)		158. (71.-244.)
1997	154. (99.-196.)		158. (70.-246.)
1998	149. (96.-200.)		158. (68.-247.)
1999	140. (76.-200.)		124. (53.-196.)
2000	131. (53.-200.)		123. (51.-194.)
2001	122. (41.-173.)		116. (48.-185.)
2002	116. (37.-172.)		110. (44.-176.)
2003	111. (40.-162.)		110. (43.-176.)
2004	106. (44.-172.)		112. (43.-180.)
2005	101. (49.-165.)		108. (41.-175.)
2006	94. (37.-162.)		104. (38.-170.)
2007	84. (33.-139.)		103. (37.-170.)
2008	76. (25.-112.)		101. (35.-167.)
2009	72. (19.-109.)		95. (33.-158.)
2010	73. (14.-133.)		97. (32.-161.)
2011	79. (17.-149.)		93. (30.-155.)
2012	83. (21.-153.)		93. (29.-156.)
2013	88. (50.-156.)	129. (83.-175.)	92. (29.-156.)
2014		129. (98.-158.)	

Table 7: Emission (Gg/yr) estimates for the UK with uncertainty (5th - 95th percentile).

5.4 Carbon dioxide (CO₂)

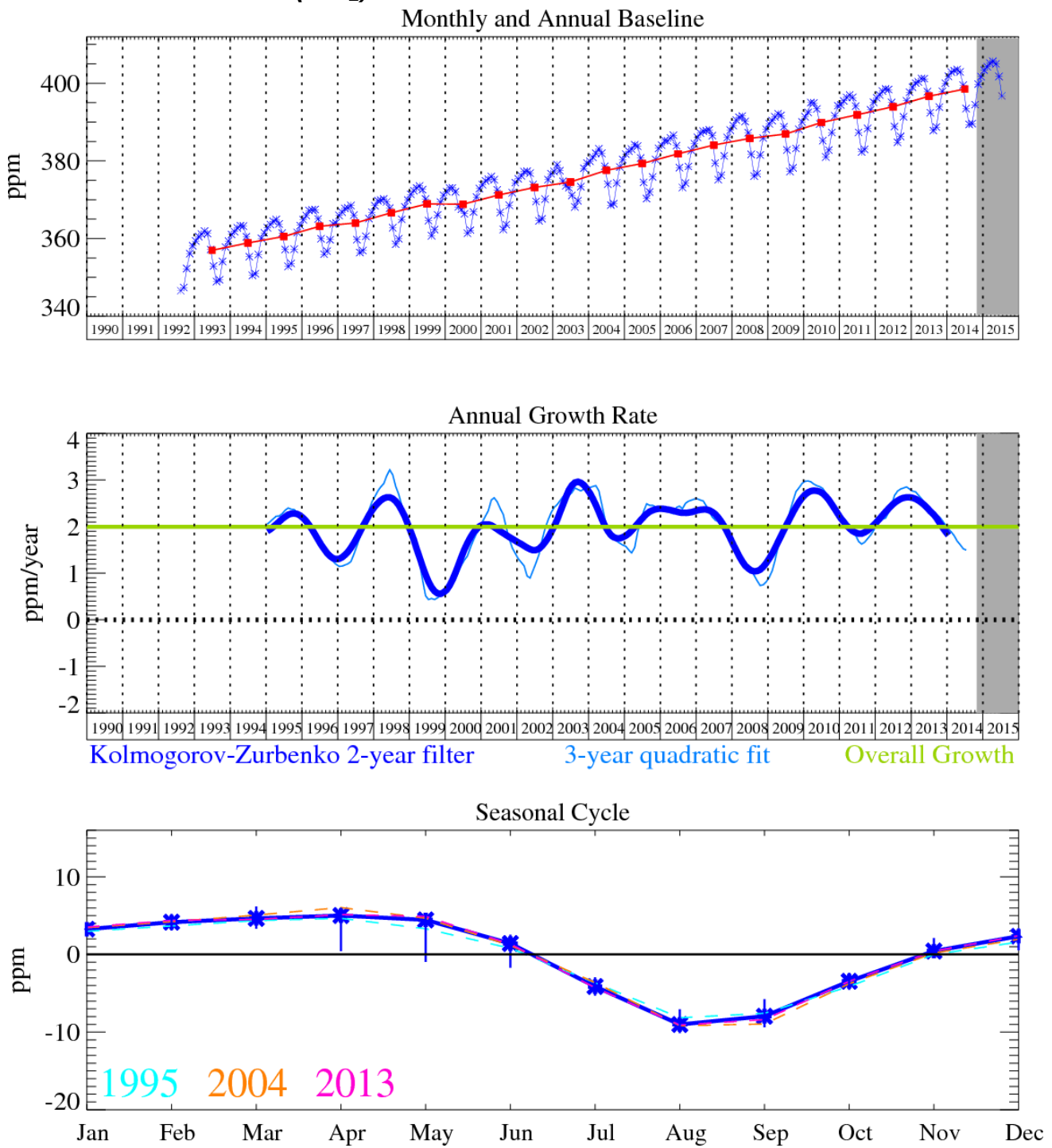


Figure 13: Carbon dioxide (CO₂): Monthly (blue) and annual (red) baseline mole fractions (top plot). Annual (blue) and overall average growth rate (green) (middle plot). Seasonal cycle (de-trended) with year-to-year variability (lower plot). Grey area covers un-ratified and therefore provisional data.

CO₂ is the most important greenhouse gas, and has steadily grown at an annual average rate of 2 ppm/yr, calculated from the baseline-selected monthly means. It has now reached a monthly mole fraction of 406 ppm (Apr 2015), the highest yet recorded at Mace Head, Ireland, and has shown significant growth rate anomalies in 1998/99 and 2002/03, which we suggest are a result of the global biomass burning events in those years. The average annual baseline mole fraction at Mace Head is estimated to be ~400 ppm in 2015. Natural CO₂ fluxes significantly influence the measured mole fractions and therefore calculations of the anthropogenic emissions component is highly uncertain. Our annual report published in May 2014 detailed an attempt to calculate emissions using a CO₂-ratio method, however, uncertainties were very large relative to the inventory estimates. Since that report further efforts have not been made to calculate anthropogenic CO₂ emissions with InTEM.

5.5 HFC-125

Hydrofluorocarbons (HFCs) are replacement chemicals for the long-lived ozone depleting substances in various applications such as refrigeration, fire extinguishers, propellants, and foam blowing. The most recent measurements of the HFCs by the UK DECC network indicate that the mixing ratios of all HFC compounds continue to grow, as is consistent with sustained emissions of these replacement compounds into the atmosphere. The only exception is HFC-152a, the growth rate of this gas is now negative. The baseline monthly mean mole fractions for all the HFCs are presented in Table 2 - Table 4.

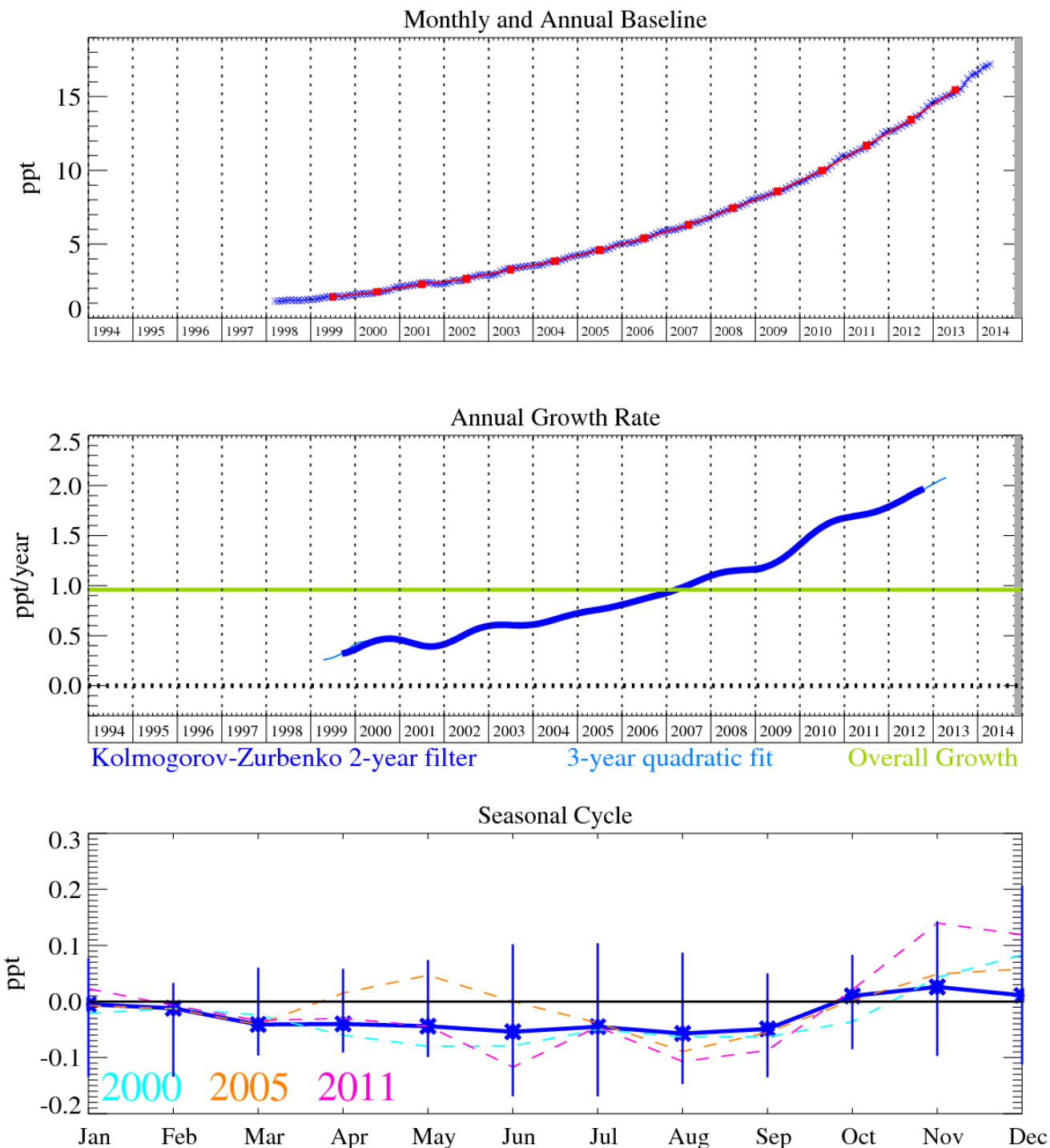


Figure 14: HFC-125 (CHF_2CF_3): Monthly (blue) and annual (red) baseline mole fractions (top plot). Annual (blue) and overall average growth rate (green) (middle plot). Seasonal cycle (de-trended) with year-to-year variability (lower plot). Grey area covers un-ratified provisional data.

HFC-125 (CHF_2CF_3): This compound is used in refrigeration blends and for fire suppression. It has a GWP₁₀₀ of 3420 and an atmospheric lifetime of 30.5 years. [Ko *et al.*, 2013]. This compound is growing rapidly in the atmosphere.

Unfortunately at Mace Head the observations of HFC-125 have been compromised by contamination (since May 2014) and have been removed. This matter has been investigated and is linked to the air conditioner leakage at the station. A temporary solution has been adopted, to flush the air sample module with clean ambient air to minimise contamination from laboratory air. A longer term solution will require modification of the contaminating air conditioner to use a chilled water heat exchanger with the contaminating refrigerant gases contained in a unit external to the laboratory. The baseline will be estimated using another Northern Hemisphere station such as Zeppelin (Ny Alesund) until the situation at Mace Head is resolved.

Relative to the magnitude of the baseline the pollution events are very significant. Therefore InTEM has plenty of clear information on which to base the emission estimates. The agreement between the inventory and InTEM for the UK is excellent up until 2009 with a strong overlap of the uncertainty bars from both methods. It is interesting to note that with InTEM the UK estimates have remained broadly constant from 2010 onwards in contrast to the inventory that continues to grow strongly. However, it is also noticeable that the NWEU InTEM estimates have continued to grow, and at a stronger rate than the inventory.

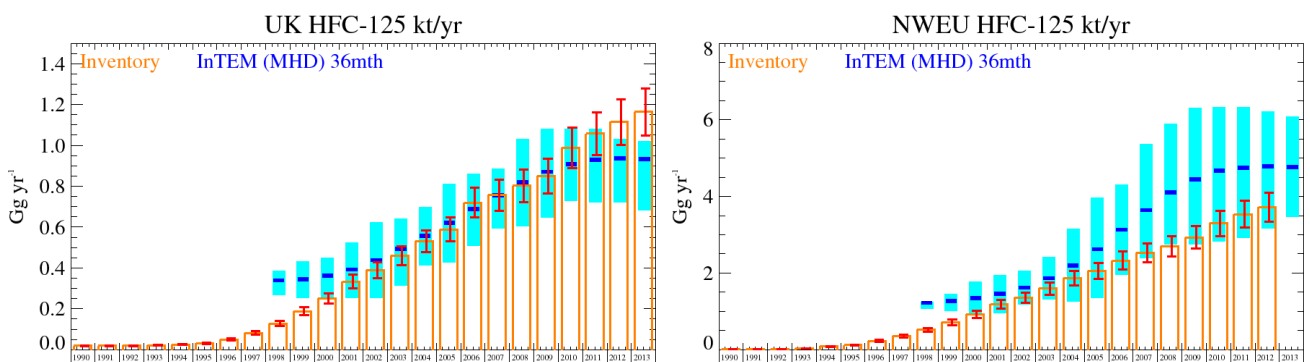


Figure 15: Emission estimates (Gg/yr) from the UNFCCC Inventory and InTEM (MHD-only) for UK and NWEU. The uncertainty bars represent the 5th and 95th percentiles.

Years	InTEM (MHD) 36mth	Inventory
1990		0.02 (0.02-0.02)
1991		0.02 (0.02-0.02)
1992		0.02 (0.02-0.02)
1993		0.02 (0.02-0.02)
1994		0.03 (0.02-0.03)
1995		0.03 (0.03-0.03)
1996		0.05 (0.05-0.06)
1997		0.08 (0.07-0.09)
1998	0.34 (0.27-0.39)	0.13 (0.12-0.14)
1999	0.35 (0.25-0.43)	0.19 (0.17-0.21)
2000	0.36 (0.25-0.45)	0.25 (0.23-0.28)
2001	0.39 (0.25-0.52)	0.33 (0.30-0.37)
2002	0.44 (0.25-0.62)	0.39 (0.35-0.43)
2003	0.49 (0.32-0.64)	0.46 (0.41-0.51)
2004	0.56 (0.41-0.70)	0.53 (0.48-0.58)
2005	0.62 (0.43-0.81)	0.59 (0.53-0.65)
2006	0.69 (0.51-0.86)	0.72 (0.65-0.79)
2007	0.76 (0.59-0.89)	0.76 (0.68-0.83)
2008	0.8 (0.6-1.0)	0.80 (0.72-0.88)
2009	0.9 (0.6-1.1)	0.85 (0.77-0.94)
2010	0.91 (0.73-1.08)	0.99 (0.89-1.09)
2011	0.93 (0.72-1.08)	1.06 (0.95-1.16)
2012	0.94 (0.72-1.03)	1.11 (1.00-1.23)
2013	0.93 (0.68-1.02)	1.16 (1.05-1.28)

Table 8: Emission (Gg/yr) estimates for the UK with uncertainty (5th – 95th percentile).

5.6 HFC-134a

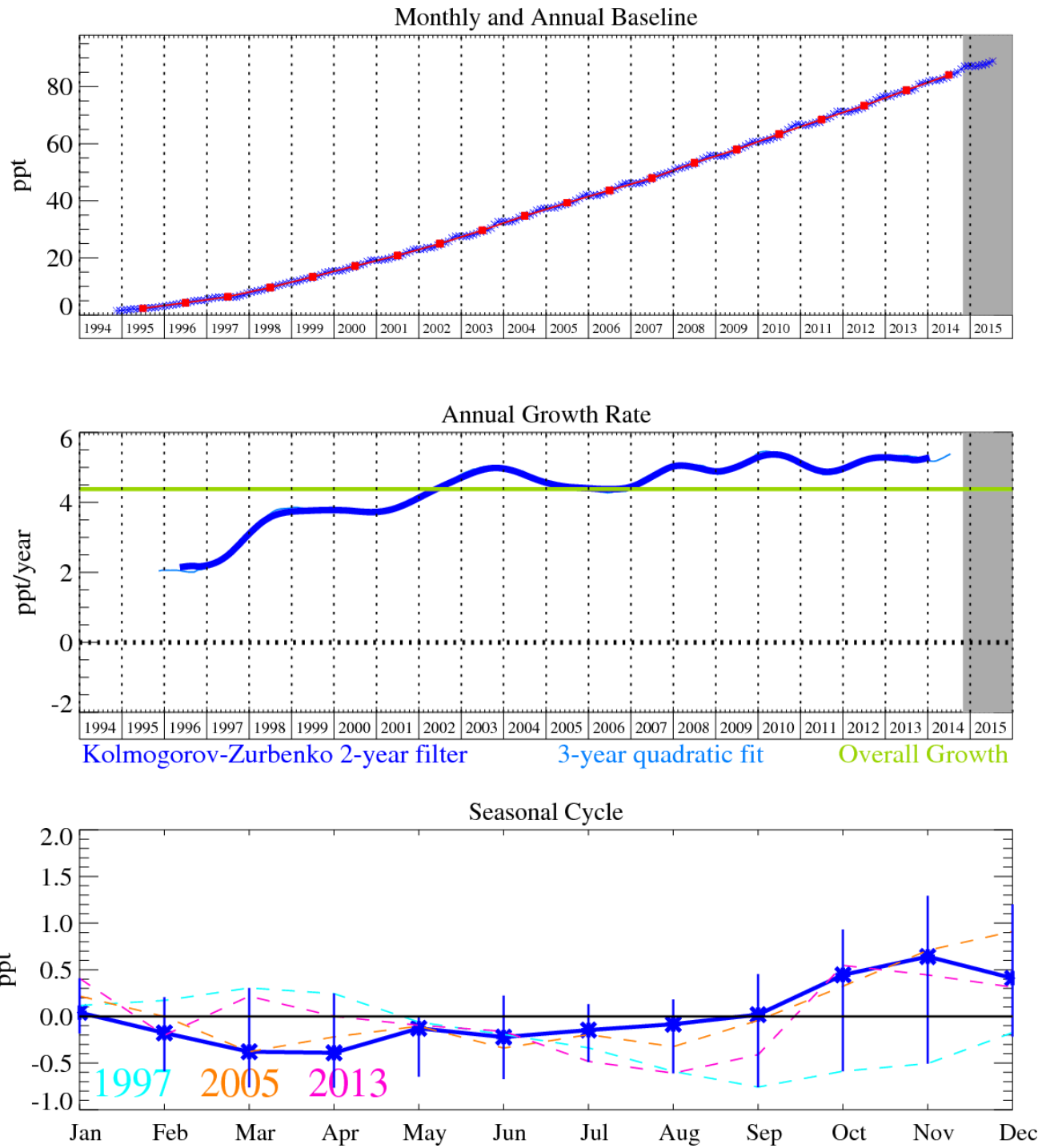


Figure 16: HFC-134a (CH_2FCF_3): Monthly (blue) and annual (red) baseline mole fractions (top plot). Annual (blue) and overall average growth rate (green) (middle plot). Seasonal cycle (de-trended) with year-to-year variability (lower plot). Grey area covers un-ratified and therefore provisional data.

HFC-134a (CH_2FCF_3): Globally HFC-134a is the most abundant HFC present in the atmosphere and is used predominantly in refrigeration and mobile air conditioning (MAC). Due to its long lifetime, 13.5 years, and relatively high GWP₁₀₀ of 1370 [Forster et al., 2007], the use of HFC-134a (and any other HFCs with a GWP₁₀₀ > 150) is being phased out in Europe between 2011 and 2017. It is proposed that a very gradual phase-out of the use of HFC-134a in cars will also take place outside Europe because of the global nature of the car industry. However in developing countries the potential for growth of HFC-134a is still large [Velders et al., 2009]. As of July 2015 the NH atmospheric mole fraction of HFC-134a reached 88.9 ppt and the recent growth is estimated to be 5.3 ppt/yr.

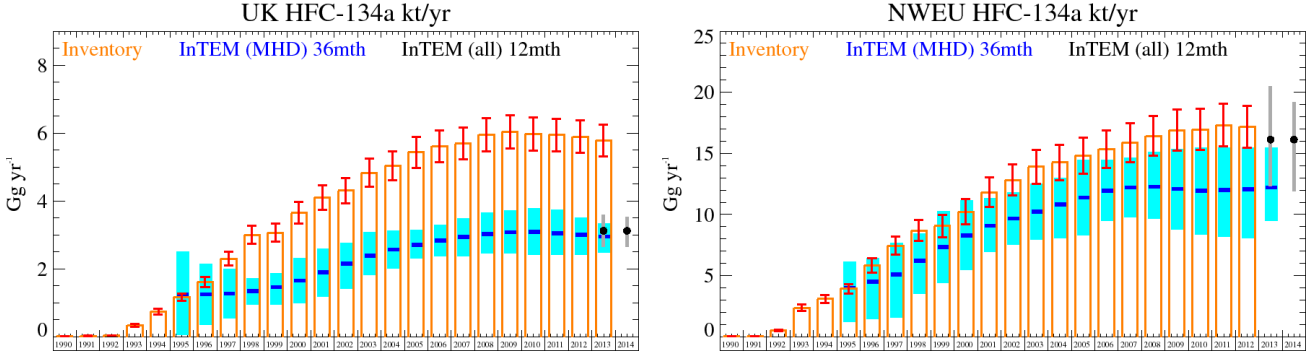


Figure 17: Emission estimates (Gg/yr) from the UNFCCC Inventory and InTEM (MHD-only and DECC network) for UK and NWEU. The uncertainty bars represent the 5th and 95th percentiles.

Years	InTEM (MHD) 36mth	InTEM (DECC) 12mth	Inventory
1990			0.02 (0.02-0.02)
1991			0.03 (0.02-0.03)
1992			0.04 (0.03-0.04)
1993			0.3 (0.3-0.4)
1994			0.7 (0.7-0.8)
1995	1.25 (0.01-2.51)		1.2 (1.1-1.3)
1996	1.3 (0.4-2.1)		1.6 (1.5-1.8)
1997	1.3 (0.5-2.0)		2.3 (2.1-2.5)
1998	1.3 (0.9-1.7)		3.0 (2.7-3.3)
1999	1.5 (1.0-1.9)		3.1 (2.8-3.3)
2000	1.7 (1.0-2.3)		3.6 (3.3-4.0)
2001	1.9 (1.2-2.6)		4.1 (3.7-4.5)
2002	2.2 (1.4-2.8)		4.3 (3.9-4.7)
2003	2.4 (1.8-3.1)		4.8 (4.4-5.2)
2004	2.6 (2.0-3.1)		5.0 (4.6-5.5)
2005	2.7 (2.3-3.1)		5.4 (5.0-5.9)
2006	2.8 (2.4-3.3)		5.6 (5.1-6.1)
2007	2.9 (2.4-3.5)		5.7 (5.2-6.2)
2008	3.0 (2.5-3.7)		5.9 (5.5-6.4)
2009	3.1 (2.5-3.7)		6.0 (5.5-6.5)
2010	3.1 (2.4-3.8)		6.0 (5.5-6.5)
2011	3.0 (2.4-3.7)		5.9 (5.5-6.4)
2012	3.0 (2.4-3.5)		5.9 (5.4-6.4)
2013	3.0 (2.5-3.3)	3.1 (2.6-3.6)	5.8 (5.3-6.2)
2014		3.1 (2.6-3.5)	

Table 9: Emission (Gg/yr) estimates for the UK with uncertainty (5th - 95th percentile).

The UK inventory and InTEM estimates increased between the mid-1990s until 2009. Since then the UK inventory and InTEM have very slightly decreased. The InTEM estimates for the UK are consistently around half to two thirds of the inventory estimates. A different picture emerges in NWEU as a whole, the inventory shows increasing emissions in recent years whereas InTEM has a flatter profile. The statistical fit between the measurements and the modelling is relatively good throughout the time-series. A significant proportion of the HFC-134a emitted is estimated to come from in-use vehicles (it is used in mobile air conditioning units). Inspection of the inventory shows that different countries across the EU use different values for the leakage rates from in-use vehicles. A full investigation of the reasons for the discrepancy between the inventory and the InTEM results has been presented in earlier reports (Oct 2014 and May 2015).

5.7 HFC-143a

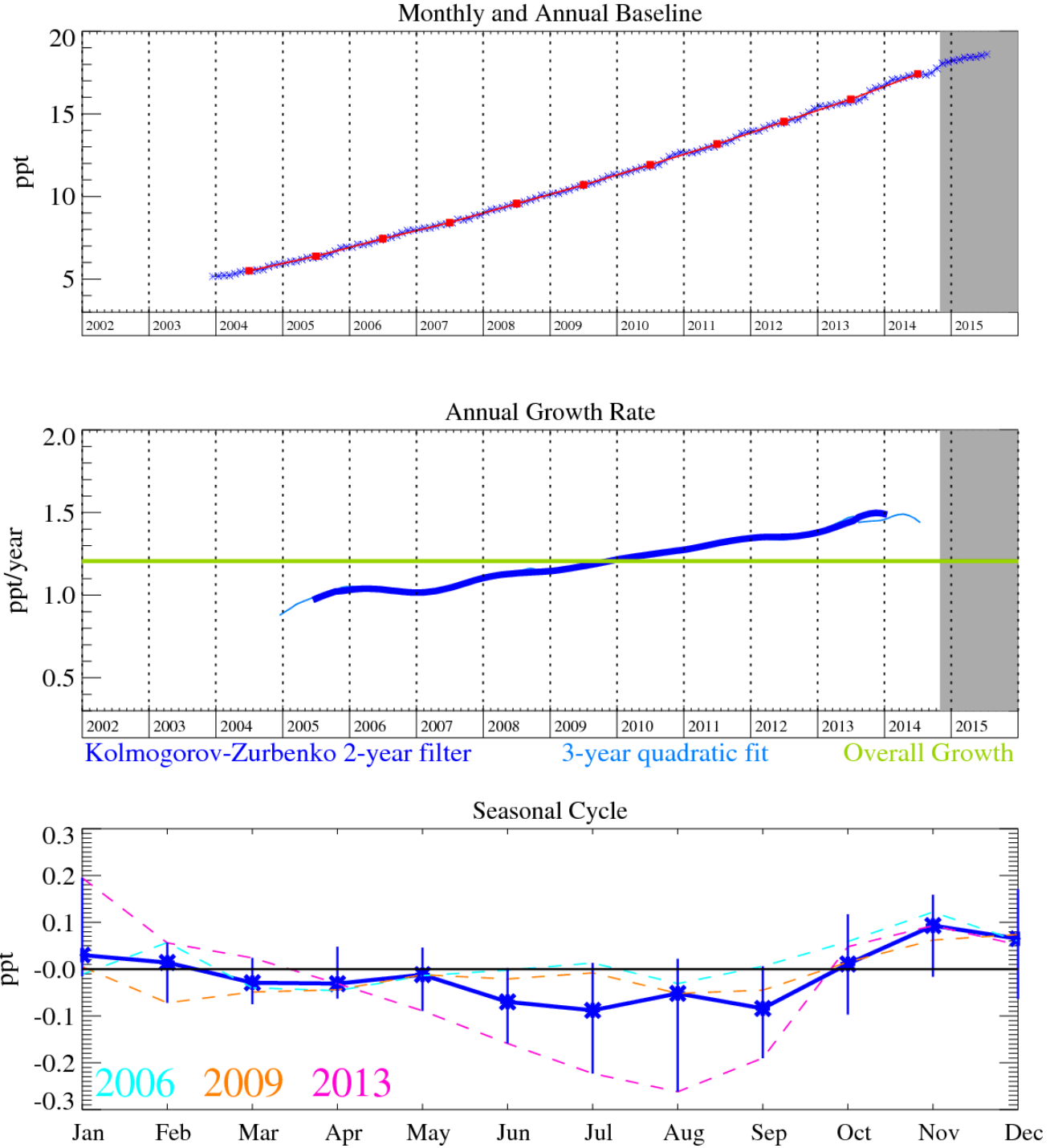


Figure 18: HFC-143a (CH_3CF_3): Monthly (blue) and annual (red) baseline mole fractions (top plot). Annual (blue) and overall average growth rate (green) (middle plot). Seasonal cycle (de-trended) with year-to-year variability (lower plot). Grey area covers un-ratified and therefore provisional data.

HFC-143a (CH_3CF_3): is used mainly as a working fluid in refrigerant blends (R-404A and R-507A) for low and medium temperature commercial refrigeration systems. In July 2015 the NH baseline mole fraction reached 18.6 ppt. These levels have increased dramatically from the low levels in 1997 with an increasing growth rate, currently estimated to be 1.4 ppt/yr. It has a relatively long atmospheric lifetime of 51.4 years and a significant radiative forcing value (third largest of all the HFCs) with a GWP₁₀₀ of 4400.

The InTEM emission estimates for the UK show a maximum was reached in 2008-09 after which they have started to decline. The inventory estimates an increase across the years. The higher frequency (1-year) DECC network InTEM estimates also show a declining UK total but are lower than the MHD-only estimates although the uncertainty bars strongly overlap. The NWEU estimates

for both InTEM and the inventory are increasing although the InTEM estimates are consistently above the inventory estimates.

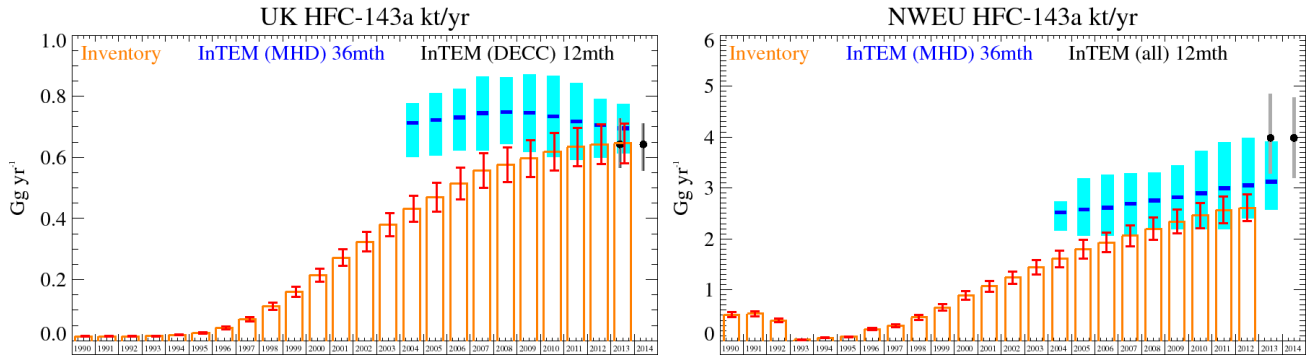


Figure 19: Emission estimates (Gg/yr) from the UNFCCC Inventory and InTEM (MHD-only and DECC network) for UK and NWEU. The uncertainty bars represent the 5th and 95th percentiles.

Years	InTEM (MHD) 36mth	InTEM (DECC) 12mth	Inventory
1990			0.01 (0.01-0.02)
1991			0.01 (0.01-0.02)
1992			0.01 (0.01-0.02)
1993			0.02 (0.01-0.02)
1994			0.02 (0.02-0.02)
1995			0.02 (0.02-0.03)
1996			0.04 (0.04-0.05)
1997			0.07 (0.06-0.08)
1998			0.11 (0.10-0.12)
1999			0.16 (0.14-0.18)
2000			0.21 (0.19-0.24)
2001			0.27 (0.25-0.30)
2002			0.32 (0.29-0.36)
2003			0.38 (0.34-0.42)
2004	0.71 (0.60-0.78)		0.43 (0.39-0.48)
2005	0.72 (0.61-0.81)		0.47 (0.42-0.52)
2006	0.73 (0.62-0.82)		0.51 (0.46-0.57)
2007	0.74 (0.62-0.86)		0.56 (0.50-0.61)
2008	0.75 (0.64-0.86)		0.58 (0.52-0.63)
2009	0.75 (0.62-0.87)		0.60 (0.54-0.66)
2010	0.73 (0.60-0.87)		0.62 (0.56-0.68)
2011	0.72 (0.59-0.84)		0.63 (0.57-0.70)
2012	0.71 (0.60-0.79)		0.64 (0.58-0.71)
2013	0.70 (0.61-0.77)	0.64 (0.56-0.73)	0.65 (0.58-0.71)
2014		0.64 (0.56-0.71)	

Table 10: Emission (Gg/yr) estimates for the UK with uncertainty (5th - 95th percentile).

5.8 HFC-152a

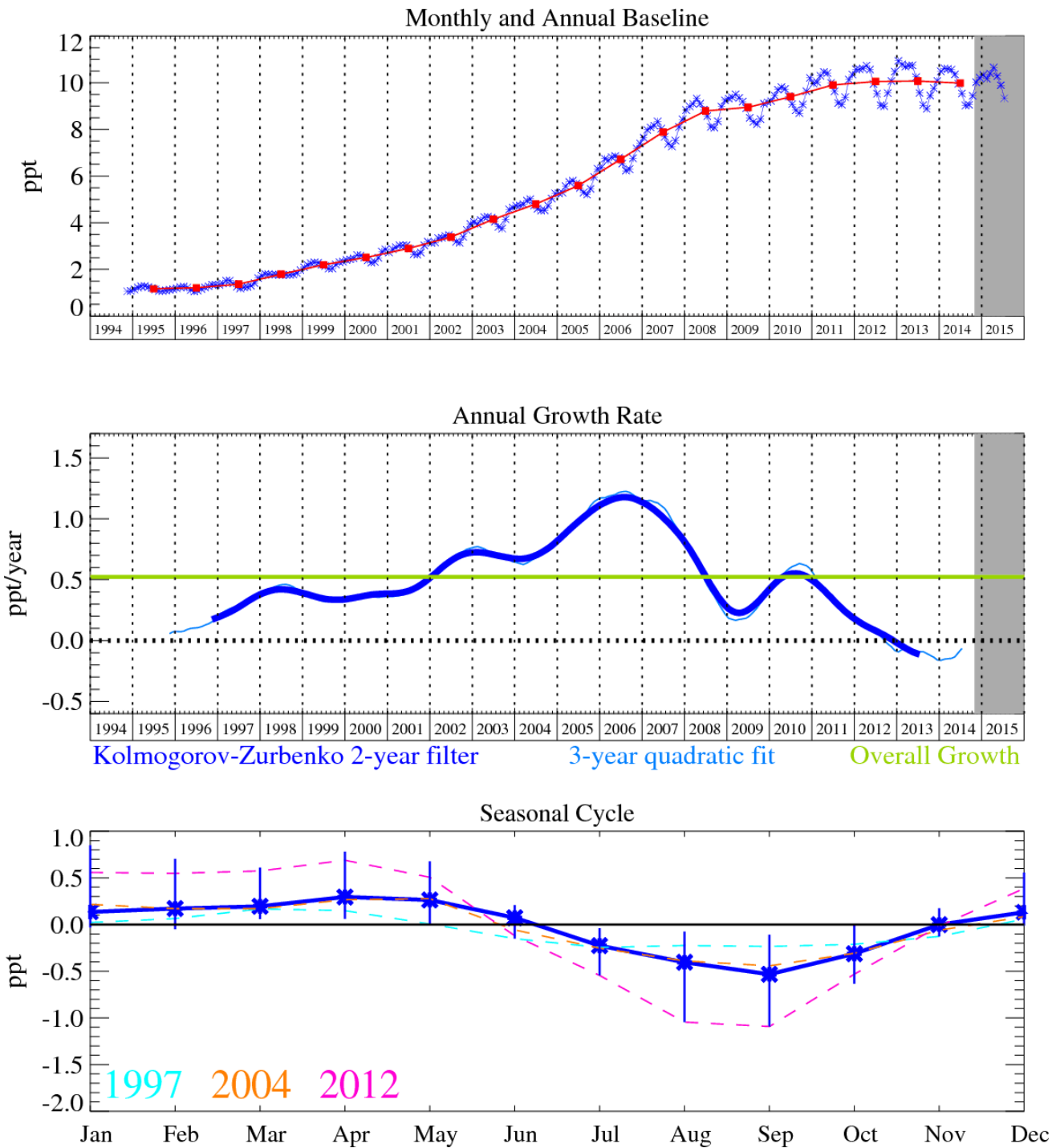


Figure 20: HFC-152a (CH_3CHF_2): Monthly (blue) and annual (red) baseline mole fractions (top plot). Annual (blue) and overall average growth rate (green) (middle plot). Seasonal cycle (de-trended) with year-to-year variability (lower plot). Grey area covers un-ratified and therefore provisional data.

HFC-152a (CH_3CHF_2): has a relatively short lifetime of 1.6 years due to its efficient removal by OH oxidation in the troposphere, consequently it has the smallest GWP₁₀₀ at 133 of all of the major HFCs. It is used as a foam-blowing agent and aerosol propellant, and given its short lifetime has exhibited substantial growth in the atmosphere since measurement began in 1994, implying a substantial increase in emissions in these years. However, in the last few years the rate of growth slowed considerably and is now negative. The maximum NH monthly mole fraction reached was 10.9 ppt (Jan 2013).

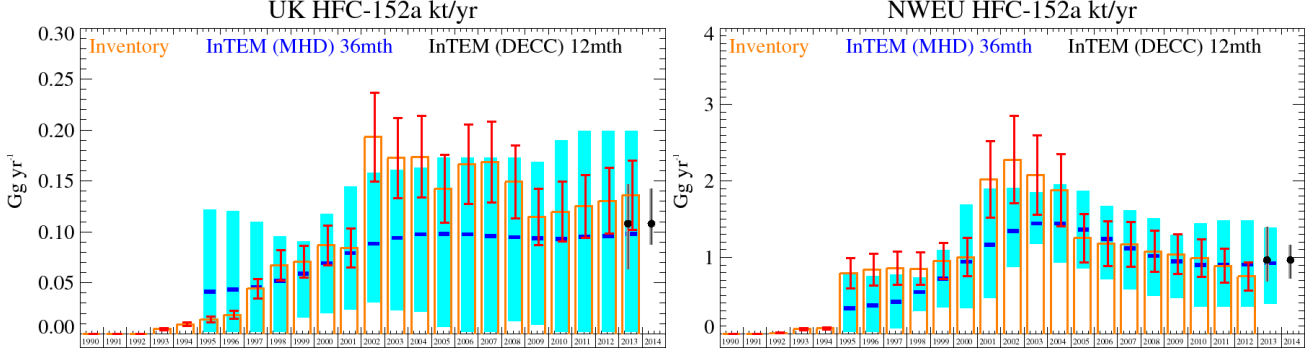


Figure 21: Emission estimates (Gg/yr) from the UNFCCC Inventory and InTEM (MHD-only and DECC network) for UK and NWEU. The uncertainty bars represent the 5th and 95th percentiles.

The NWEU emission estimates from both InTEM and the inventory match very well. The comparison for the UK is less well matched between 2002-2008, when the inventory exhibited a substantial increase in emissions compared to InTEM. The UK comparison either side of this time window is good.

Years	InTEM (MHD) 36mth	InTEM (DECC) 12mth	Inventory
1990			0.0 (0.0-0.0)
1991			0.0 (0.0-0.0)
1992			0.0 (0.0-0.0)
1993			0.005 (0.004-0.006)
1994			0.01 (0.01-0.01)
1995	0.04 (0.00-0.12)		0.01 (0.01-0.02)
1996	0.04 (0.00-0.12)		0.02 (0.01-0.02)
1997	0.05 (0.00-0.11)		0.04 (0.03-0.05)
1998	0.05 (0.00-0.10)		0.07 (0.05-0.08)
1999	0.06 (0.02-0.09)		0.07 (0.06-0.09)
2000	0.07 (0.02-0.12)		0.09 (0.07-0.11)
2001	0.08 (0.02-0.14)		0.08 (0.07-0.10)
2002	0.09 (0.03-0.16)		0.19 (0.15-0.24)
2003	0.09 (0.02-0.16)		0.17 (0.13-0.21)
2004	0.10 (0.02-0.16)		0.17 (0.13-0.21)
2005	0.10 (0.01-0.17)		0.14 (0.11-0.18)
2006	0.10 (0.00-0.17)		0.17 (0.13-0.21)
2007	0.10 (0.00-0.17)		0.17 (0.13-0.21)
2008	0.09 (0.01-0.17)		0.15 (0.11-0.18)
2009	0.09 (0.01-0.17)		0.11 (0.09-0.14)
2010	0.09 (0.00-0.19)		0.12 (0.09-0.15)
2011	0.09 (0.00-0.20)		0.13 (0.09-0.16)
2012	0.10 (0.00-0.20)		0.13 (0.10-0.16)
2013	0.10 (0.00-0.20)	0.11 (0.06-0.15)	0.14 (0.10-0.17)
2014		0.11 (0.09-0.14)	

Table 11: Emission (Gg/yr) estimates for the UK with uncertainty (5th - 95th percentile).

5.9 HFC-23

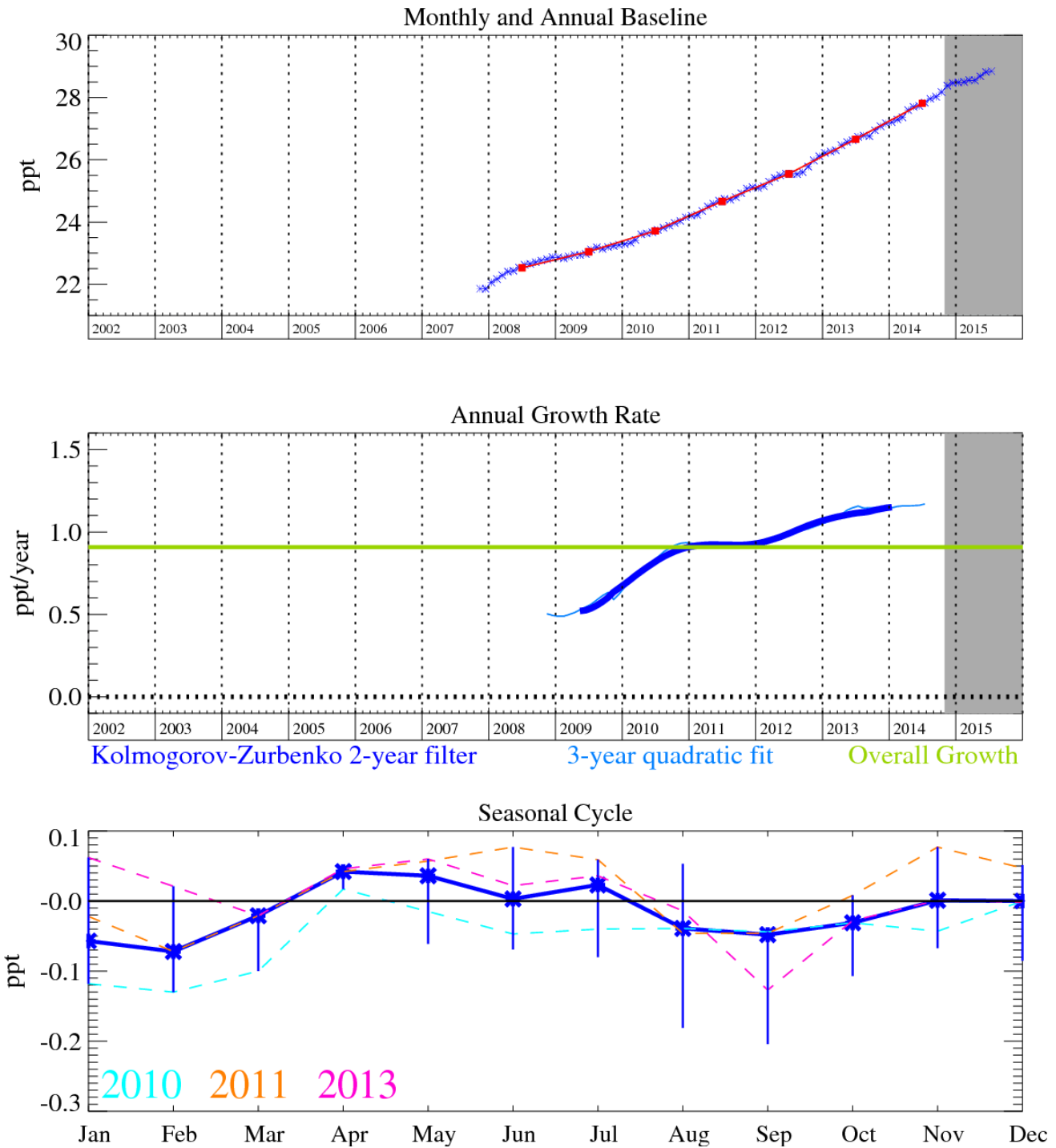


Figure 22: HFC-23 (CHF_3): Monthly (blue) and annual (red) baseline mole fractions. Annual (blue) and overall average growth rate (green) (lower plot). Grey area covers un-ratified and therefore provisional data.

HFC-23 (CHF_3): is primarily a by-product formed by the over fluorination of chloroform during the production of HCFC-22; other minor emissions arise from the electronic industry and fire extinguishers. For this reason it has grown at an average rate of 0.9 ppt/yr and by July 2015 the NH mole fraction was 28.8 ppt. It is the second most abundant HFC in the atmosphere after HFC-134a; this combined with a long atmospheric lifetime of 228 years makes this compound a potent GHG. Emissions of HFC-23 in developed countries have declined due to the Montreal Protocol phase-out schedule for HCFC-22, however, emissions from developing countries continue to drive global mixing ratios up.

The statistical fit between the model time-series and the observations is not strong and this is reflected in the significant uncertainty bars for the InTEM emission estimates. Although the InTEM estimates on average are higher than the inventory estimates, the uncertainty ranges entirely overlap for the UK. The baseline uncertainty is of a similar magnitude to the pollution events and so the emission estimates are very uncertain. The use of the Mace Head baseline at Tacobness is a particular concern for this gas because of this issue, hence the even larger uncertainty when the DECC network observations are included.

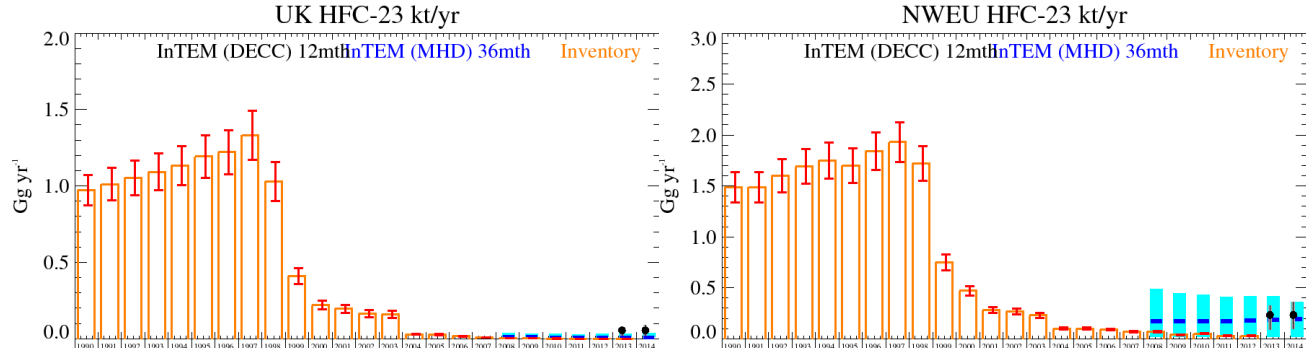


Figure 23: Emission estimates (Gg/yr) from the UNFCCC Inventory and InTEM (MHD-only and DECC network) for UK and NWEU. The uncertainty bars represent the 5th and 95th percentiles.

Years	InTEM (MHD) 36mth	InTEM (DECC) 12mth	Inventory
1990			0.97 (0.88-1.07)
1991			1.01 (0.91-1.12)
1992			1.05 (0.94-1.16)
1993			1.09 (0.97-1.21)
1994			1.13 (1.01-1.26)
1995			1.19 (1.06-1.33)
1996			1.22 (1.08-1.37)
1997			1.33 (1.17-1.49)
1998			1.03 (0.90-1.16)
1999			0.41 (0.36-0.46)
2000			0.22 (0.19-0.25)
2001			0.20 (0.17-0.22)
2002			0.17 (0.14-0.19)
2003			0.16 (0.14-0.18)
2004			0.03 (0.03-0.03)
2005			0.03 (0.02-0.03)
2006			0.02 (0.01-0.02)
2007			0.008 (0.007-0.010)
2008	0.01 (0.00-0.04)		0.005 (0.004-0.005)
2009	0.01 (0.00-0.03)		0.004 (0.003-0.004)
2010	0.01 (0.00-0.03)		0.001 (0.001-0.001)
2011	0.01 (0.00-0.03)		0.001 (0.001-0.001)
2012	0.01 (0.00-0.03)		0.001 (0.001-0.001)
2013	0.01 (0.00-0.03)	0.05 (0.02-0.08)	0.001 (0.001-0.001)
2014	0.01 (0.00-0.04)	0.05 (0.02-0.09)	

Table 12: Emission (Gg/yr) estimates for the UK with uncertainty (5th - 95th percentile).

5.10 HFC-32

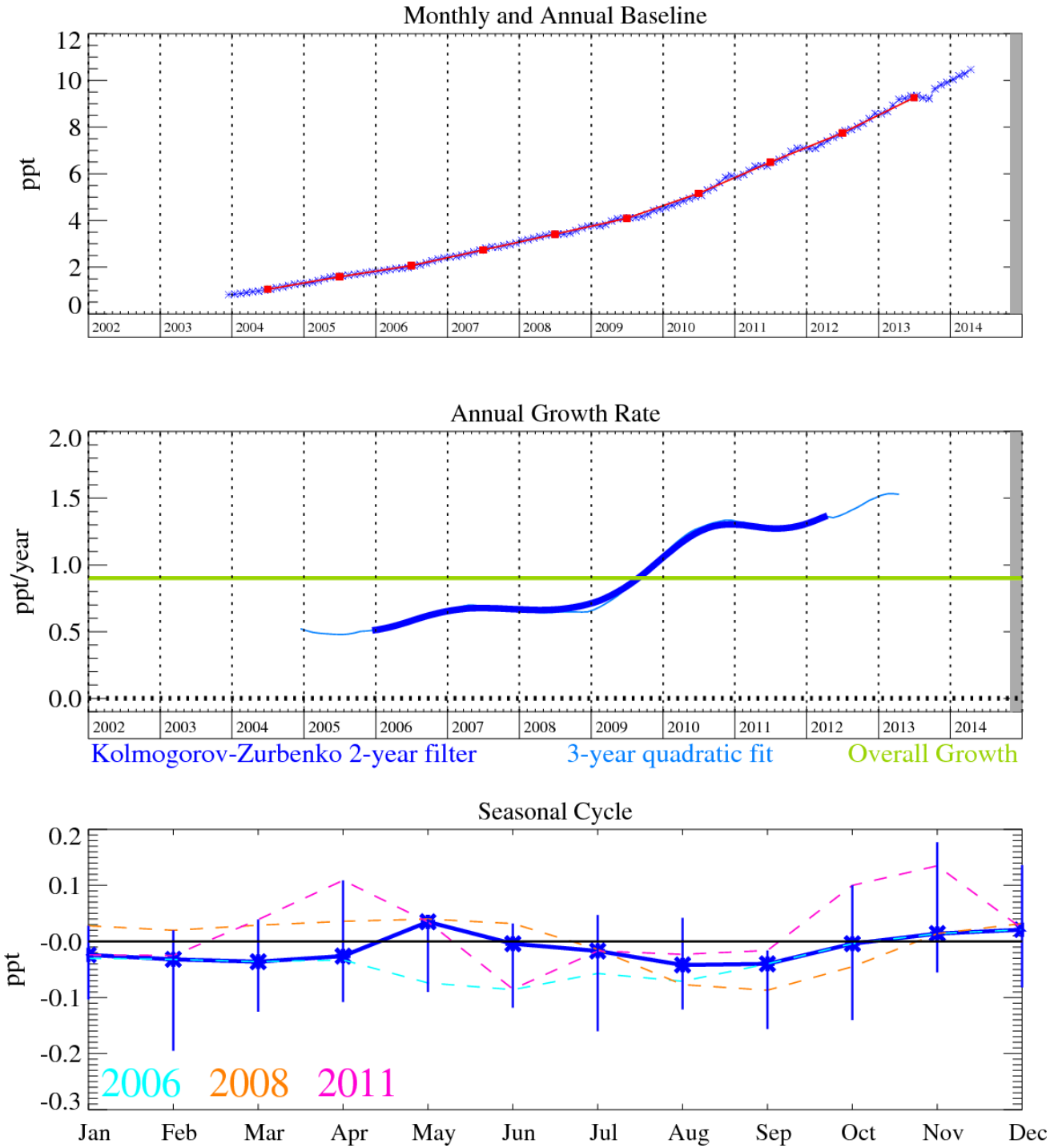


Figure 24: HFC-32 (CH_2F_2): Monthly (blue) and annual (red) baseline mole fractions (top plot). Annual (blue) and overall average growth rate (green) (middle plot). Seasonal cycle (de-trended) with year-to-year variability (lower plot). Grey area covers un-ratified and therefore provisional data.

HFC-32 (CH_2F_2): has an atmospheric lifetime of 5.4 years and a GWP_{100} of 716. It is used in air conditioning and refrigeration applications; R-410A (50% HFC-32, 50% HFC-125 by weight) and R-407C (23% HFC-32, 52% HFC-134a, 25% HFC-125 by weight) are used as replacements to HCFC-22. As the phase-out of HCFC-22 gains momentum it might be expected that demand for these refrigerant blends will increase. The pollution events measured at Mace Head are highly correlated with that of HFC-125.

Unfortunately at Mace Head the observations of HFC-32 (and HFC-125) have been compromised by contamination (since May 2014) and have been removed. This matter has been investigated and

is linked to the air conditioner leakage at the station. A temporary solution has been adopted, to flush the air sample module with clean ambient air to minimise contamination from laboratory air. A longer term solution will require modification of the contaminating air conditioner to use a chilled water heat exchanger with the contaminating refrigerant gases contained in an unit external to the laboratory. The baseline will be estimated using another Northern Hemisphere station such as Zeppelin (Ny Alesund) until the situation at Mace Head is resolved.

The UK emission estimates from the inventory and InTEM are both growing but the inventory is growing faster than the InTEM estimates. The NWEU estimates from InTEM are very similar to the inventory estimates. This might indicate that inventory estimates for such a gas by NWEU countries as a collective are better than the UK's in isolation, however, analysis of emissions from individual countries may be no better than for the UK.

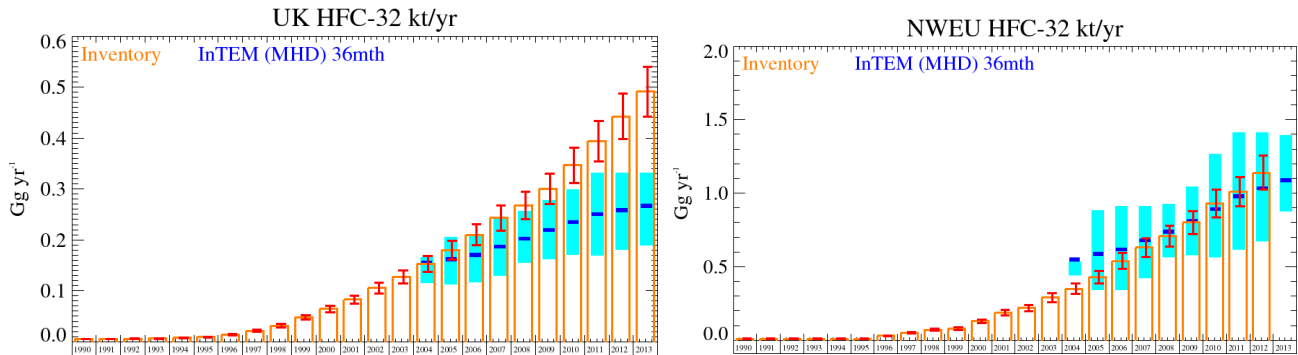


Figure 25: Emission estimates (Gg/yr) from the UNFCCC Inventory and InTEM (MHD-only) for UK and NWEU. The uncertainty bars represent the 5th and 95th percentiles.

Years	InTEM (MHD) 36mth	Inventory
1990		0.005 (0.005-0.006)
1991		0.005 (0.005-0.006)
1992		0.006 (0.005-0.006)
1993		0.006 (0.006-0.007)
1994		0.008 (0.007-0.008)
1995		0.01 (0.01-0.01)
1996		0.01 (0.01-0.01)
1997		0.02 (0.02-0.02)
1998		0.03 (0.03-0.03)
1999		0.05 (0.04-0.05)
2000		0.06 (0.06-0.07)
2001		0.08 (0.07-0.09)
2002		0.11 (0.10-0.12)
2003		0.13 (0.11-0.14)
2004	0.15 (0.11-0.17)	0.15 (0.14-0.17)
2005	0.16 (0.11-0.21)	0.18 (0.16-0.20)
2006	0.17 (0.12-0.21)	0.21 (0.19-0.23)
2007	0.19 (0.13-0.24)	0.24 (0.22-0.27)
2008	0.20 (0.16-0.26)	0.27 (0.24-0.30)
2009	0.22 (0.16-0.28)	0.30 (0.27-0.33)
2010	0.24 (0.17-0.30)	0.35 (0.31-0.38)
2011	0.25 (0.17-0.33)	0.39 (0.35-0.43)
2012	0.26 (0.18-0.33)	0.44 (0.40-0.49)
2013	0.27 (0.19-0.33)	0.49 (0.44-0.54)

Table 13: Emission (Gg/yr) estimates for the UK with uncertainty (5th - 95th percentile).

5.11 HFC-227ea

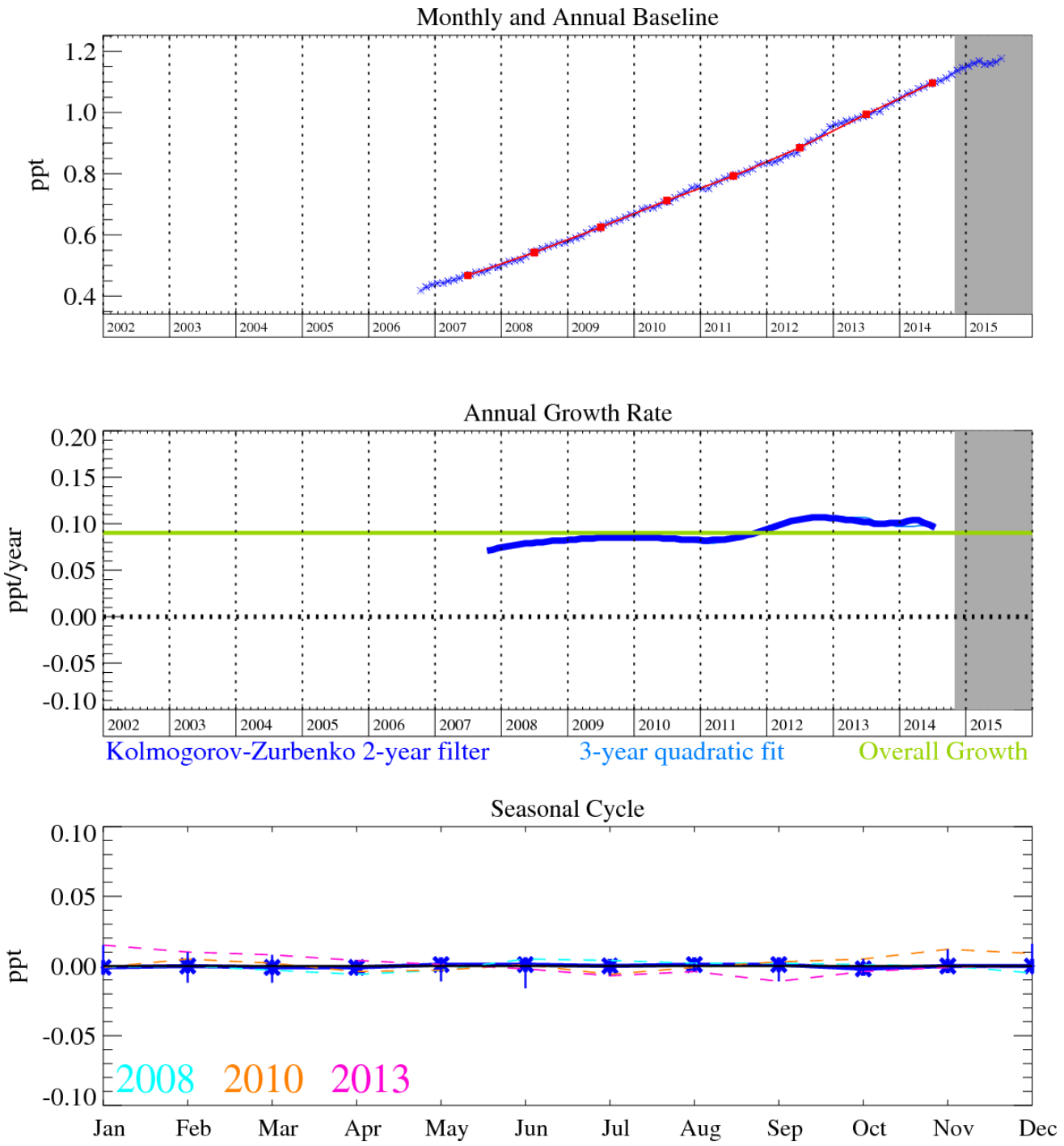


Figure 26: HFC-227ea (C_3HF_7): Monthly (blue) and annual (red) baseline mole fractions (top plot). Annual (blue) and overall average growth rate (green) (middle plot). Seasonal cycle (de-trended) with year-to-year variability (lower plot). Grey area covers un-ratified and therefore provisional data.

HFC-227ea (C_3HF_7): was added to the Medusa analysis in October 2006. HFC-227ea is used as a propellant for medical aerosols and a fire-fighting agent and to a lesser extent in metered-dose inhalers, and foam blowing (atmospheric lifetime 35.8 years and GWP₁₀₀ of 3580). The NH mole fraction was 1.2 ppt in July 2015 with a growth rate of 0.1 ppt/yr.

The InTEM results are significantly lower (50%) than the inventory estimates. The reason for this difference is unknown. The results, when the new observations from Taconheston are incorporated, are similar to the Mace Head only InTEM results. The statistical match between the model time-series and the observations is reasonable.

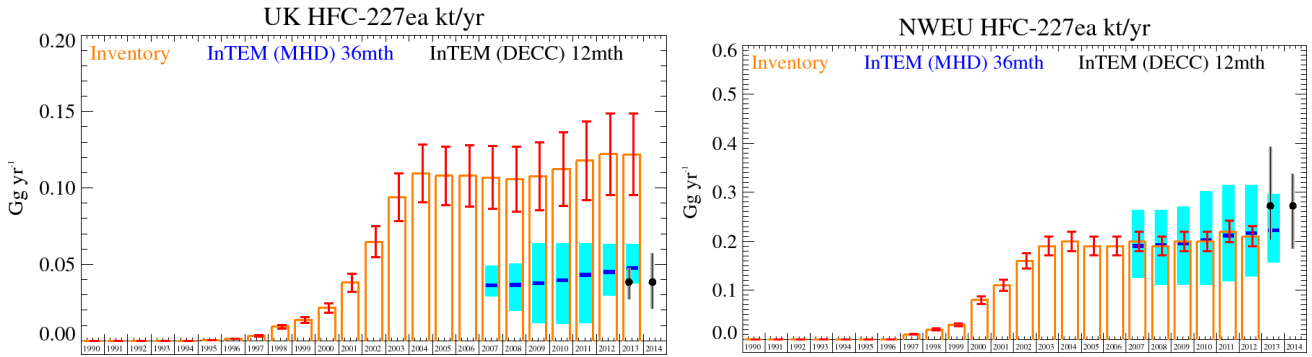


Figure 27: Emission estimates (Gg/yr) from the UNFCCC Inventory and InTEM (MHD-only and DECC network) for UK and NWEU. The uncertainty bars represent the 5th and 95th percentiles.

Years	InTEM (MHD) 36mth	InTEM (DECC) 12mth	Inventory
1990			0.0 (0.0-0.0)
1991			0.0 (0.0-0.0)
1992			0.0 (0.0-0.0)
1993			0.0 (0.0-0.0)
1994			0.0 (0.0-0.0)
1995			0.0003 (0.0003-0.0004)
1996			0.001 (0.001-0.001)
1997			0.003 (0.003-0.004)
1998			0.01 (0.01-0.01)
1999			0.01 (0.01-0.02)
2000			0.02 (0.02-0.02)
2001			0.04 (0.03-0.04)
2002			0.06 (0.05-0.08)
2003			0.09 (0.08-0.11)
2004			0.11 (0.09-0.13)
2005			0.11 (0.09-0.13)
2006			0.11 (0.09-0.13)
2007	0.04 (0.03-0.05)		0.11 (0.09-0.13)
2008	0.04 (0.02-0.05)		0.11 (0.08-0.13)
2009	0.04 (0.01-0.06)		0.11 (0.09-0.13)
2010	0.04 (0.01-0.06)		0.11 (0.09-0.14)
2011	0.04 (0.01-0.06)		0.12 (0.09-0.14)
2012	0.05 (0.03-0.06)		0.12 (0.10-0.15)
2013	0.05 (0.04-0.06)	0.04 (0.03-0.05)	0.12 (0.10-0.15)
2014		0.04 (0.02-0.06)	

Table 14: Emission (Gg/yr) estimates for the UK with uncertainty (5th - 95th percentile).

5.12 HFC-43-10mee

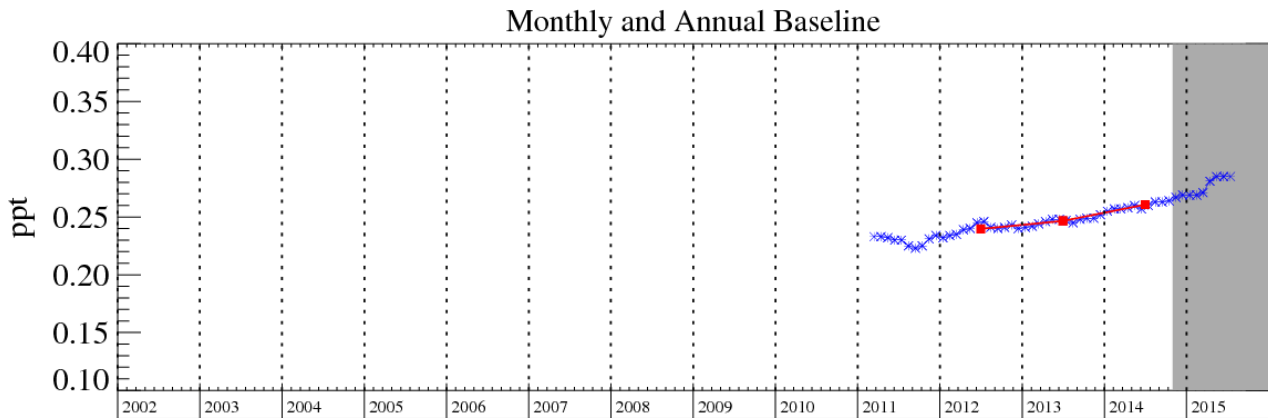


Figure 28: HFC-43-10mee ($\text{C}_5\text{H}_2\text{F}_{10}$): Monthly (blue) and annual (red) baseline mole fractions.

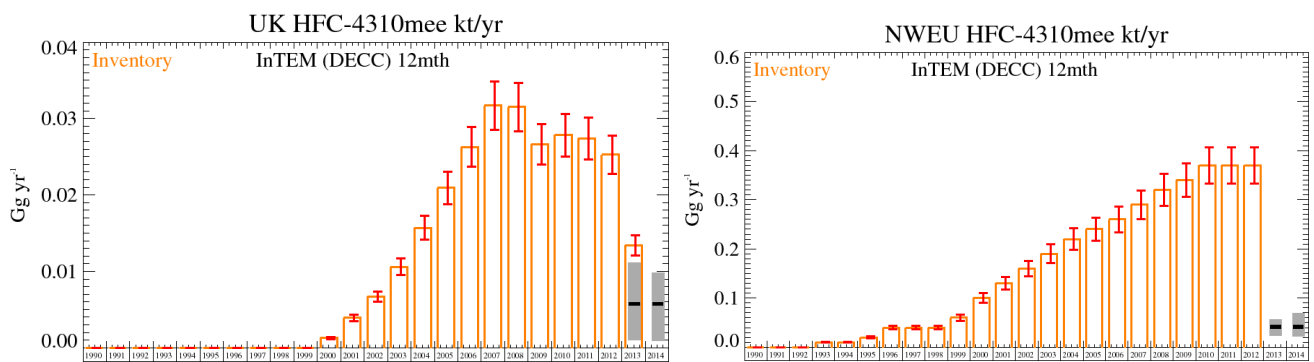


Figure 29: Emission estimates (Gg/yr) from the UNFCCC Inventory and InTEM (DECC network) for UK and NWEU. The uncertainty bars represent the 5th and 95th percentiles.

Years	InTEM (DECC) 12mth	Inventory
1990		0.0 (0.0-0.0)
1991		0.0 (0.0-0.0)
1992		0.0 (0.0-0.0)
1993		0.0 (0.0-0.0)
1994		0.0 (0.0-0.0)
1995		0.0 (0.0-0.0)
1996		0.0 (0.0-0.0)
1997		0.0 (0.0-0.0)
1998		0.0 (0.0-0.0)
1999		0.0 (0.0-0.0)
2000		0.001 (0.001-0.001)
2001		0.004 (0.004-0.004)
2002		0.007 (0.006-0.007)
2003		0.01 (0.01-0.01)
2004		0.02 (0.01-0.02)
2005		0.02 (0.02-0.02)
2006		0.03 (0.02-0.03)
2007		0.03 (0.03-0.03)
2008		0.03 (0.03-0.03)
2009		0.03 (0.02-0.03)
2010		0.03 (0.03-0.03)
2011		0.03 (0.02-0.03)
2012		0.03 (0.02-0.03)
2013	0.01 (0.00-0.01)	0.01 (0.01-0.01)
2014	0.006 (0.001-0.010)	

Table 15: Emission (Gg/yr) estimates for the UK with uncertainty (5th - 95th percentile).

HFC-43-10mee ($C_5H_2F_{10}$): Introduced in the mid-1990s as a replacement for CFC-113. It meets many requirements in the electronics industries and replaces PFCs in some uses such as a carrier fluid for lubricants applied to computer hard disks. It has an atmospheric lifetime of 16.1 years, a GWP₁₀₀ of 1,650 and a radiative efficiency of $0.42 \text{ W m}^{-2} \text{ ppb}^{-1}$.

The NH growth rate for this gas is estimated to be around 0.01 ppt/yr. The first inversion results for HFC-43-10mee show that there is some disagreement between the inventory and the InTEM results, although the emissions are relatively small.

5.13 HFC-365mfc

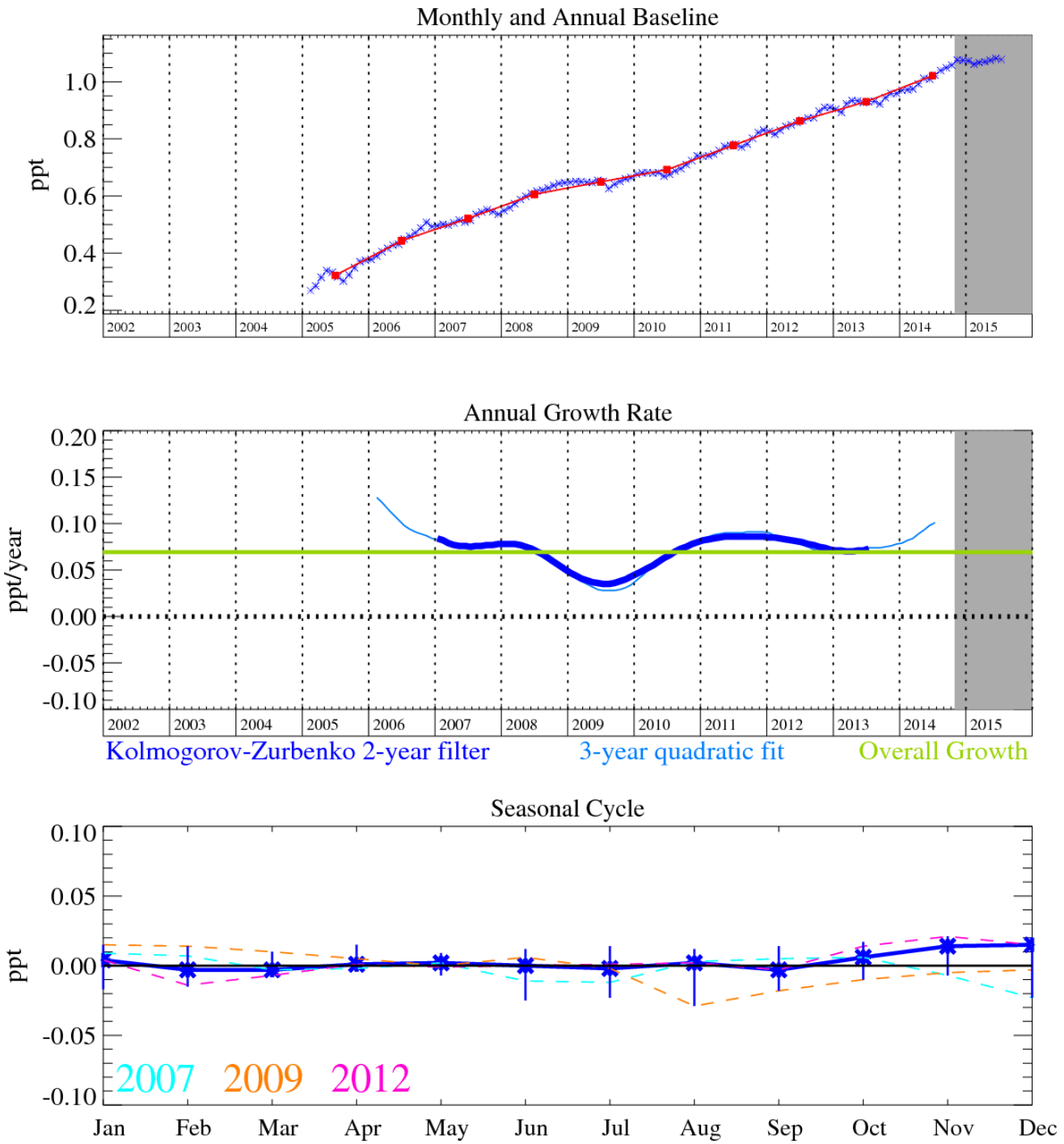


Figure 30: HFC-365mfc ($C_4H_5F_5$): Monthly (blue) and annual (red) baseline (top plot). Annual (blue) and overall average growth rate (green) (middle plot). Seasonal cycle (de-trended) with year-to-year variability (lower plot). Grey area covers un-rated and therefore provisional data.

HFC-365mfc ($C_4H_5F_5$) is used mainly for polyurethane structural foam blowing as a replacement for HCFC-141b, and to a minor extent as a blend component for solvents. It has an atmospheric lifetime of 8.6 years and a GWP estimated at 790-997 (100-year time horizon). It is currently growing in the atmosphere at a rate of 0.08 ppt/yr and in the NH in July 2015 reached a mole fraction of 1.08 ppt.

The statistical match between the modelled and observed time-series is good. The emissions in the UK decreased significantly between 2005-2009 and then remained static, whereas those in NWEU have slowly grown over the last few years.

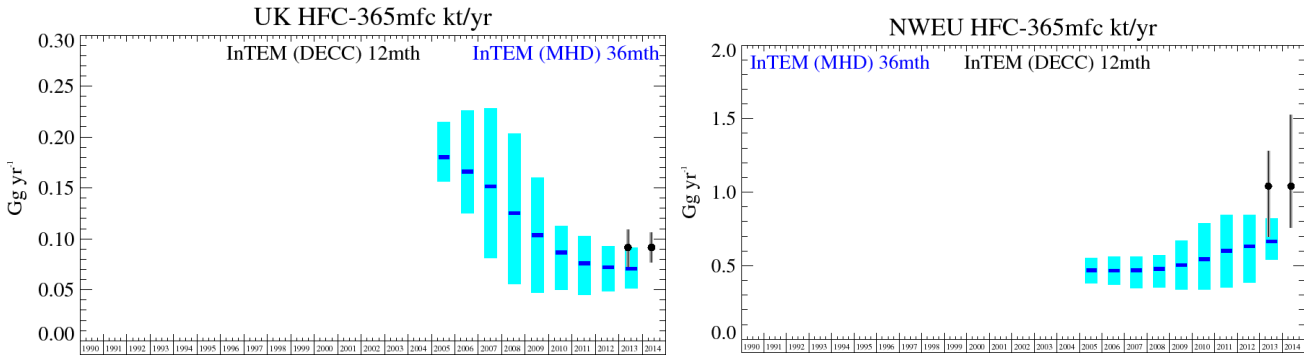


Figure 31: Emission estimates (Gg/yr) from InTEM (MHD-only and DECC network) for UK and NWEU. The uncertainty bars represent the 5th and 95th percentiles. Inventory estimates have not been made for HFC-365 alone.

Years	InTEM (MHD) 36mth	InTEM (DECC) 12mth
2005	0.18 (0.16-0.21)	
2006	0.17 (0.12-0.23)	
2007	0.15 (0.08-0.23)	
2008	0.13 (0.06-0.20)	
2009	0.10 (0.05-0.16)	
2010	0.09 (0.05-0.11)	
2011	0.08 (0.04-0.10)	
2012	0.07 (0.05-0.09)	
2013	0.07 (0.05-0.09)	0.09 (0.07-0.11)
2014		0.09 (0.08-0.11)

Table 16: Emission (Gg/yr) estimates for the UK with uncertainty (5th - 95th percentile).

5.14 PFC-14 (CF_4)

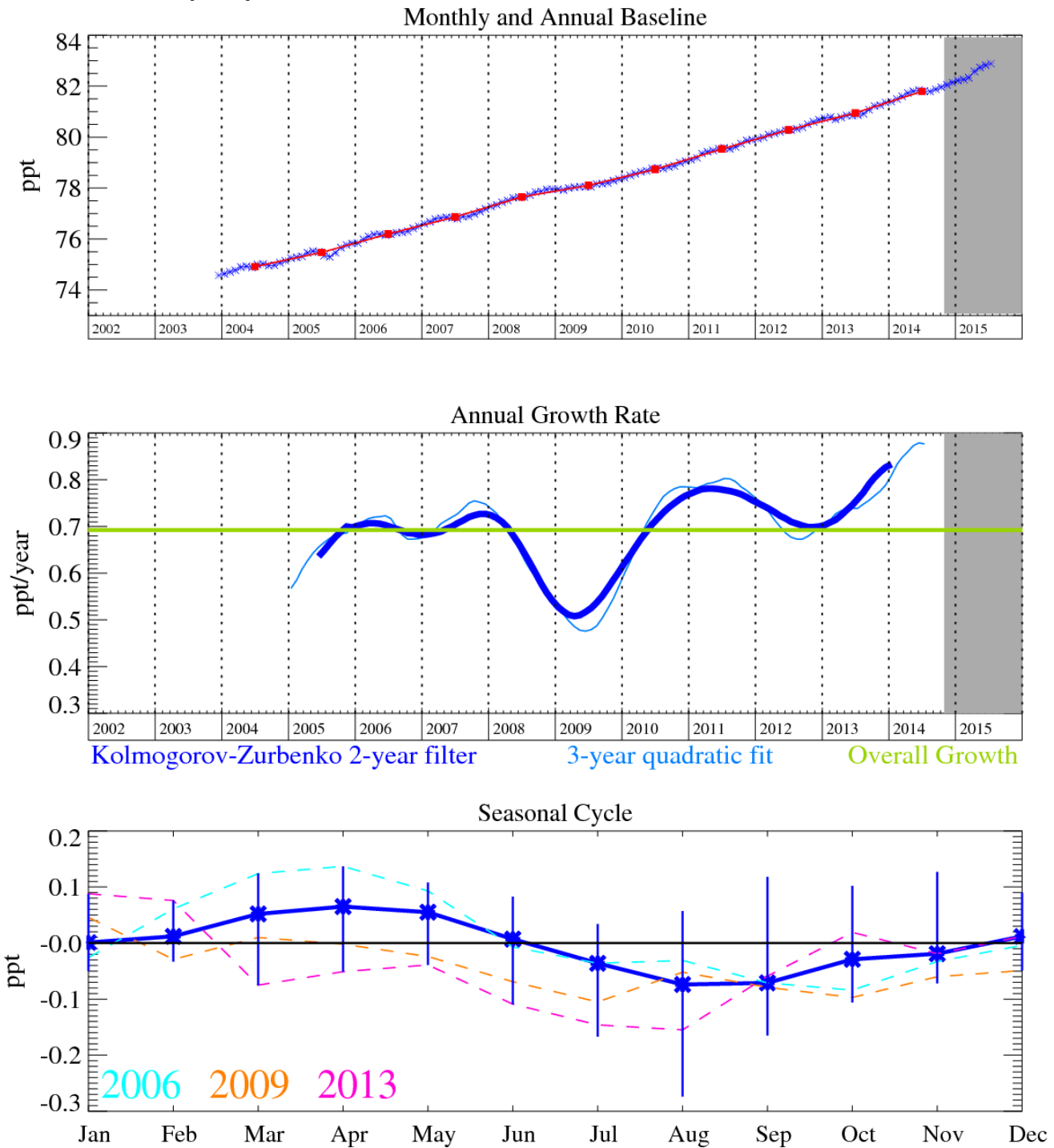


Figure 32: PFC-14 (CF_4): Monthly (blue) and annual (red) baseline mole fractions (top plot). Annual (blue) and overall average growth rate (green) (middle plot). Seasonal cycle (de-trended) with year-to-year variability (lower plot). Grey area covers un-ratified and therefore provisional data.

PFC-14 (CF_4) possesses the longest known lifetime of anthropogenic molecules (>50,000 yrs), which, when coupled with its high absolute radiative forcing ($0.08 \text{ W m}^{-2} \text{ ppb}^{-1}$) gives rise to a high GWP₁₀₀ of 5,820 and can equate to upwards of 1% of total radiative forcing. Its primary emission source is as an unwanted by-product of aluminium smelting during a fault condition known as the Anode Effect. Thus the frequency of occurrence and duration of an anode effect event will determine the regional and global CF_4 emission. CF_4 has some additional minor applications in the semiconductor industry (as a source of F radicals), but industry has shied away from using CF_4 knowing that its GWP is so high. The aluminium industry has recognised the CF_4 (and C_2F_6) emission problem and has been undergoing processes of replacement of older, less efficient aluminium production cells with more efficient designs, and automated and quicker intervention

policies to prevent the occurrence of these anode effects. It is also thought that CF_4 has a natural source from crustal degassing.

The current growth rate of atmospheric CF_4 in the NH is 0.8 ppt/yr. This compound will continue to accumulate in the atmosphere due to its very long atmospheric lifetime. In July 2015 the mole fraction of CF_4 was close to 83 ppt.

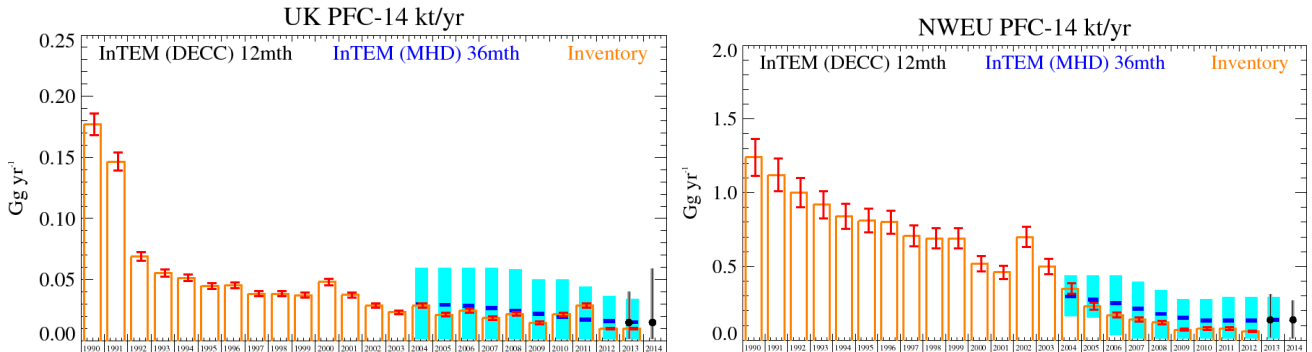


Figure 33: Emission estimates (Gg/yr) from the UNFCCC Inventory and InTEM (MHD-only and DECC network) for UK and NWEU. The uncertainty bars represent the 5th and 95th percentiles.

The significant uncertainties in the InTEM results entirely overlap with the inventory estimates although the median results are consistently higher. In the standard InTEM inversion, the statistical match between the model time-series and the observations is weak. This is because the emissions are principally from point sources (aluminium smelters). If the locations of the smelters are included and solved for as single grid cells (25 km) then the agreement between model and observation is much improved. The largest smelter in the UK, at Lynemouth on the north east coast of England ceased operations in March 2012. This is very clearly seen in the modelled emissions when the smelter locations are included as prior information – please refer to the Annual report 2014.

Years	InTEM (MHD) 36mth	InTEM (DECC) 12mth	Inventory
1990			0.18 (0.17-0.19)
1991			0.15 (0.14-0.15)
1992			0.07 (0.07-0.07)
1993			0.06 (0.05-0.06)
1994			0.05 (0.05-0.05)
1995			0.04 (0.04-0.05)
1996			0.05 (0.04-0.05)
1997			0.04 (0.04-0.04)
1998			0.04 (0.04-0.04)
1999			0.04 (0.04-0.04)
2000			0.05 (0.05-0.05)
2001			0.04 (0.04-0.04)
2002			0.03 (0.03-0.03)
2003			0.02 (0.02-0.02)
2004	0.03 (0.00-0.06)		0.03 (0.03-0.03)
2005	0.03 (0.00-0.06)		0.02 (0.02-0.02)
2006	0.03 (0.00-0.06)		0.02 (0.02-0.03)
2007	0.03 (0.00-0.06)		0.02 (0.02-0.02)
2008	0.02 (0.00-0.06)		0.02 (0.02-0.02)
2009	0.02 (0.00-0.05)		0.01 (0.01-0.02)
2010	0.02 (0.00-0.05)		0.02 (0.02-0.02)
2011	0.02 (0.00-0.04)		0.03 (0.03-0.03)
2012	0.02 (0.00-0.04)		0.01 (0.01-0.01)
2013	0.02 (0.00-0.03)	0.01 (0.00-0.04)	0.01 (0.01-0.01)
2014		0.01 (0.00-0.06)	

Table 17: Emission (Gg/yr) estimates for the UK with uncertainty (5th - 95th percentile).

5.15 PFC-116

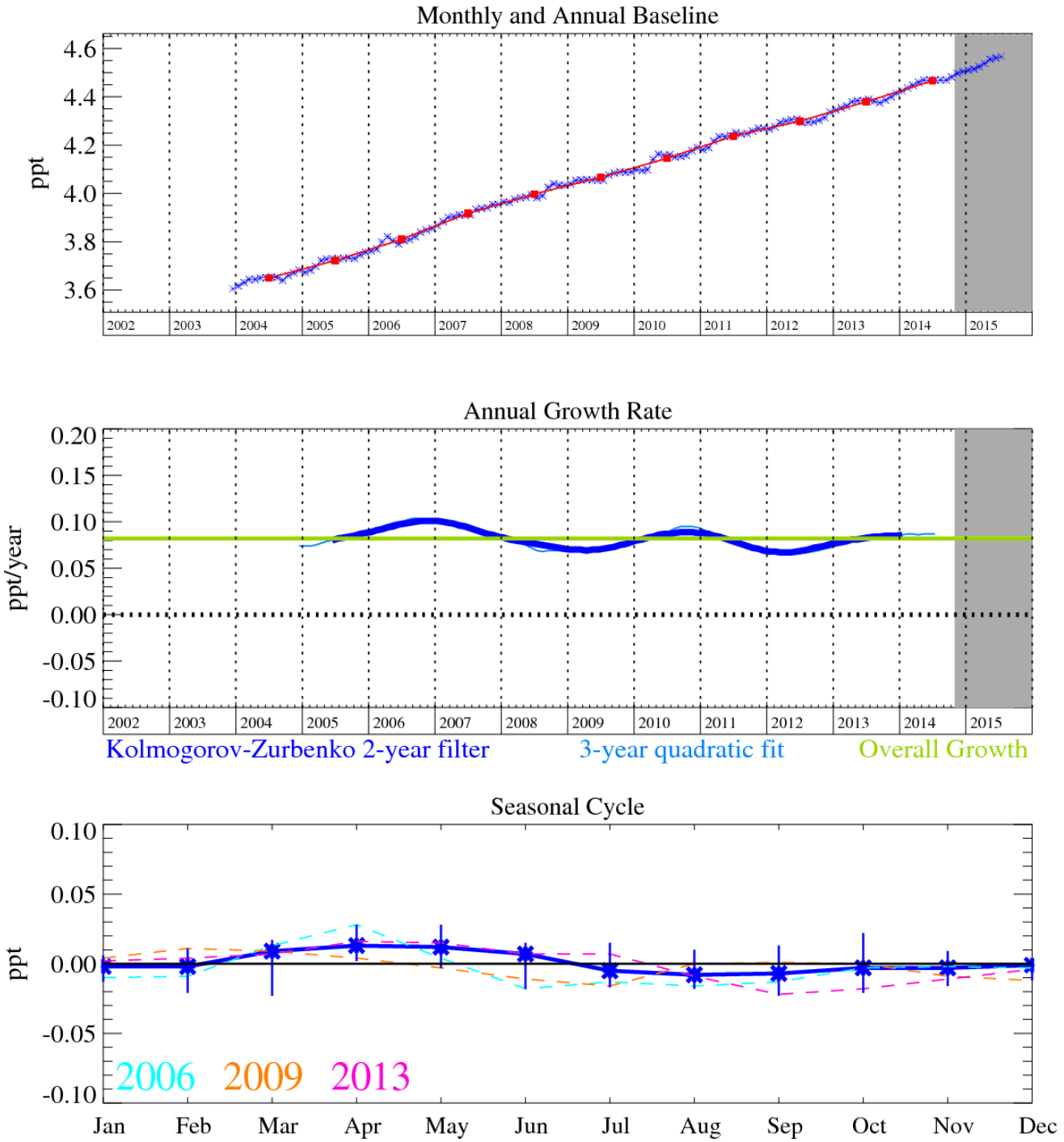


Figure 34: PFC-116 (C_2F_6): Monthly (blue) and annual (red) baseline mole fractions (top plot). Annual (blue) and overall average growth rate (green) (middle plot). Seasonal cycle (de-trended) with year-to-year variability (lower plot). Grey area covers un-ratified and therefore provisional data.

PFC-116 (C_2F_6) is also a potent greenhouse gas with an atmospheric lifetime of >10,000 years. It has common sources to CF_4 , and serves to help explain why most of the CF_4 above-baseline (pollution) events are correlated with those of C_2F_6 . However, we note that there are more frequent and greater magnitude emissions of C_2F_6 relative to CF_4 . This is due to the dominant source of C_2F_6 being from semiconductor industries (plasma etching).

The current growth rate of NH atmospheric C_2F_6 is 0.09 ppt/yr. In July 2015 the NH mole fraction of C_2F_6 was 4.57 ppt.

The InTEM uncertainty ranges for the regional emissions are large but consistently overlap the inventory estimates. The statistical match between the estimated model time-series and the observations is fair to weak.

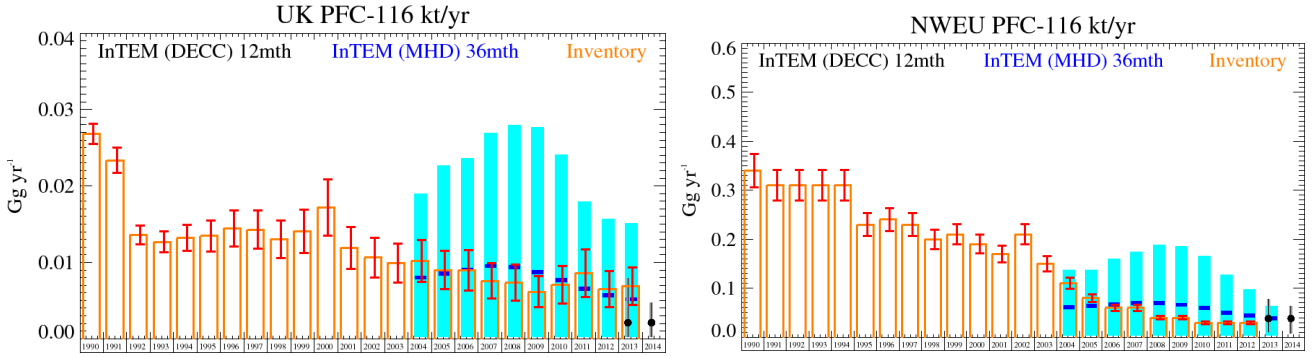


Figure 35: Emission estimates (Gg/yr) from the UNFCCC Inventory and InTEM (MHD-only and DECC network) for UK and NWEU. The uncertainty bars represent the 5th and 95th percentiles.

Years	InTEM (MHD) 36mth	InTEM (DECC) 12mth	Inventory
1990			0.03 (0.03-0.03)
1991			0.02 (0.02-0.02)
1992			0.01 (0.01-0.01)
1993			0.01 (0.01-0.01)
1994			0.01 (0.01-0.01)
1995			0.01 (0.01-0.02)
1996			0.01 (0.01-0.02)
1997			0.01 (0.01-0.02)
1998			0.01 (0.01-0.02)
1999			0.01 (0.01-0.02)
2000			0.02 (0.01-0.02)
2001			0.01 (0.01-0.01)
2002			0.01 (0.01-0.01)
2003			0.01 (0.01-0.01)
2004	0.01 (0.00-0.02)		0.01 (0.01-0.01)
2005	0.01 (0.00-0.02)		0.01 (0.01-0.01)
2006	0.01 (0.00-0.02)		0.01 (0.01-0.01)
2007	0.01 (0.00-0.03)		0.008 (0.005-0.010)
2008	0.01 (0.00-0.03)		0.007 (0.005-0.010)
2009	0.01 (0.00-0.03)		0.006 (0.004-0.008)
2010	0.01 (0.00-0.02)		0.007 (0.005-0.010)
2011	0.01 (0.00-0.02)		0.01 (0.01-0.01)
2012	0.01 (0.00-0.02)		0.007 (0.004-0.009)
2013	0.01 (0.00-0.02)	0.002 (0.000-0.008)	0.007 (0.004-0.009)
2014		0.002 (0.000-0.005)	

Table 18: Emission (Gg/yr) estimates for the UK with uncertainty (5th - 95th percentile).

5.16 PFC-218

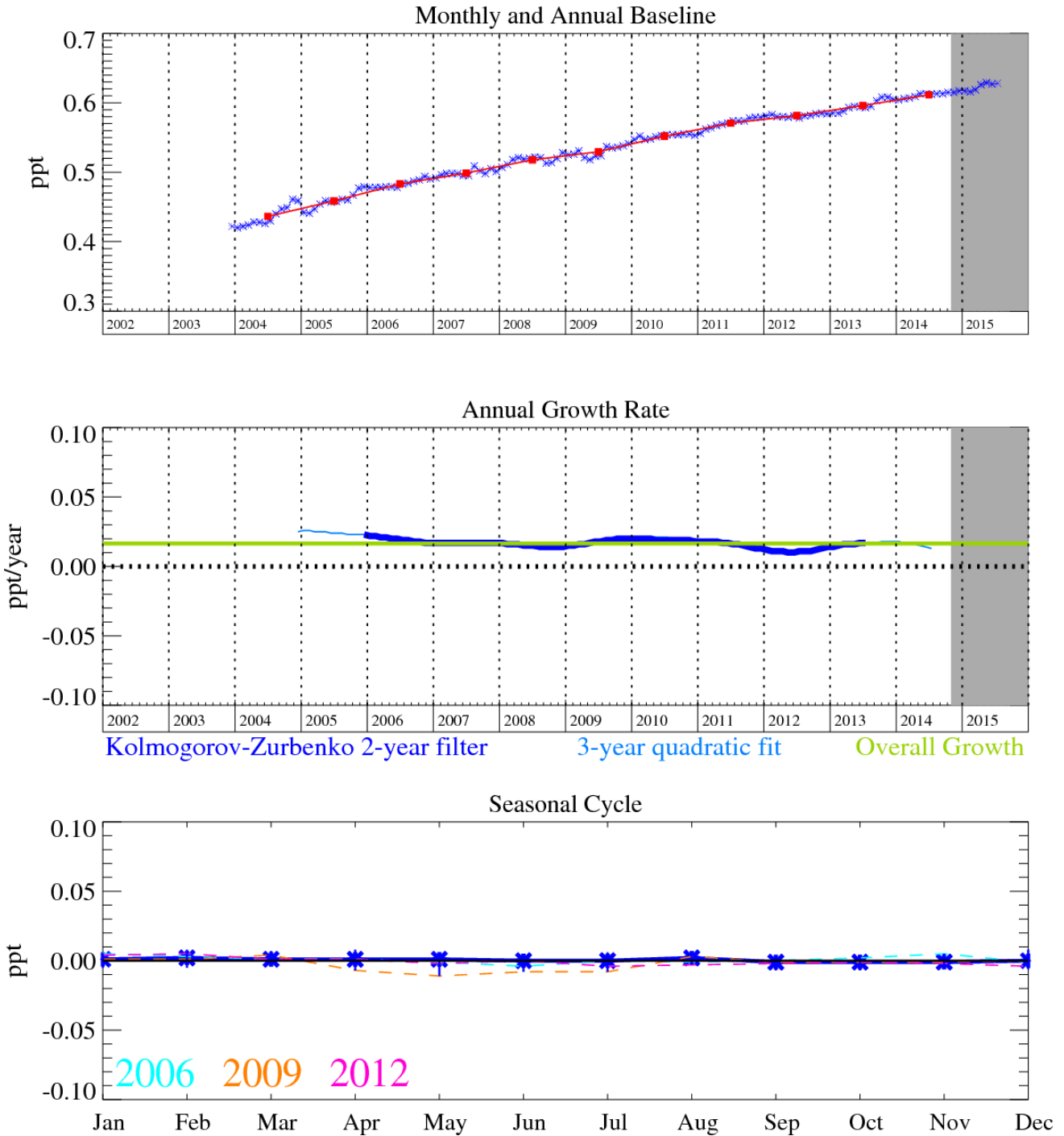


Figure 36: PFC-218 (C_3F_8): Monthly (blue) and annual (red) baseline mole fractions (top plot). Annual (blue) and overall average growth rate (green) (middle plot). Seasonal cycle (de-trended) with year-to-year variability (lower plot). Grey area covers un-ratified and therefore provisional data.

PFC-218 (C_3F_8) has an atmospheric lifetime of 2600 years and a GWP₁₀₀ of 8690. It is also used in semiconductor manufacturing, but to a lesser extent than C_2F_6 . It also has a very small contribution from aluminium smelting and has an increasing contribution from refrigeration use. Observations of above-baseline C_3F_8 emissions are less frequent than those of C_2F_6 but are of a higher relative magnitude.

The current growth rate of atmospheric C_3F_8 is very low at 0.02 ppt/yr. In July 2015 the NH mole fraction of C_3F_8 was 0.63 ppt.

There is a large uncertainty in the InTEM emission estimates because the pollution events are relatively difficult to model because the significant sources are probably specific point sources that

cannot be readily resolved by the large inversion grids used. Prior knowledge is required to pin-point the significant point sources in a similar analysis as conducted for PFC-14. Within the InTEM and inventory uncertainty the results are consistent.

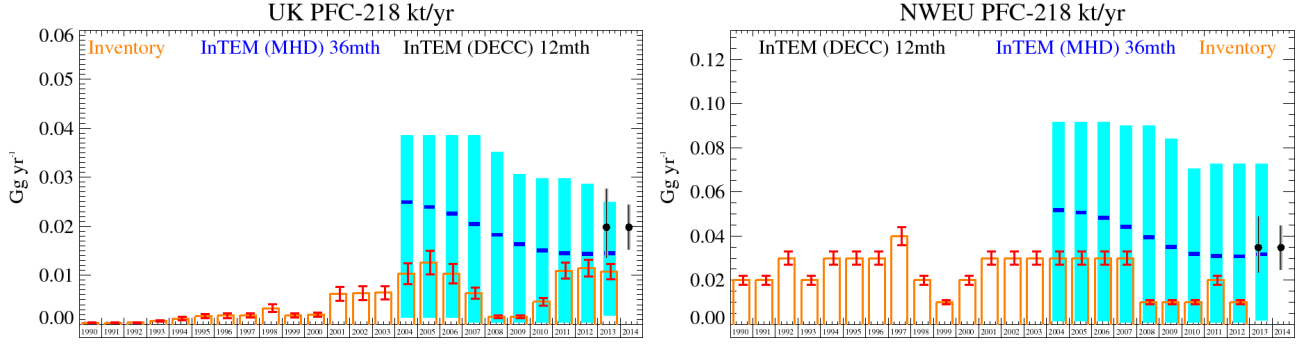


Figure 37: Emission estimates (Gg/yr) from the UNFCCC Inventory and InTEM (MHD-only and DECC network) for UK and NWEU. The uncertainty bars represent the 5th and 95th percentiles.

Years	InTEM (MHD) 36mth	InTEM (DECC) 12mth	Inventory
1990			0.0003 (0.0002-0.0004)
1991			0.0003 (0.0002-0.0004)
1992			0.0003 (0.0002-0.0004)
1993			0.0007 (0.0005-0.0009)
1994			0.001 (0.001-0.001)
1995			0.002 (0.001-0.002)
1996			0.002 (0.001-0.002)
1997			0.002 (0.001-0.002)
1998			0.003 (0.002-0.004)
1999			0.002 (0.001-0.002)
2000			0.002 (0.002-0.002)
2001			0.006 (0.005-0.008)
2002			0.006 (0.005-0.008)
2003			0.006 (0.005-0.008)
2004	0.02 (0.00-0.04)		0.01 (0.01-0.01)
2005	0.02 (0.00-0.04)		0.01 (0.01-0.02)
2006	0.02 (0.00-0.04)		0.01 (0.01-0.01)
2007	0.02 (0.00-0.04)		0.006 (0.005-0.008)
2008	0.02 (0.00-0.04)		0.002 (0.001-0.002)
2009	0.02 (0.00-0.03)		0.002 (0.001-0.002)
2010	0.02 (0.00-0.03)		0.005 (0.004-0.005)
2011	0.01 (0.00-0.03)		0.01 (0.01-0.01)
2012	0.01 (0.00-0.03)		0.01 (0.01-0.01)
2013	0.01 (0.00-0.02)	0.02 (0.01-0.03)	0.01 (0.01-0.01)
2014		0.02 (0.02-0.02)	

Table 19: Emission (Gg/yr) estimates for the UK with uncertainty (5th - 95th percentile).

5.17 PFC-318

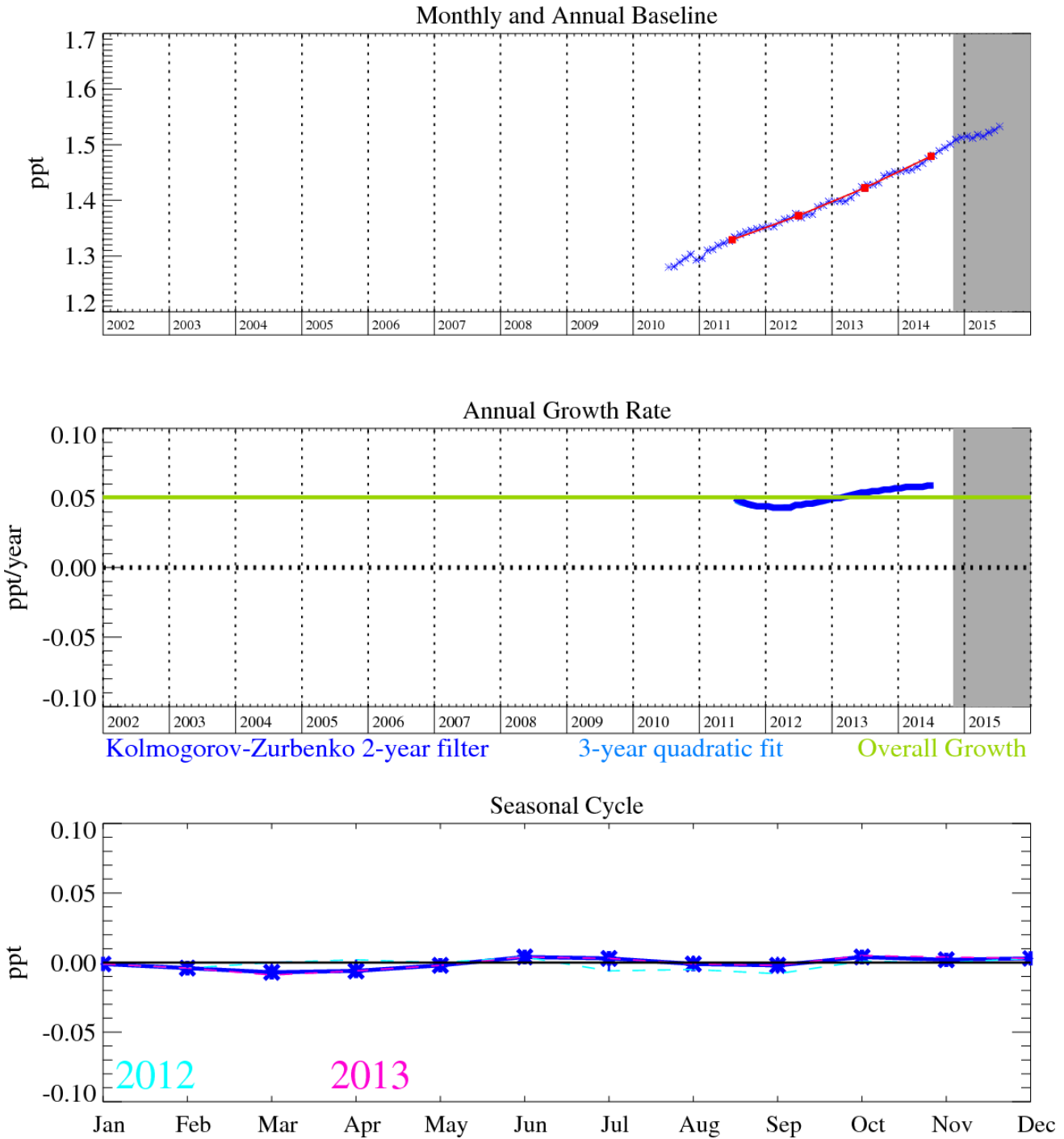


Figure 38: PFC-318 (c-C₄F₈): Monthly (blue) and annual (red) baseline mole fractions (top plot). Annual (blue) and overall average growth rate (green) (middle plot). Seasonal cycle (de-trended) with year-to-year variability (lower plot). Grey area covers un-ratified and therefore provisional data.

This gas is increasingly used in the semiconductor and electronics industries for cleaning, plasma etching and deposition gas, also it has more minor use in aerolyzed foods, retinal detachment surgery, size estimation of natural gas and oil reservoirs, specialist military applications, tracer experiments and may also replace SF₆ as an electrically insulating gas. It has an atmospheric lifetime of 3,200 years, a GWP₁₀₀ of 10,300 and a radiative efficiency of 0.32 W m⁻² ppb⁻¹.

The reported inventory emissions of PFC-318 are very small compared to the median InTEM emission estimates. However the InTEM estimates have significant uncertainty; it is likely that significant amounts of this gas are released intermittently thereby challenging one of the InTEM assumptions of uniform emissions in time in the inversion time-window.

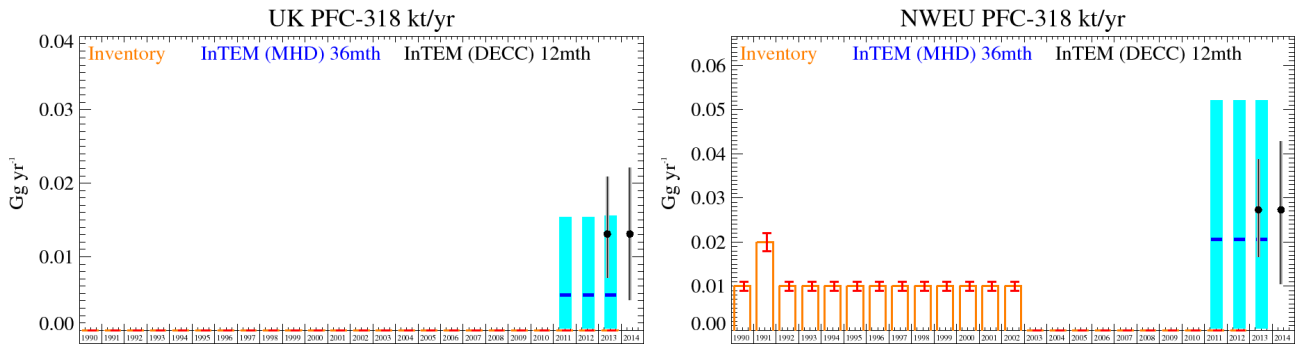


Figure 39: Emission estimates (Gg/yr) from the UNFCCC Inventory and InTEM (MHD-only and DECC network) for UK and NWEU. The uncertainty bars represent the 5th and 95th percentiles

Years	InTEM (MHD) 36mth	InTEM (DECC) 12mth	Inventory
1990			0.0000013 (0.0-0.0)
1991			0.0000014 (0.0-0.0)
1992			0.0000017 (0.0-0.0)
1993			0.0000019 (0.0-0.0)
1994			0.0000022 (0.0-0.0)
1995			0.0000025 (0.0-0.0)
1996			0.0000029 (0.0-0.0)
1997			0.0000033 (0.0-0.0)
1998			0.0000038 (0.0-0.0)
1999			0.0000044 (0.0-0.0)
2000			0.0000051 (0.0-0.0)
2001			0.0000032 (0.0-0.0)
2002			0.0000032 (0.0-0.0)
2003			0.0000032 (0.0-0.0)
2004			0.0000030 (0.0-0.0)
2005			0.0000030 (0.0-0.0)
2006			0.0000032 (0.0-0.0)
2007			0.0000033 (0.0-0.0)
2008			0.0000035 (0.0-0.0)
2009			0.0000036 (0.0-0.0)
2010			0.0000038 (0.0-0.0)
2011	0.00 (0.00-0.02)		0.0000038 (0.0-0.0)
2012	0.00 (0.00-0.02)		0.0000042 (0.0-0.0)
2013	0.00 (0.00-0.02)	0.01 (0.01-0.02)	0.0000045 (0.0-0.0)
2014		0.01 (0.00-0.02)	

Table 20: Emission (Gg/yr) estimates for the UK with uncertainty (5th - 95th percentile).

5.18 SF₆

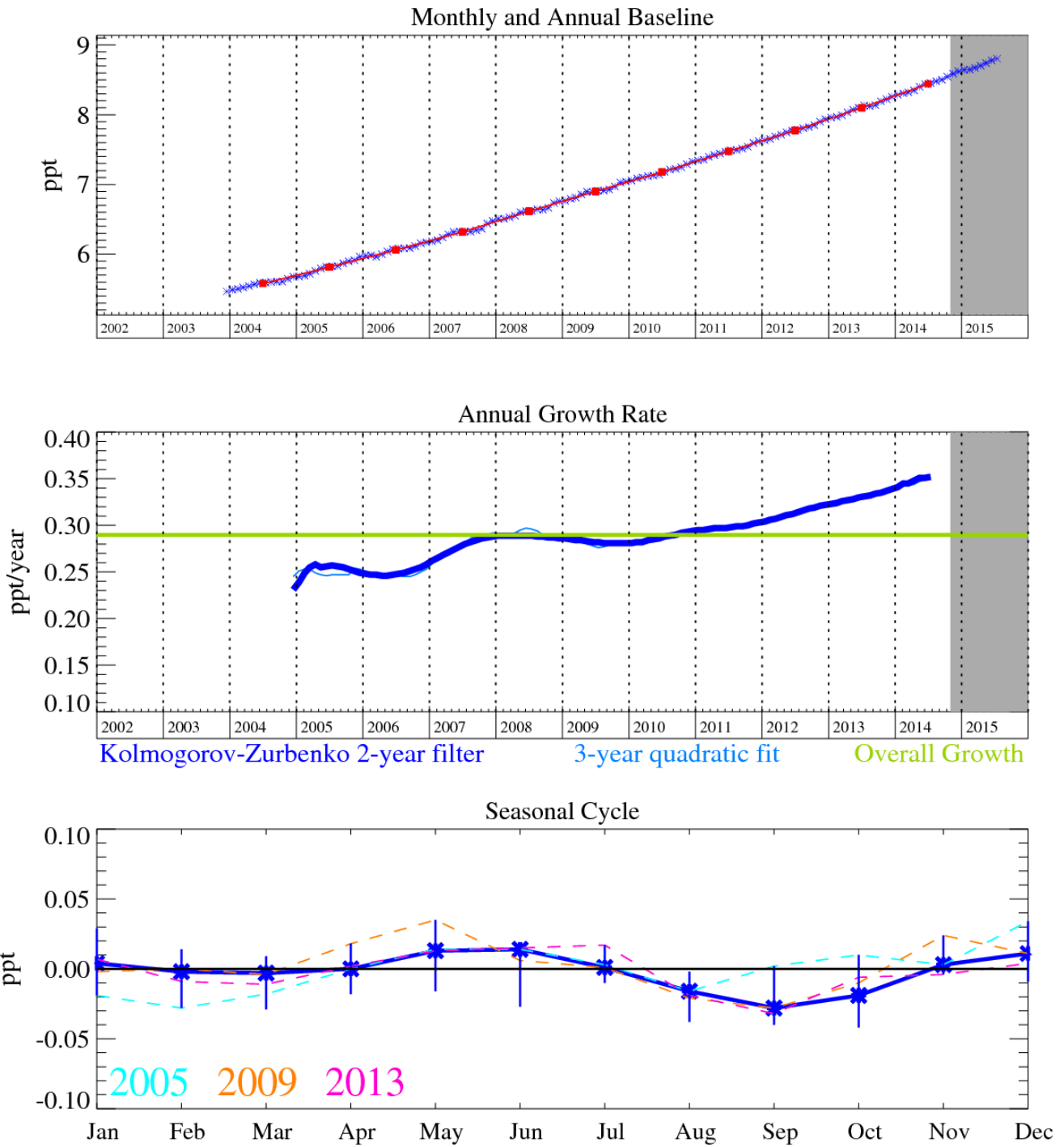


Figure 40: SF₆: Monthly (blue) and annual (red) baseline mole fractions (top plot). Annual (blue) and overall average growth rate (green) (middle plot). Seasonal cycle (de-trended) with year-to-year variability (lower plot). Grey area covers un-ratified and therefore provisional data.

SF₆ is an important greenhouse gas since it has a long atmospheric lifetime of 3,200 years and a high radiative efficiency; giving rise to a GWP₁₀₀ of 22,800. Its current growth rate is 0.35 ppt/yr and in July 2015 reached the NH mole fraction was 8.8 ppt. Although having minor usage in the semiconductor industry, it is predominantly used in electrical circuit breakers, heavy-duty gas-insulated switchgear (GIS) for systems with voltages from 5,000-38,000 volts, and other switchgear used in the electrical transmission systems to manage high voltages (>38 kV). The electrical power industry uses roughly 80% of all SF₆ produced worldwide. Although the units themselves are hermetically sealed and pressurised, aging equipment, breakdown and disposal, alongside leakage from wear-and-tear will cause this sector to emit SF₆. A minor use of this gas is also reported in its use as a blanketing (i.e. oxygen inhibiting inert gas) agent during magnesium production. Hence SF₆

will have many, and more diffuse, sources relative to the other perfluorinated species. Its atmospheric trend was predicted to rise at a rate faster than linear, as older electrical switchgear is switched to higher efficiency units; this is corroborated by the constantly increasing growth rate over the last several years

The UK InTEM estimates are consistently elevated compared to the inventory, however, the InTEM uncertainty ranges do encompass the inventory estimates. The NWEU InTEM estimates are higher than the inventory until 2010 after which the agreement is good. The statistical match between the model time-series and the observations is reasonable.

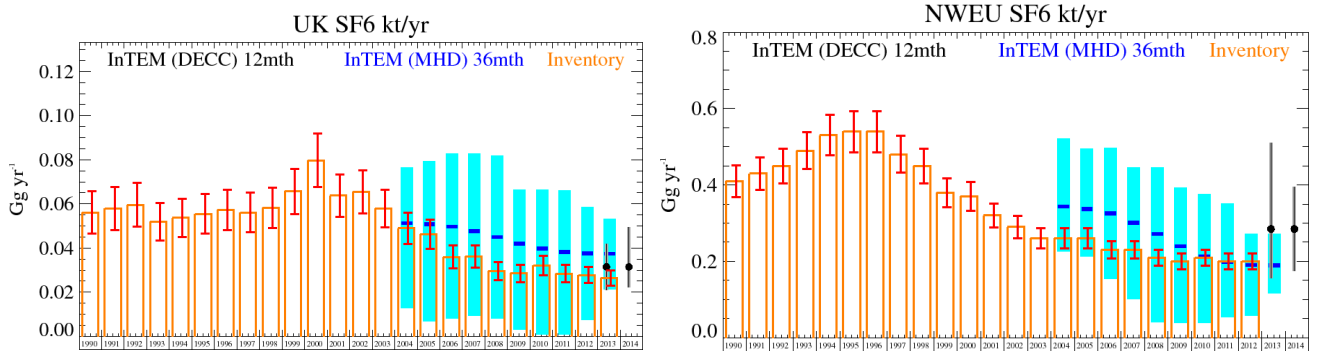


Figure 41: Emission estimates (Gg/yr) from the UNFCCC Inventory and InTEM (MHD-only and DECC network) for UK and NWEU. The uncertainty bars represent the 5th and 95th percentiles.

Years	InTEM (MHD) 36mth	InTEM (DECC) 12mth	Inventory
1990			0.06 (0.05-0.07)
1991			0.06 (0.05-0.07)
1992			0.06 (0.05-0.07)
1993			0.05 (0.04-0.06)
1994			0.05 (0.04-0.06)
1995			0.06 (0.05-0.06)
1996			0.06 (0.05-0.07)
1997			0.06 (0.05-0.07)
1998			0.06 (0.05-0.07)
1999			0.07 (0.06-0.08)
2000			0.08 (0.07-0.09)
2001			0.06 (0.05-0.07)
2002			0.07 (0.06-0.08)
2003			0.06 (0.05-0.07)
2004	0.05 (0.01-0.08)		0.05 (0.04-0.06)
2005	0.05 (0.01-0.08)		0.05 (0.04-0.05)
2006	0.05 (0.01-0.08)		0.04 (0.03-0.04)
2007	0.05 (0.01-0.08)		0.04 (0.03-0.04)
2008	0.04 (0.01-0.08)		0.03 (0.03-0.03)
2009	0.04 (0.00-0.07)		0.03 (0.02-0.03)
2010	0.04 (0.00-0.07)		0.03 (0.03-0.04)
2011	0.04 (0.00-0.07)		0.03 (0.02-0.03)
2012	0.04 (0.01-0.06)		0.03 (0.02-0.03)
2013	0.04 (0.02-0.05)	0.03 (0.02-0.04)	0.03 (0.02-0.03)
2014		0.03 (0.02-0.05)	

Table 21: Emission (Gg/yr) estimates for the UK with uncertainty (5th - 95th percentile).

5.19 NF₃

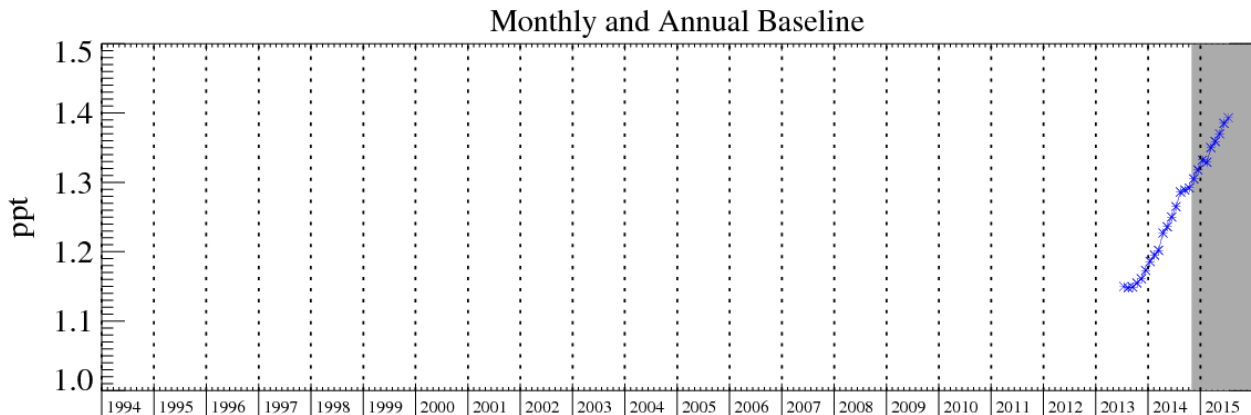


Figure 42: NF₃: Monthly (blue) baseline mole fractions. Grey area covers un-ratified and therefore provisional data.

Production of nitrogen trifluoride (NF₃) has been increasing rapidly to meet demand in end use applications (the manufacture of semiconductor devices, flat panel displays and photovoltaic cells). The new ambient air measurements from the Advanced Global Atmospheric Gases Experiment have shown the rapidly rising global atmospheric abundance of this gas due to this market expansion. Although the current contribution of NF₃ to radiative forcing is small, its potential to impact the climate is significant (its 100 year global warming potential is 16,100).

Years	InTEM (MHD) 36mth	Inventory
1990		0.02 (0.02-0.03)
1991		0.03 (0.02-0.03)
1992		0.03 (0.03-0.04)
1993		0.04 (0.03-0.04)
1994		0.04 (0.04-0.05)
1995		0.05 (0.04-0.05)
1996		0.06 (0.05-0.06)
1997		0.06 (0.06-0.07)
1998		0.07 (0.07-0.08)
1999		0.08 (0.08-0.09)
2000		0.10 (0.09-0.11)
2001		0.06 (0.05-0.07)
2002		0.06 (0.05-0.07)
2003		0.06 (0.05-0.06)
2004		0.03 (0.03-0.04)
2005		0.02 (0.02-0.02)
2006		0.02 (0.01-0.02)
2007		0.02 (0.01-0.02)
2008		0.02 (0.01-0.02)
2009		0.01 (0.01-0.02)
2010		0.02 (0.01-0.02)
2011		0.02 (0.02-0.02)
2012		0.02 (0.02-0.02)
2013	0.003 (0.002-0.004)	0.02 (0.02-0.02)
2014	0.003 (0.002-0.004)	

Table 22: Emission (t/yr) estimates for the UK with uncertainty (5th - 95th percentile).

6 Results and analysis of additional gases

6.1 Introduction

This section discusses the atmospheric trends and regional emissions of the other gases that are measured at Mace Head. The table below describes, if applicable, the principle uses of each of the gases, their radiative efficiency, atmospheric lifetime, global warming potential in a 100-year framework (GWP₁₀₀) and ozone depleting potential (ODP). In the following sections each of these gases are presented.

Gas	Primary use	Radiative Efficiency (W m ⁻² ppb ⁻¹)	Atmospheric Lifetime (years)	GWP ₁₀₀	ODP
CFC-11	Widespread	0.26	45	4,660	1
CFC-12	Refrigerant	0.32	100	10,200	0.82
CFC-113	Coolant, electronics	0.30	85	5,820	0.85
CFC-115	Refrigerant	0.20	1,020	7,670	0.57
HCFC-124	Refrigerant, fire suppression	0.20	5.9	527	0.02
HCFC-141b	Foam blowing	0.16	9.2	782	0.12
HCFC-142b	Chem. synthesis/foam blowing	0.19	17.2	1,980	0.06
HCFC-22	Propellant, air conditioning	0.21	11.9	1,760	0.04
HFC-236fa	Fire extinguisher	0.24	242	8060	
HFC-245fa	Foam blowing	0.24	7.7	858	
SO ₂ F ₂	Fumigant	0.2	36	4090	
CH ₃ Cl	Natural, refrigerant	0.01	1	12	0.02
CH ₂ Cl ₂	Foam plastic, solvent, natural		144 days		
CHCl ₃	Bi-product, natural		149 days		
CCl ₄	Fire suppression, precursor	0.17	26	1,730	0.82
CH ₃ CCl ₃	Solvent	0.07	5.0	160	0.16
CHClCCl ₂	Degreasing solvent		5 days	5	
CCl ₂ CCl ₂	Solvent, dry cleaning		90 days	15	
CH ₃ Br	Natural (seaweed), fumigant		0.8		
CH ₂ Br ₂	Natural (seaweed)		123 days		
CHBr ₃	Natural (seaweed)		24 days		0.66
CBrClF ₂	Fire suppression (military)	0.29	16	1,750	7.9
CBrF ₃	Fire suppression	0.30	65	6,290	15.9
C ₂ Br ₂ F ₄	Fire suppression	0.31	20	1,470	13.0
CH ₃ I	Natural (seaweed)		7 days		
C ₂ H ₆	Combustion, gas leakage				
CO	Combustion		30-90 days		
O ₃	Reactions in atmosphere				
H ₂	Combustion, photolysis				

Table 23: The principle uses of the gases observed at Mace Head, their radiative efficiency, atmospheric lifetime, global warming potential in a 100-year framework (GWP₁₀₀) and ozone depleting potential (ODP). The gases listed in red are specifically covered by the Montreal Protocol. All of the gases with a GWP are GHGs but not all GHGs are covered by the Kyoto Protocol.

6.2 CFC-11

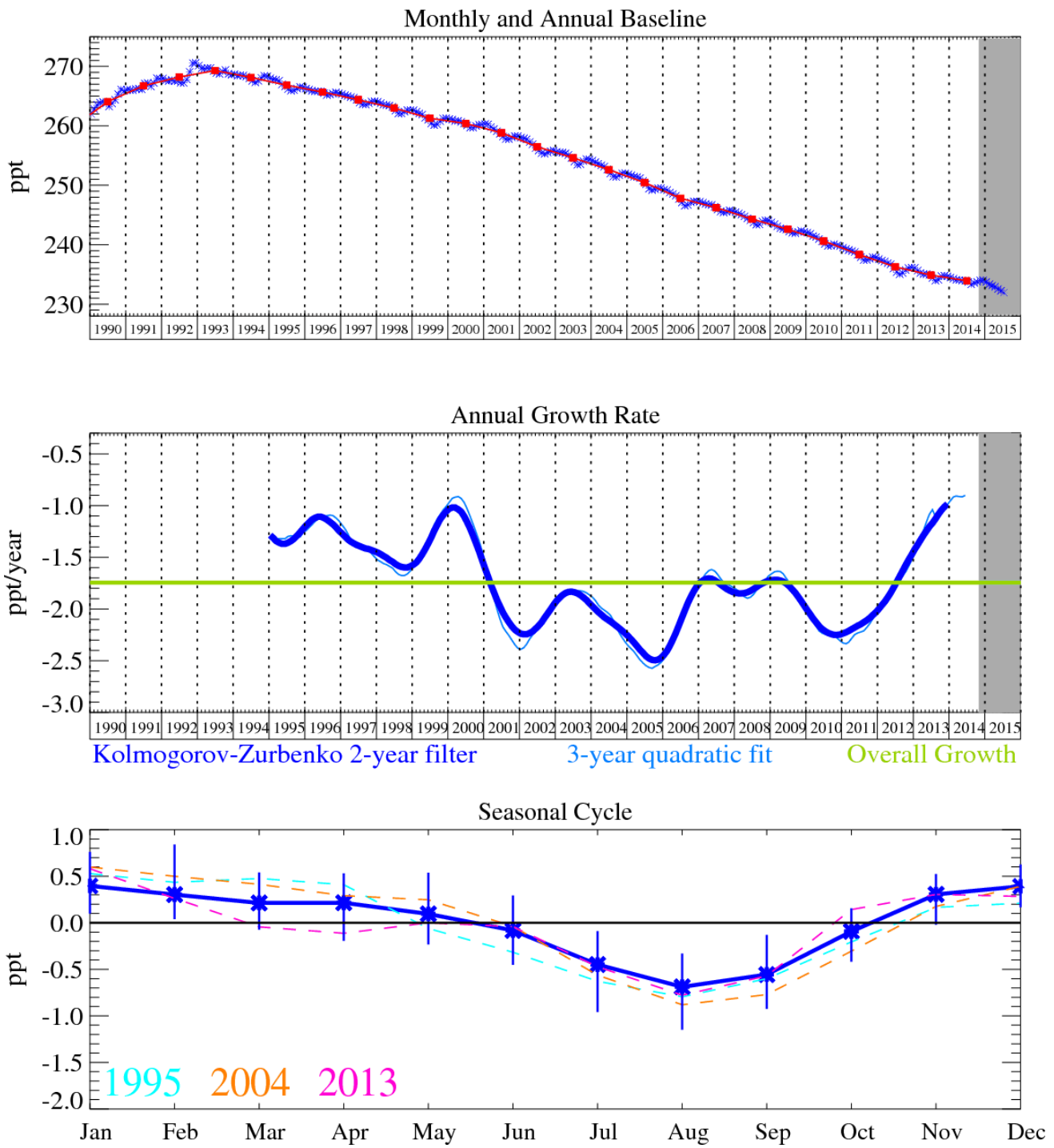


Figure 43: CFC-11 (CCl_3F): Monthly (blue) and annual (red) baseline (top plot). Annual (blue) and overall average growth rate (green) (middle plot). Seasonal cycle (de-trended) with year-to-year variability (lower plot). The grey area covers un-ratified and therefore provisional data.

6.3 CFC-12

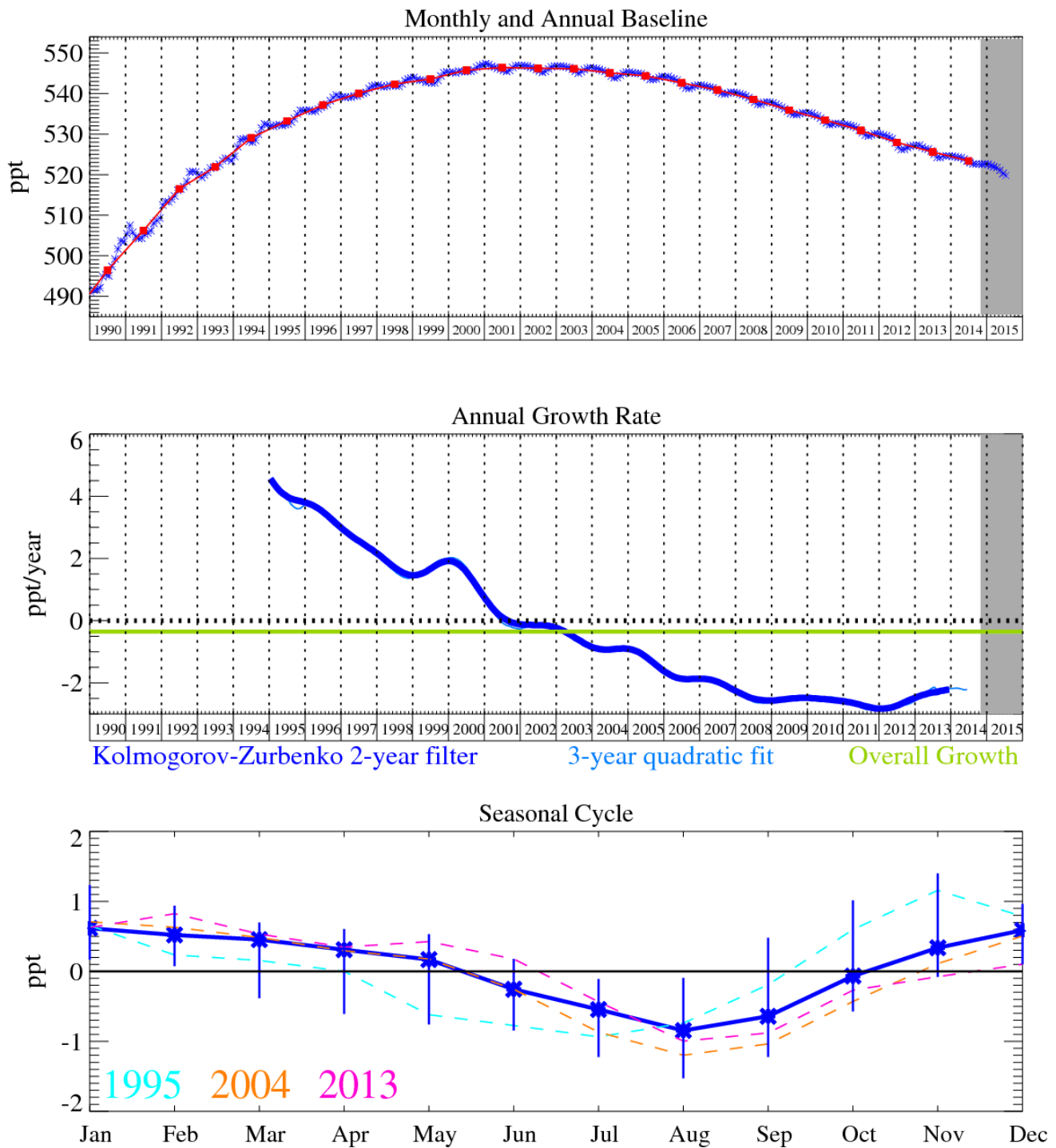


Figure 44: CFC-12 (CCl_2F_2): Monthly (blue) and annual (red) baseline (top plot). Annual (blue) and overall average growth rate (green) (middle plot). Seasonal cycle (de-trended) with year-to-year variability (lower plot). The grey area covers un-ratified and therefore provisional data.

6.4 CFC-113

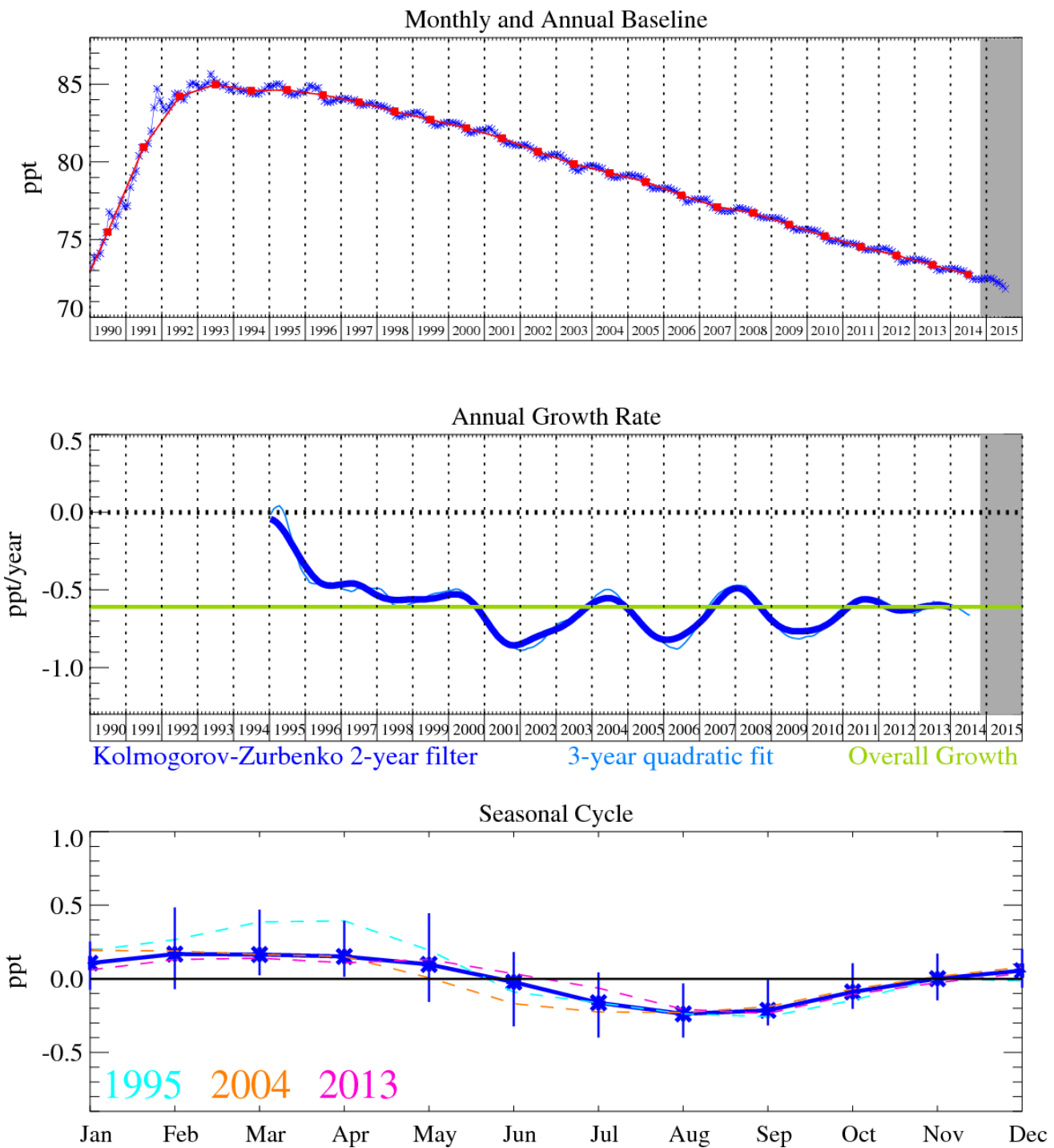


Figure 45: CFC-113 ($\text{C}_2\text{Cl}_3\text{F}_3$): Monthly (blue) and annual (red) baseline (top plot). Annual (blue) and overall average growth rate (green) (middle plot). Seasonal cycle (de-trended) with year-to-year variability (lower plot). The grey area covers un-ratified and therefore provisional data.

6.5 HCFC-124

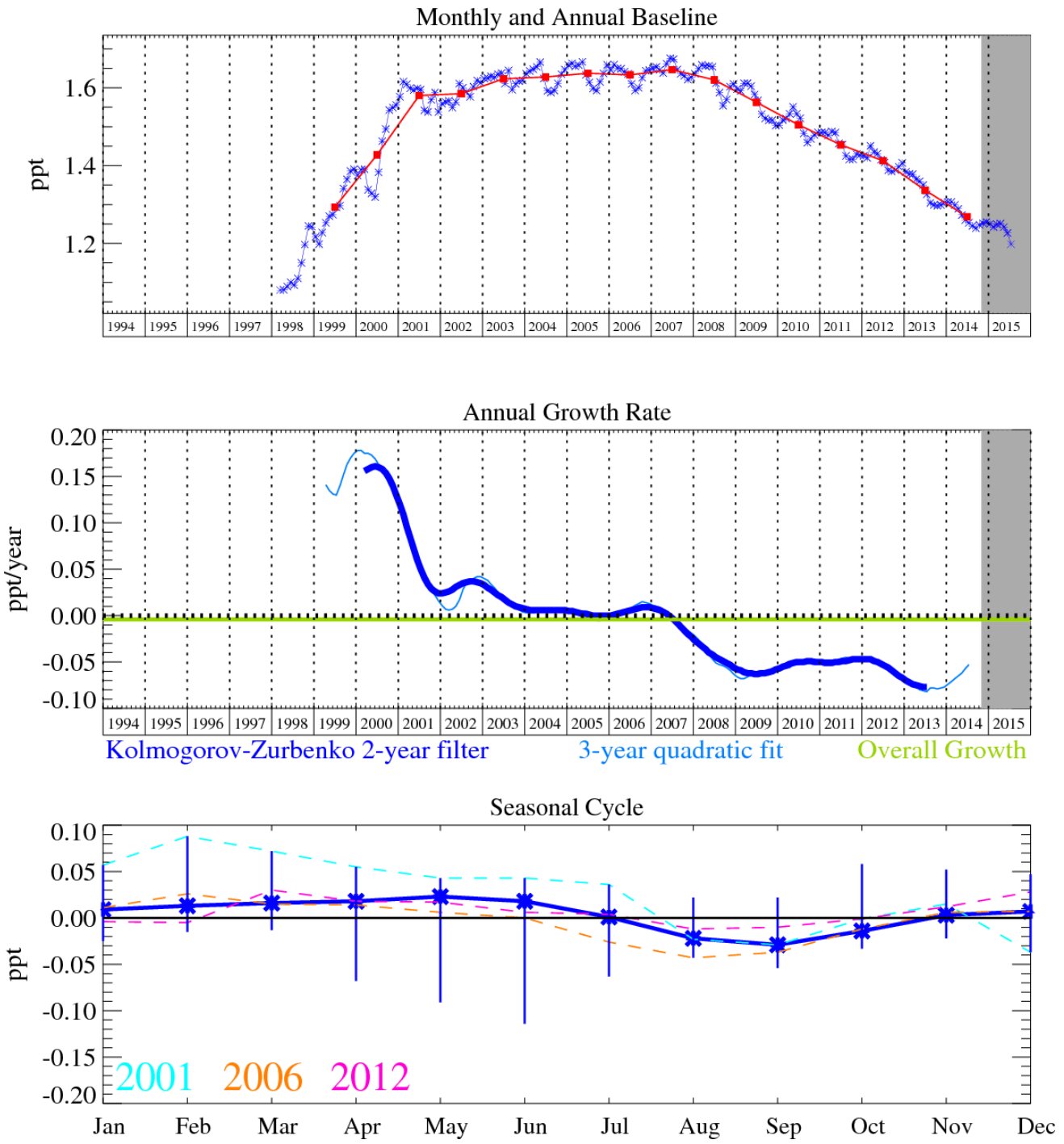


Figure 46: HCFC-124 (C_2HCIF_4): Monthly (blue) and annual (red) baseline (top plot). Annual (blue) and overall average growth rate (green) (middle plot). Seasonal cycle (de-trended) with year-to-year variability (lower plot). The grey area covers un-ratified and therefore provisional data.

6.6 HCFC-141b

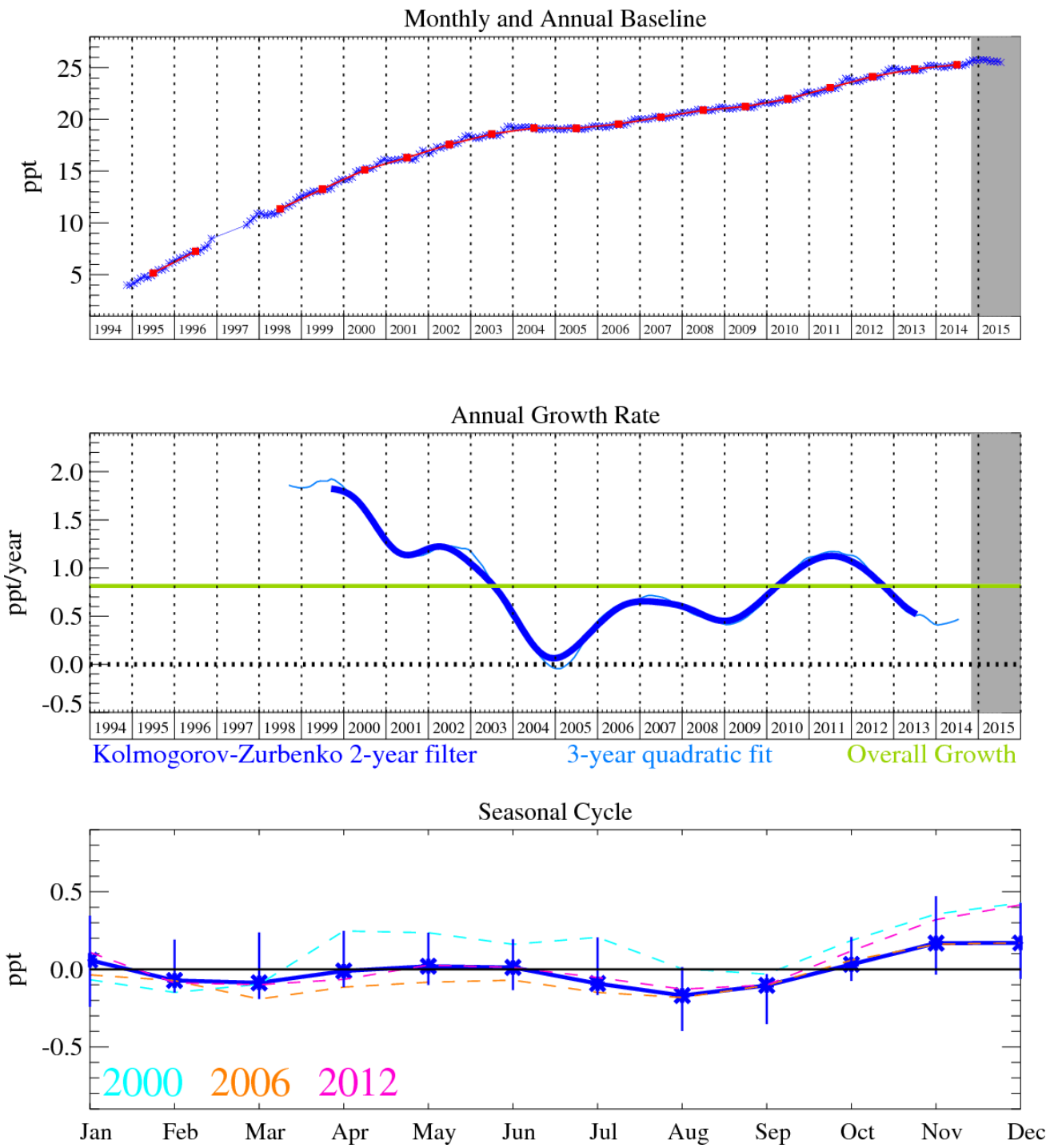


Figure 47: HCFC-141b (C₂H₃Cl₂F): Monthly (blue) and annual (red) baseline (top). Annual (blue) and overall average growth rate (green) (middle plot). Seasonal cycle (de-trended) with year-to-year variability (lower plot). The grey area covers un-ratified and therefore provisional data.

6.7 HCFC-142b

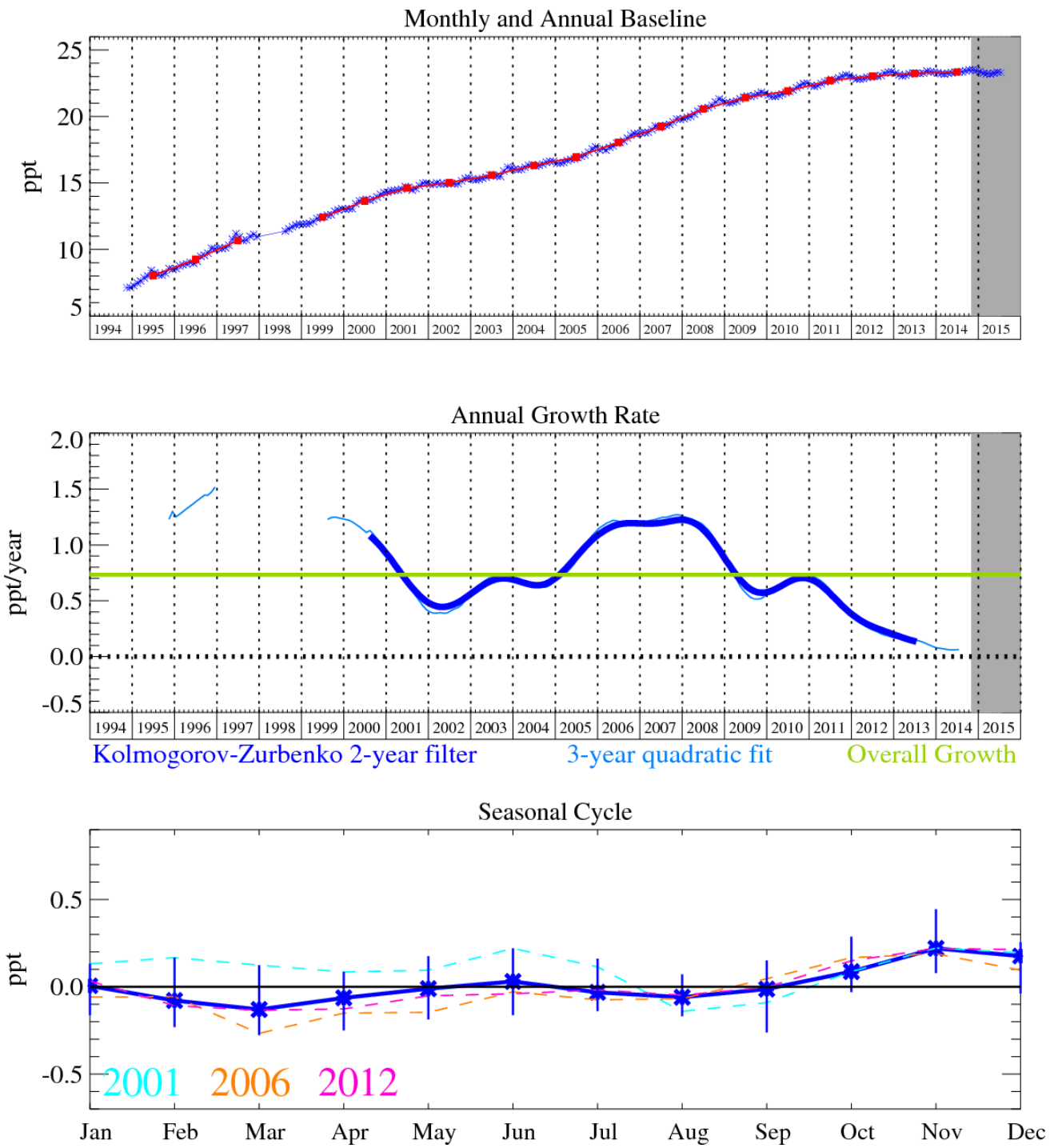


Figure 48: HCFC-142b ($\text{C}_2\text{H}_3\text{ClF}_2$): Monthly (blue) and annual (red) baseline (top). Annual (blue) and overall average growth rate (green) (middle plot). Seasonal cycle (de-trended) with year-to-year variability (lower plot). The grey area covers un-ratified and therefore provisional data.

6.8 HCFC-22

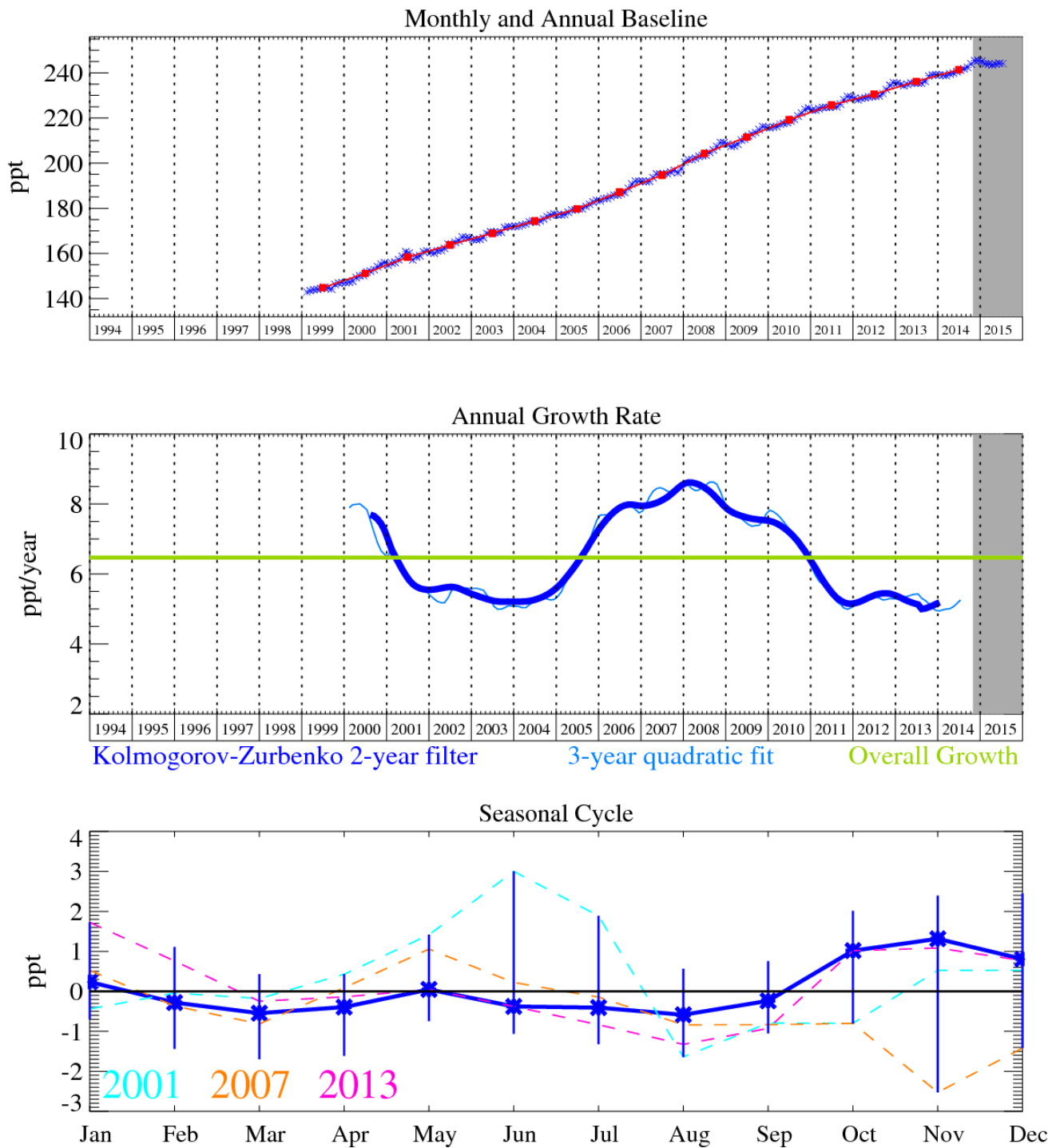


Figure 49: HCFC-22 (CHClF_2): Monthly (blue) and annual (red) baseline (top plot). Annual (blue) and overall average growth rate (green) (middle plot). Seasonal cycle (de-trended) with year-to-year variability (lower plot). Grey area covers un-ratified and therefore provisional data.

6.9 HFC-236fa

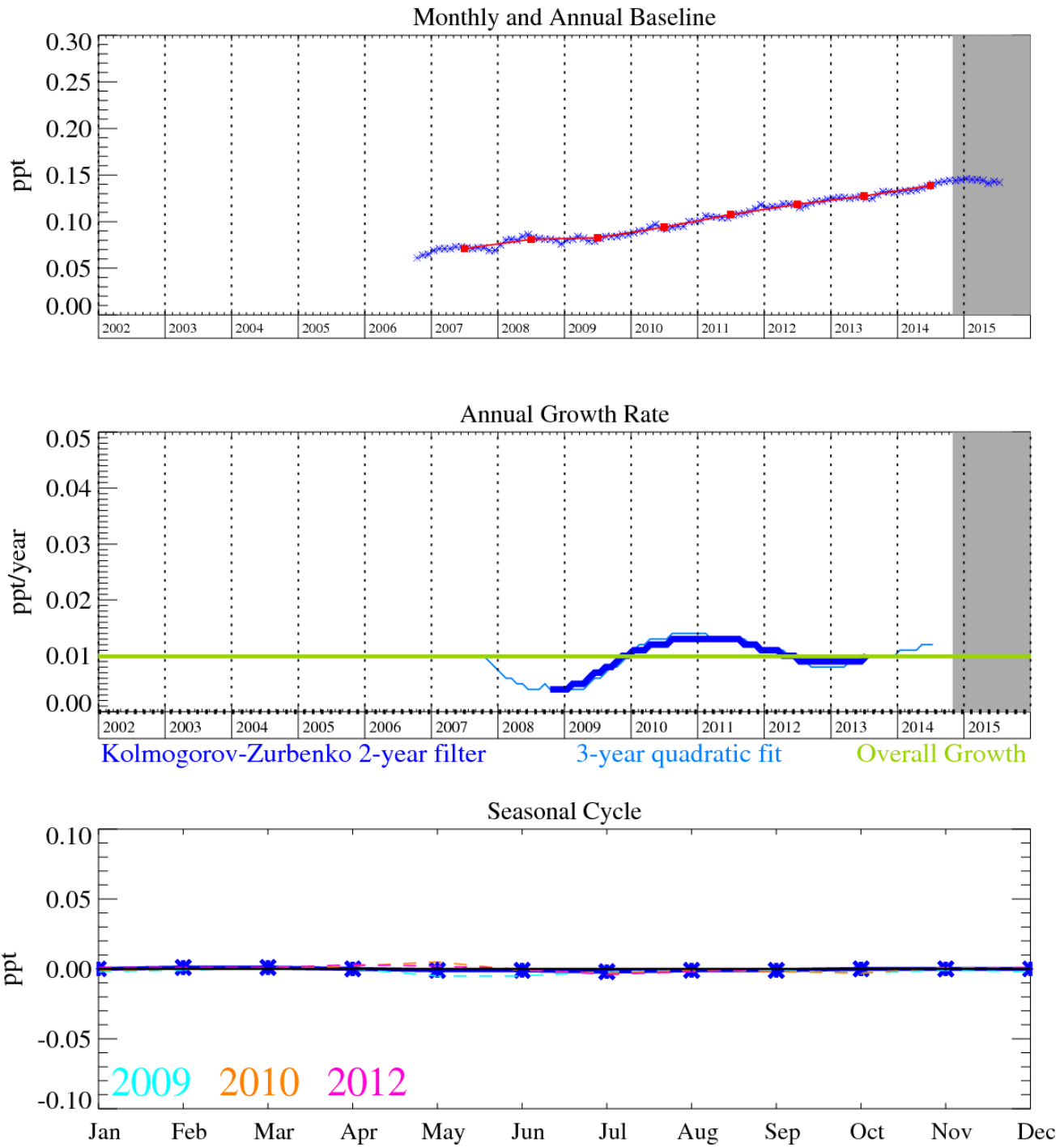


Figure 50: HFC-236fa ($C_3H_2F_6$): Monthly (blue) and annual (red) baseline (top plot). Annual (blue) and overall average growth rate (green) (middle plot). Seasonal cycle (de-trended) with year-to-year variability (lower plot). Grey area covers un-ratified and therefore provisional data.

6.10 HFC-245fa

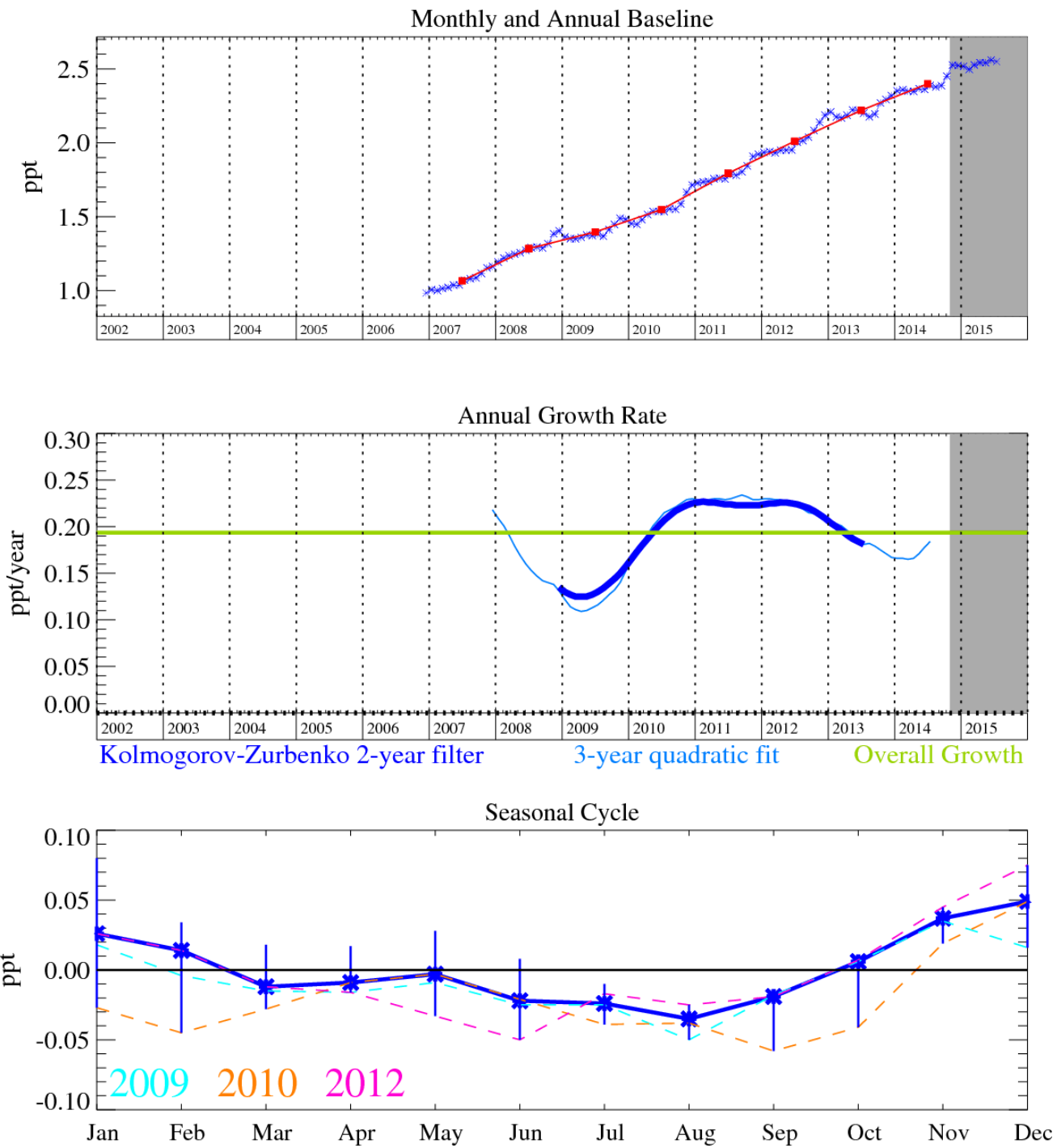
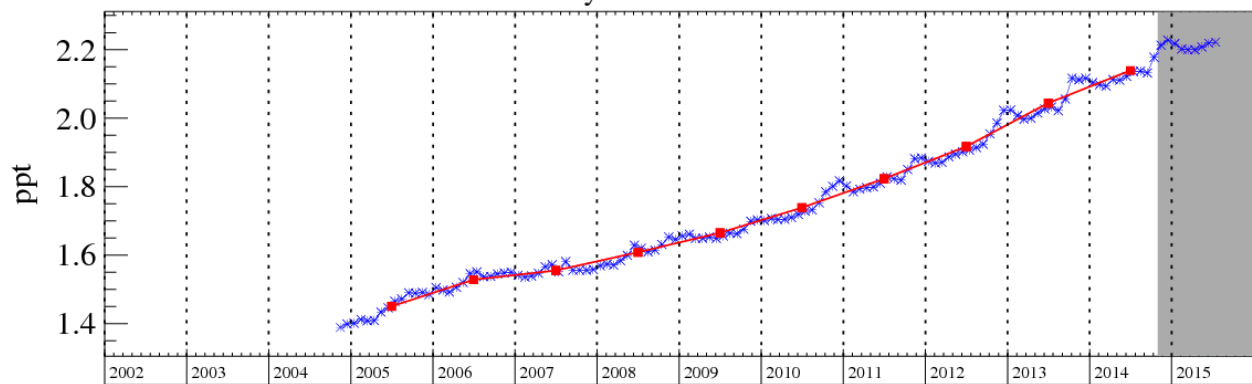


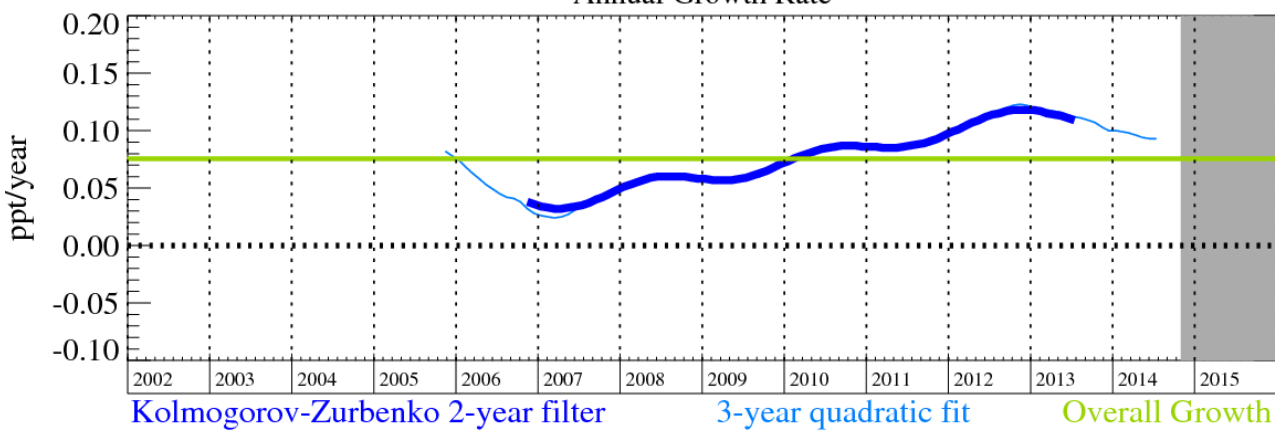
Figure 51: HFC-245fa ($C_3H_3F_5$): Monthly (blue) and annual (red) baseline (top plot). Annual (blue) and overall average growth rate (green) (middle plot). Seasonal cycle (de-trended) with year-to-year variability (lower plot). Grey area covers un-rated and therefore provisional data.

6.11 SO₂F₂

Monthly and Annual Baseline



Annual Growth Rate



Seasonal Cycle

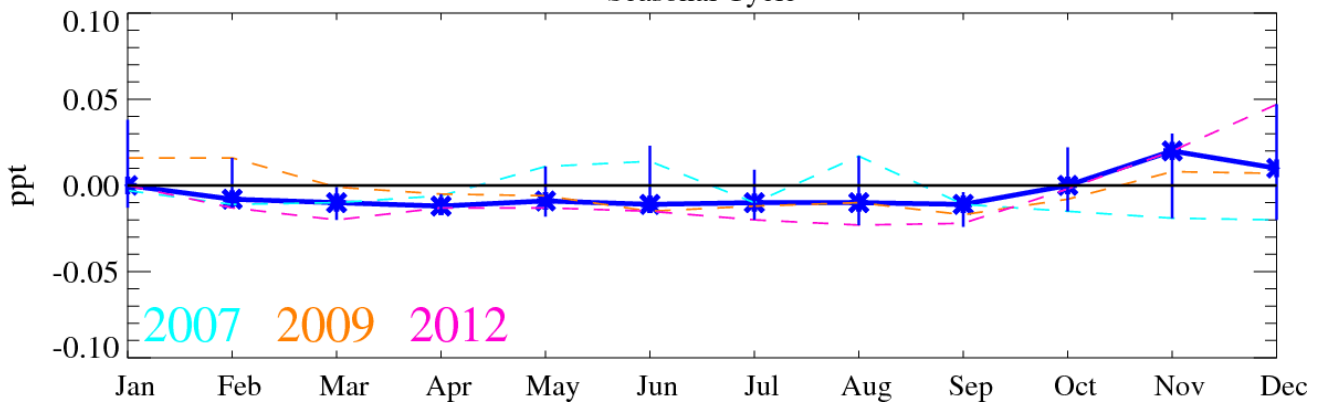


Figure 52: SO₂F₂: Monthly (blue) and annual (red) baseline mole fractions (top plot). Annual (blue) and overall average growth rate (green) (middle plot). Seasonal cycle (de-trended) with year-to-year variability (lower plot). Grey area covers un-rated and therefore provisional data.

6.12 CH₃Cl

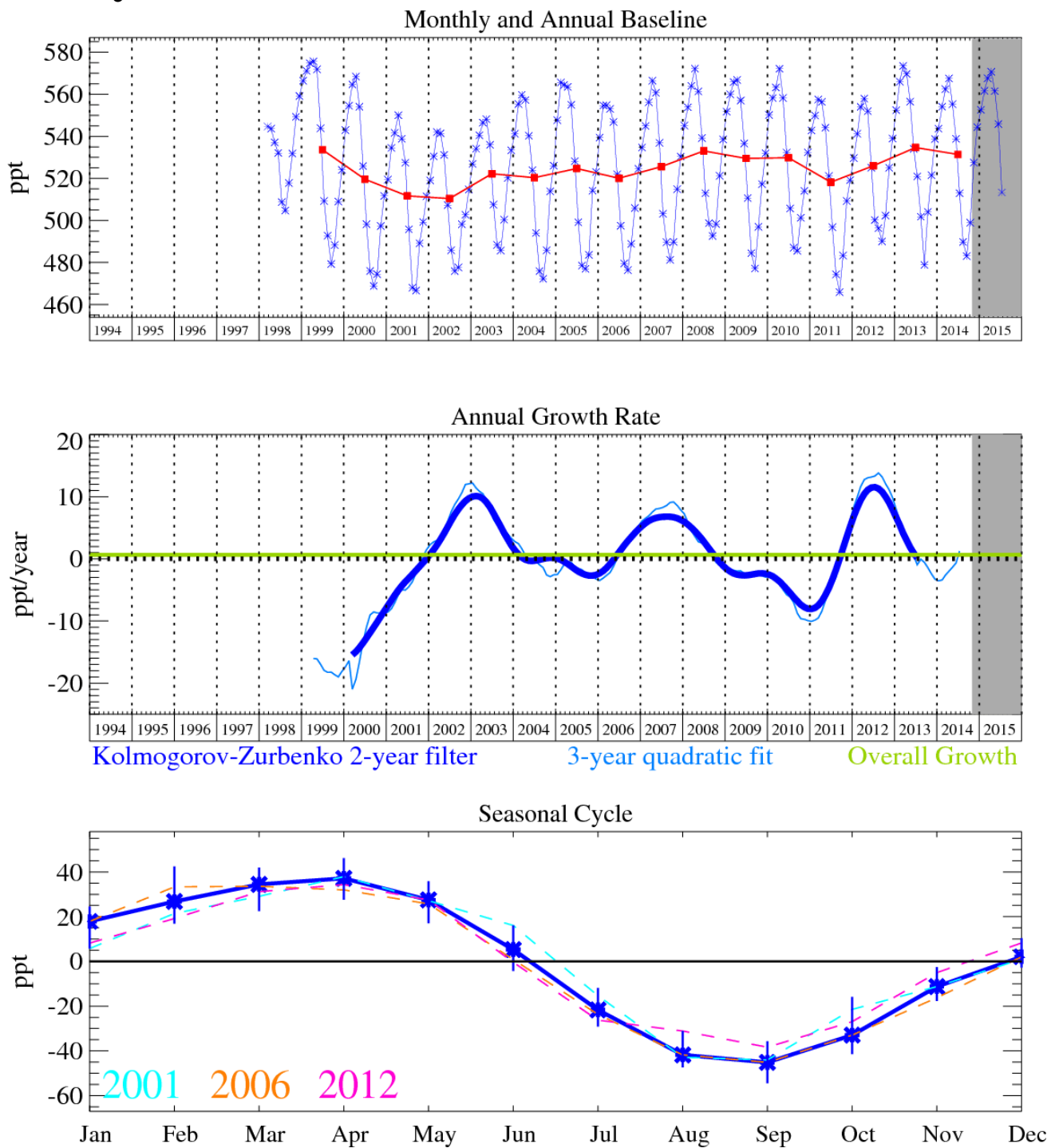


Figure 53: CH₃Cl: Monthly (blue) and annual (red) baseline mole fractions (top plot). Annual (blue) and overall growth rate (green) (middle). Seasonal cycle (de-trended) with year-to-year variability (lower plot). Grey area covers un-ratified and therefore provisional data.

6.13 CH_2Cl_2

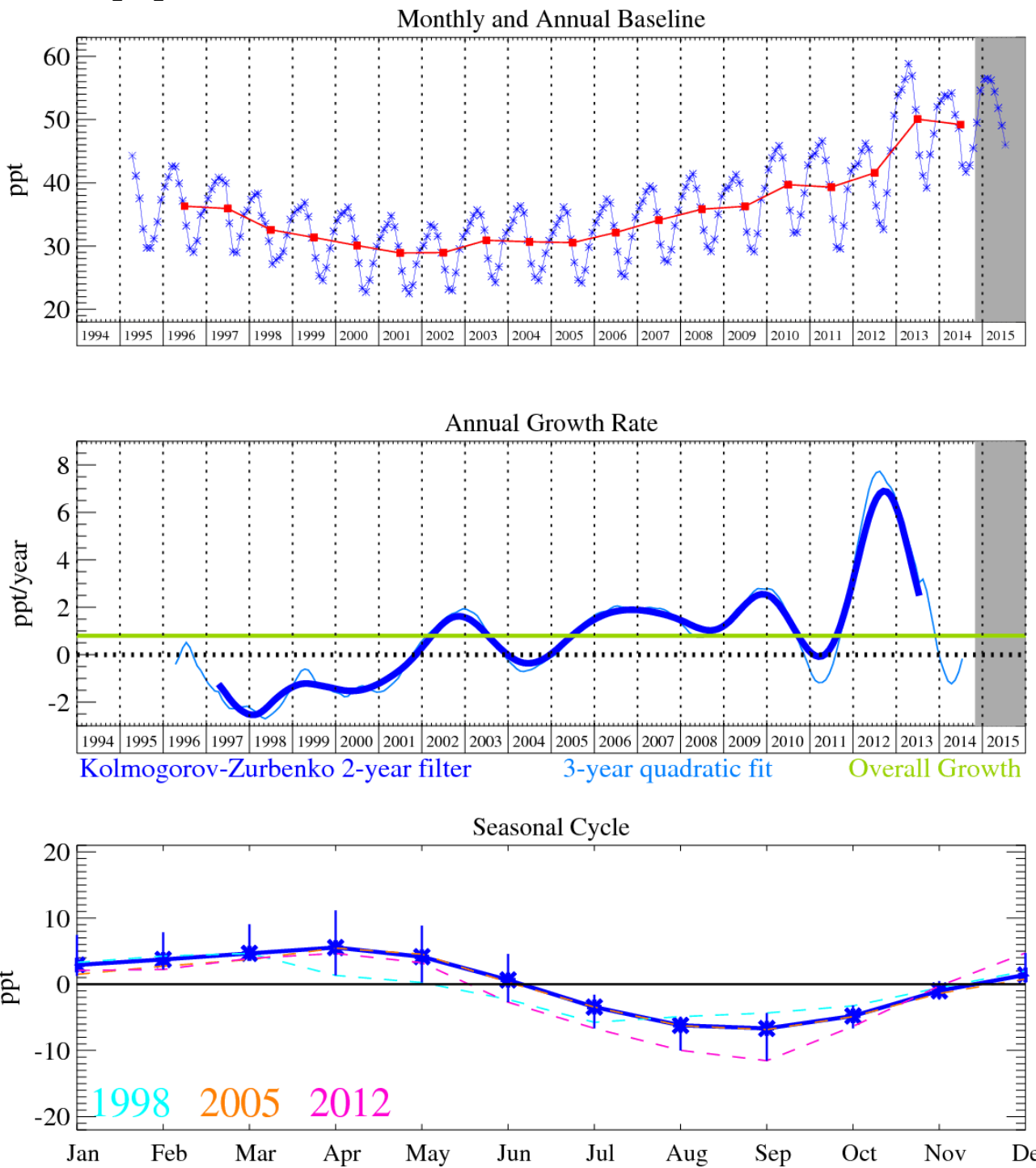


Figure 54: CH_2Cl_2 : Monthly (blue) and annual (red) baseline mole fractions (top plot). Annual (blue) and overall average growth rate (green) (middle plot). Seasonal cycle (de-trended) with year-to-year variability (lower plot). Grey area covers un-ratified and therefore provisional data.

6.14 CHCl₃ (chloroform)

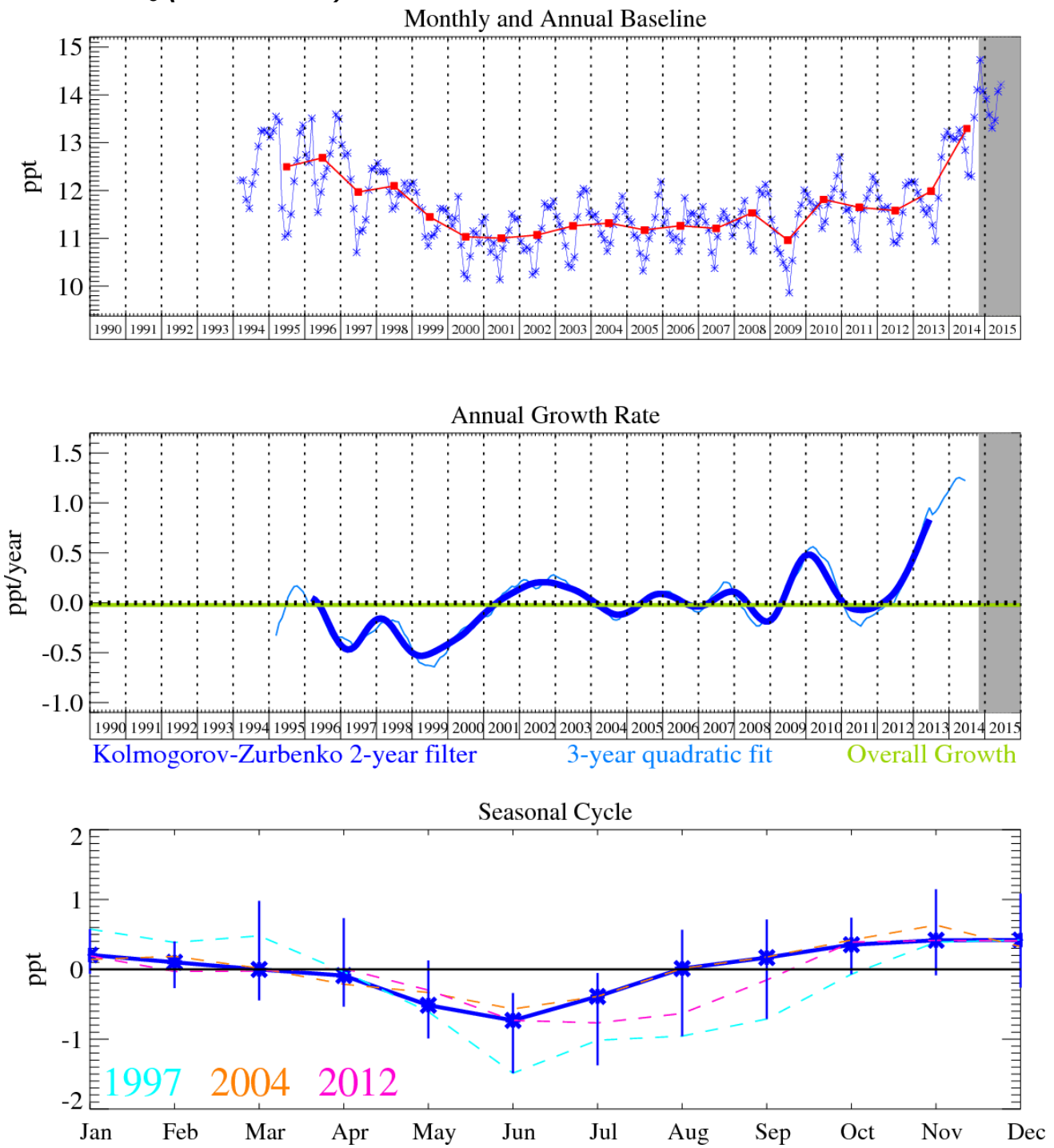


Figure 55: CHCl₃: Monthly (blue) and annual (red) baseline mole fractions (top plot). Annual (blue) and overall average growth rate (green) (middle plot). Seasonal cycle (de-trended) with year-to-year variability (lower plot). Grey area covers un-ratified and therefore provisional data.

6.15 CCl₄ (carbon tetrachloride)

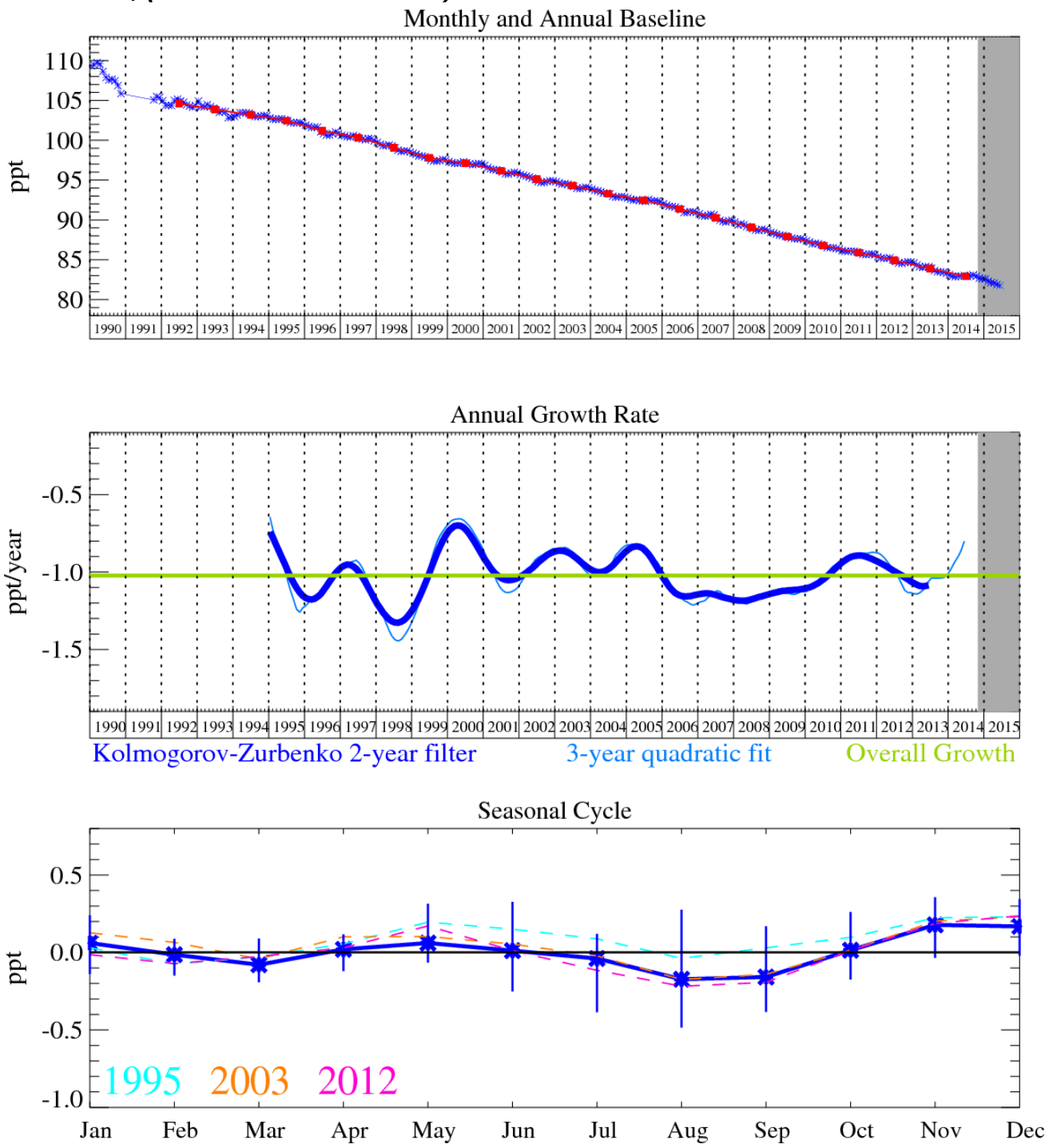
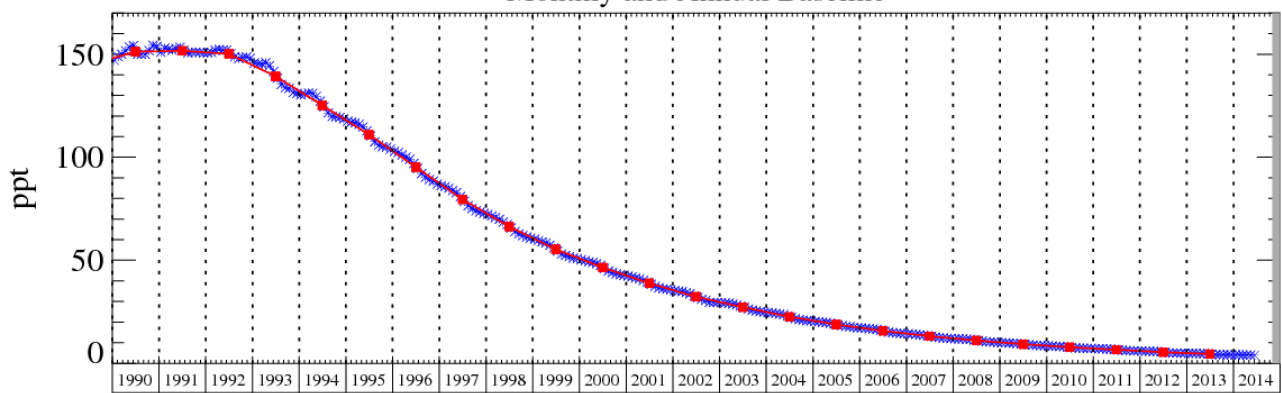


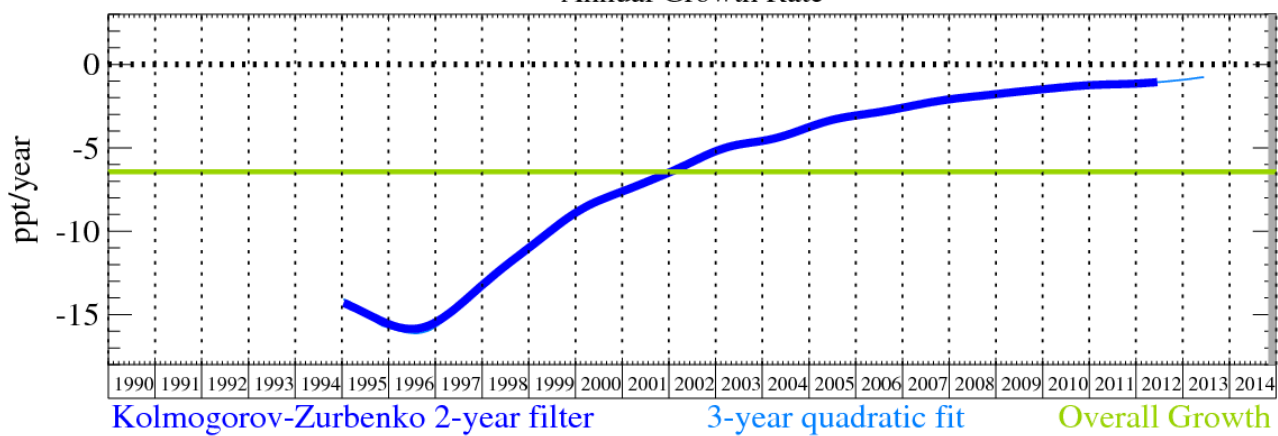
Figure 56: CCl₄: Monthly (blue) and annual (red) baseline mole fractions (top plot). Annual (blue) and overall average growth rate (green) (middle plot). Seasonal cycle (de-trended) with year-to-year variability (lower plot). Grey area covers un-ratified and therefore provisional data.

6.16 CH_3CCl_3 (methyl chloroform)

Monthly and Annual Baseline



Annual Growth Rate



Seasonal Cycle

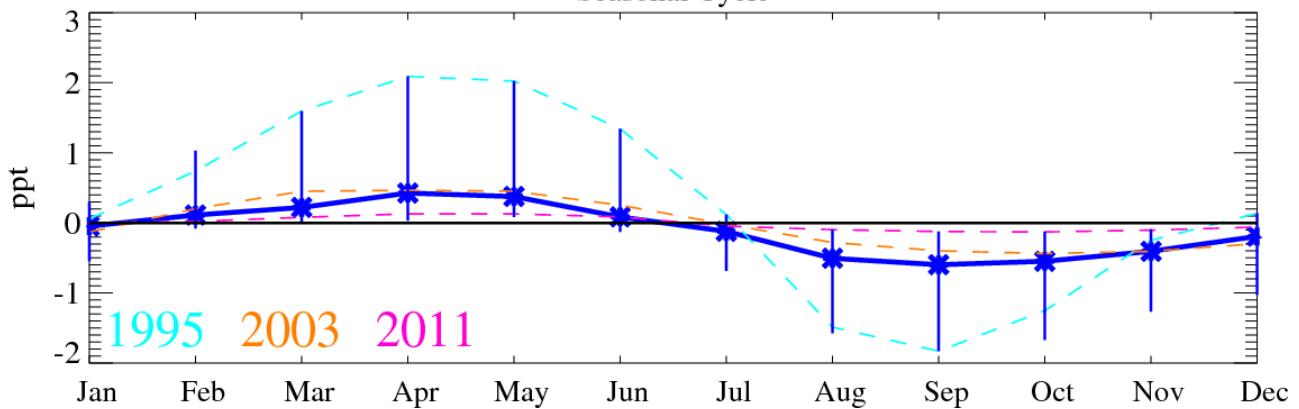


Figure 57: CH_3CCl_3 : Monthly (blue) and annual (red) baseline mole fractions (top plot). Annual (blue) and overall average growth rate (green) (middle plot). Seasonal cycle (de-trended) with year-to-year variability (lower plot). Grey area covers un-rated and therefore provisional data.

6.17 CCl_2CCl_2

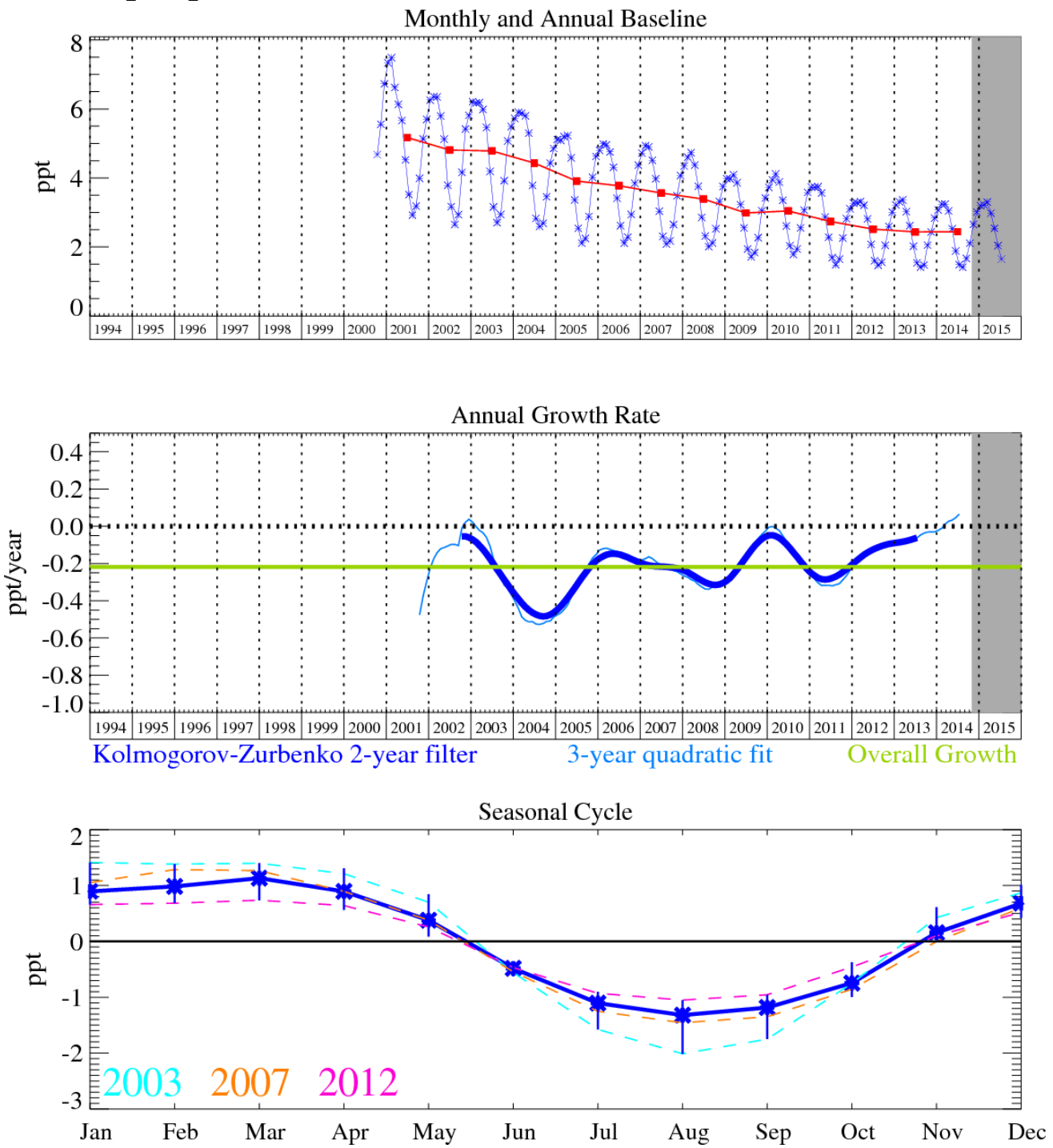


Figure 58: CCl_2CCl_2 : Monthly (blue) and annual (red) baseline mole fractions (top plot). Annual (blue) and overall average growth rate (green) (middle plot). Seasonal cycle (de-trended) with year-to-year variability (lower plot). Grey area covers un-ratified and therefore provisional data.

6.18 Methyl bromide (CH_3Br)

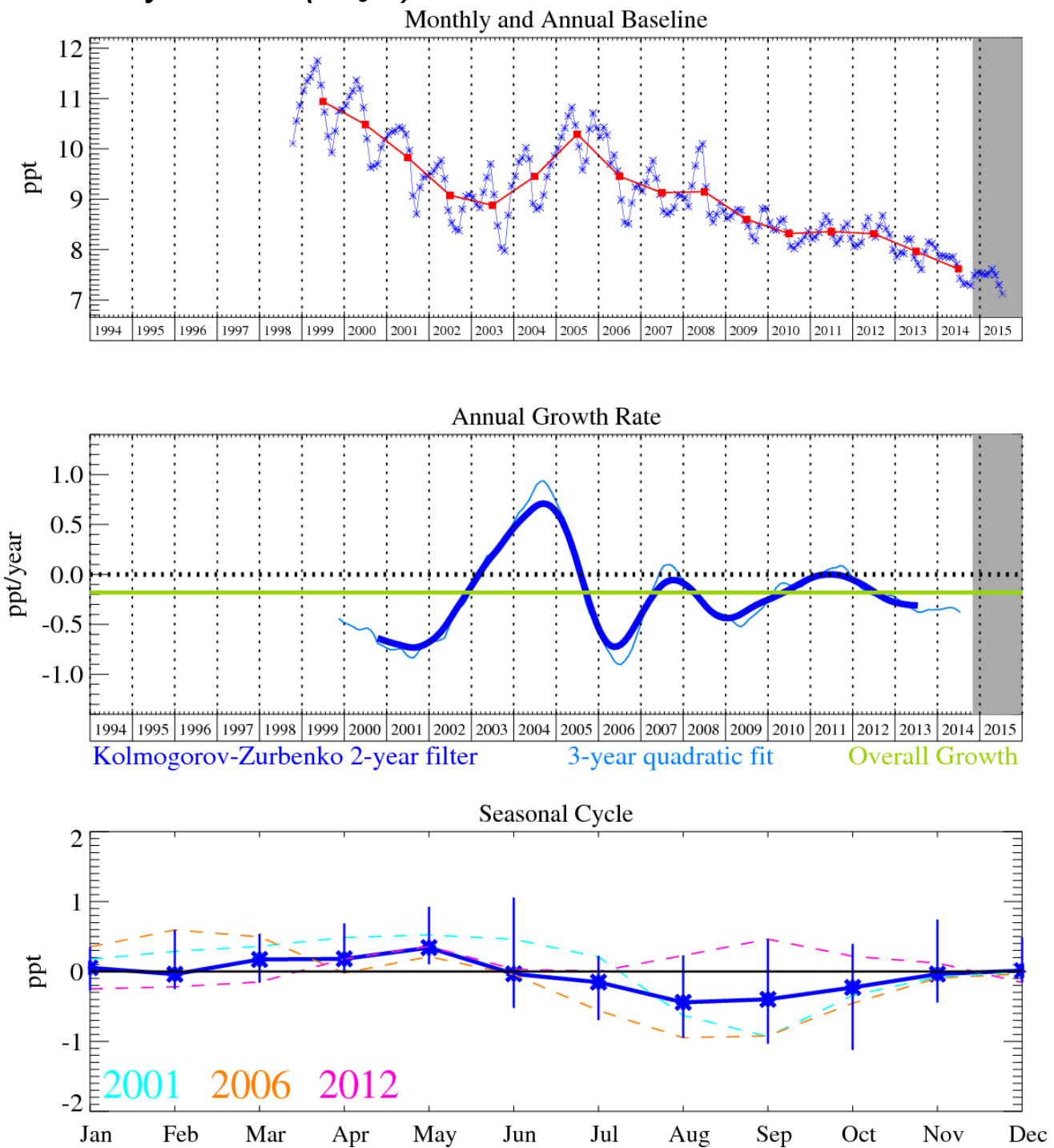


Figure 59: Methyl bromide: Monthly (blue) and annual (red) baseline (top plot). Annual (blue) and overall average growth rate (green) (middle plot). Seasonal cycle (de-trended) with year-to-year variability (lower plot). Grey area covers un-ratified and therefore provisional data.

The instrument change in 2005 to the Medusa system produced a discontinuity in the methyl bromide record, this jump should be discounted as it is an artefact of the measurement system.

6.19 Halon-1211

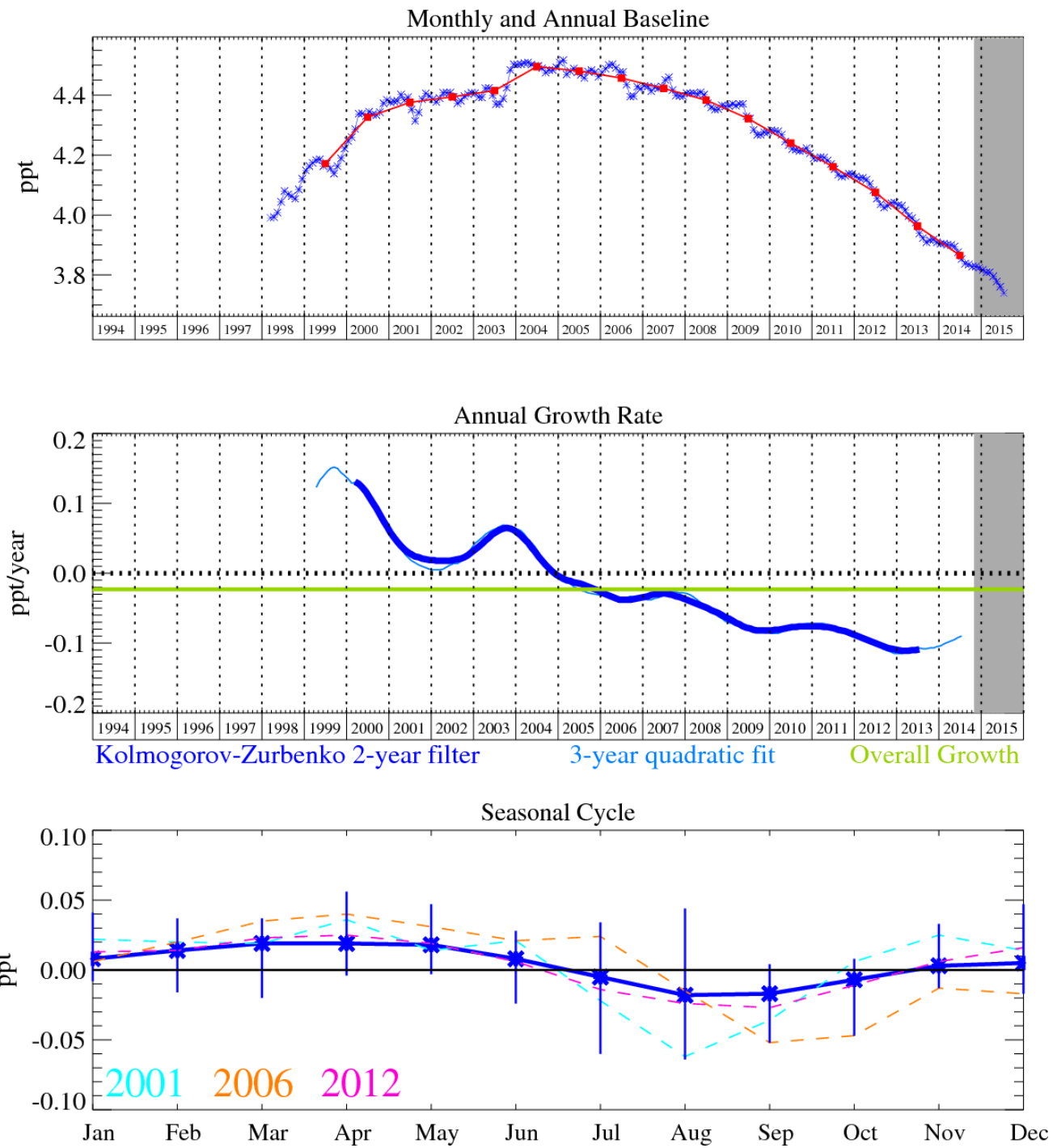


Figure 60: Halon-1211 (CBrClF_2): Monthly (blue) and annual (red) baseline (top plot). Annual (blue) and overall average growth rate (green) (middle plot). Seasonal cycle (de-trended) with year-to-year variability (lower plot). Grey area covers un-rated and therefore provisional data.

6.20 Halon-1301

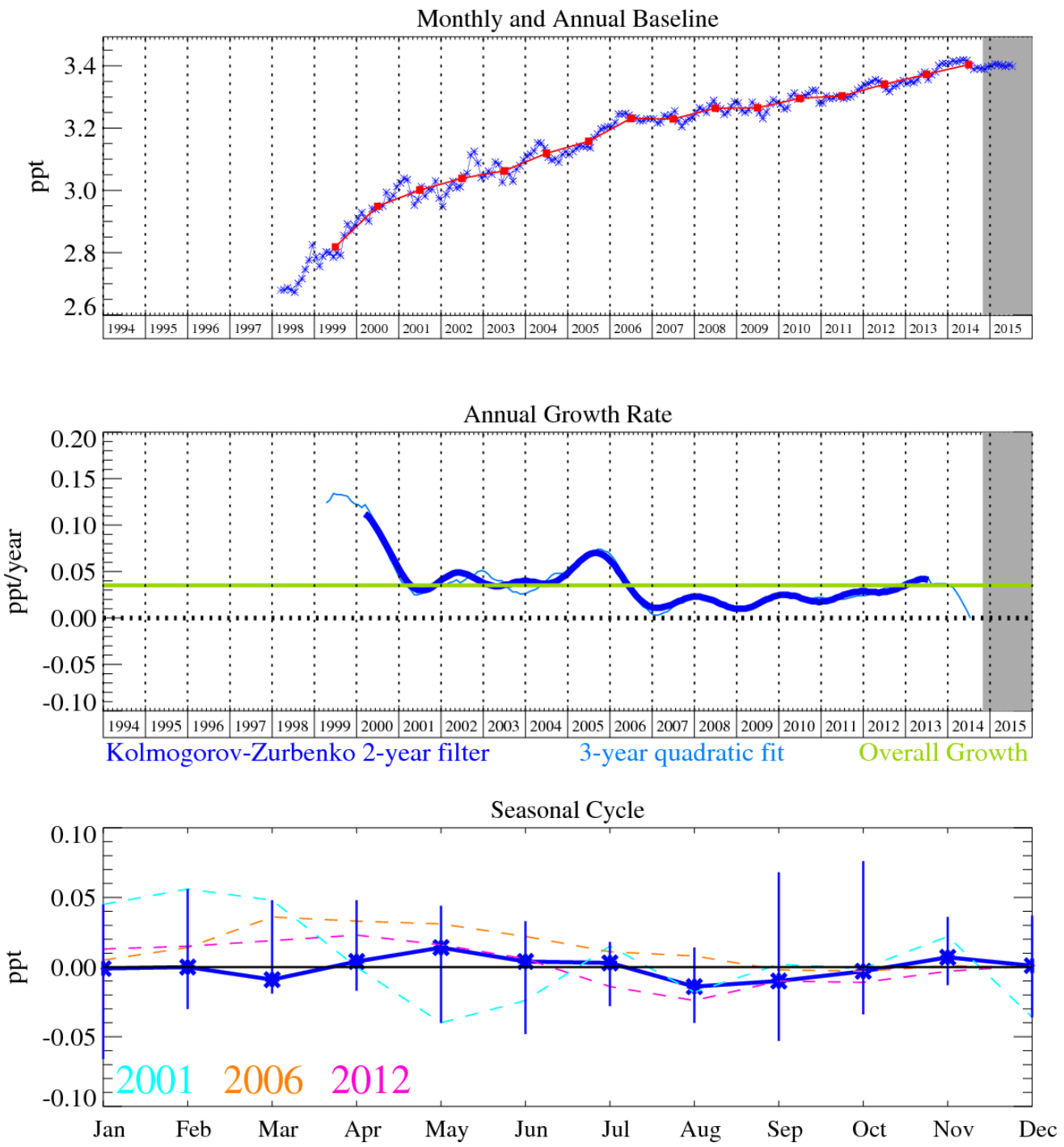


Figure 61: Halon-1301 (CBrF_3): Monthly (blue) and annual (red) baseline (top plot). Annual (blue) and overall average growth rate (green) (middle plot). Seasonal cycle (de-trended) with year-to-year variability (lower plot). Grey area covers un-rated and therefore provisional data.

6.21 Halon-2402

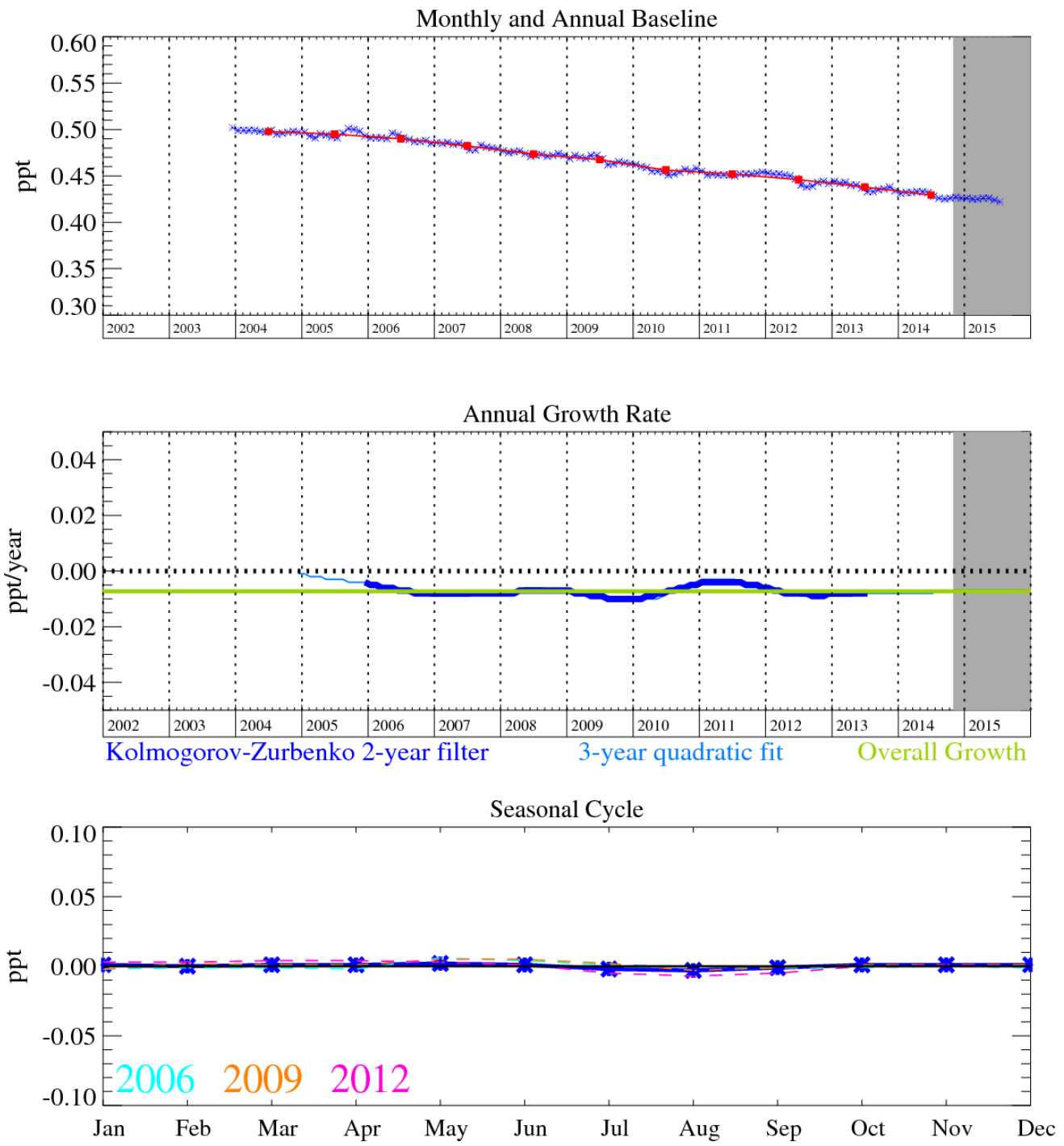


Figure 62: Halon-2402 ($\text{C}_2\text{Br}_2\text{F}_4$): Monthly (blue) and annual (red) baseline (top plot). Annual (blue) and overall average growth rate (green) (middle plot). Seasonal cycle (de-trended) with year-to-year variability (lower plot). Grey area covers un-rated and therefore provisional data.

6.22 Carbon monoxide (CO)

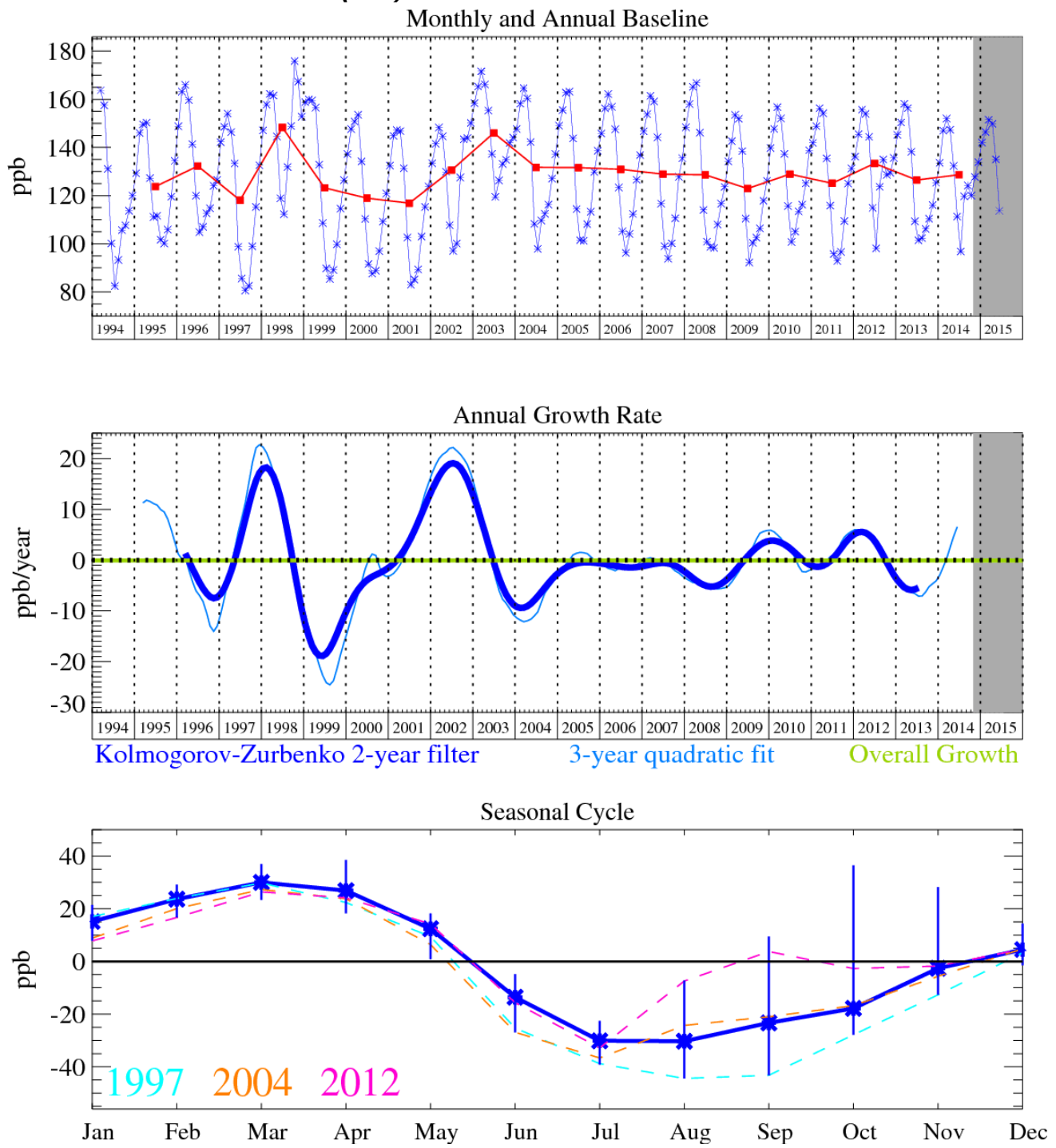


Figure 63: CO: Monthly (blue) and annual (red) baseline mole fractions (top plot). Annual (blue) and overall average growth rate (green) (middle plot). Seasonal cycle (de-trended) with year-to-year variability (lower plot). Grey area covers un-ratified and therefore provisional data.

6.23 Ozone (O_3)

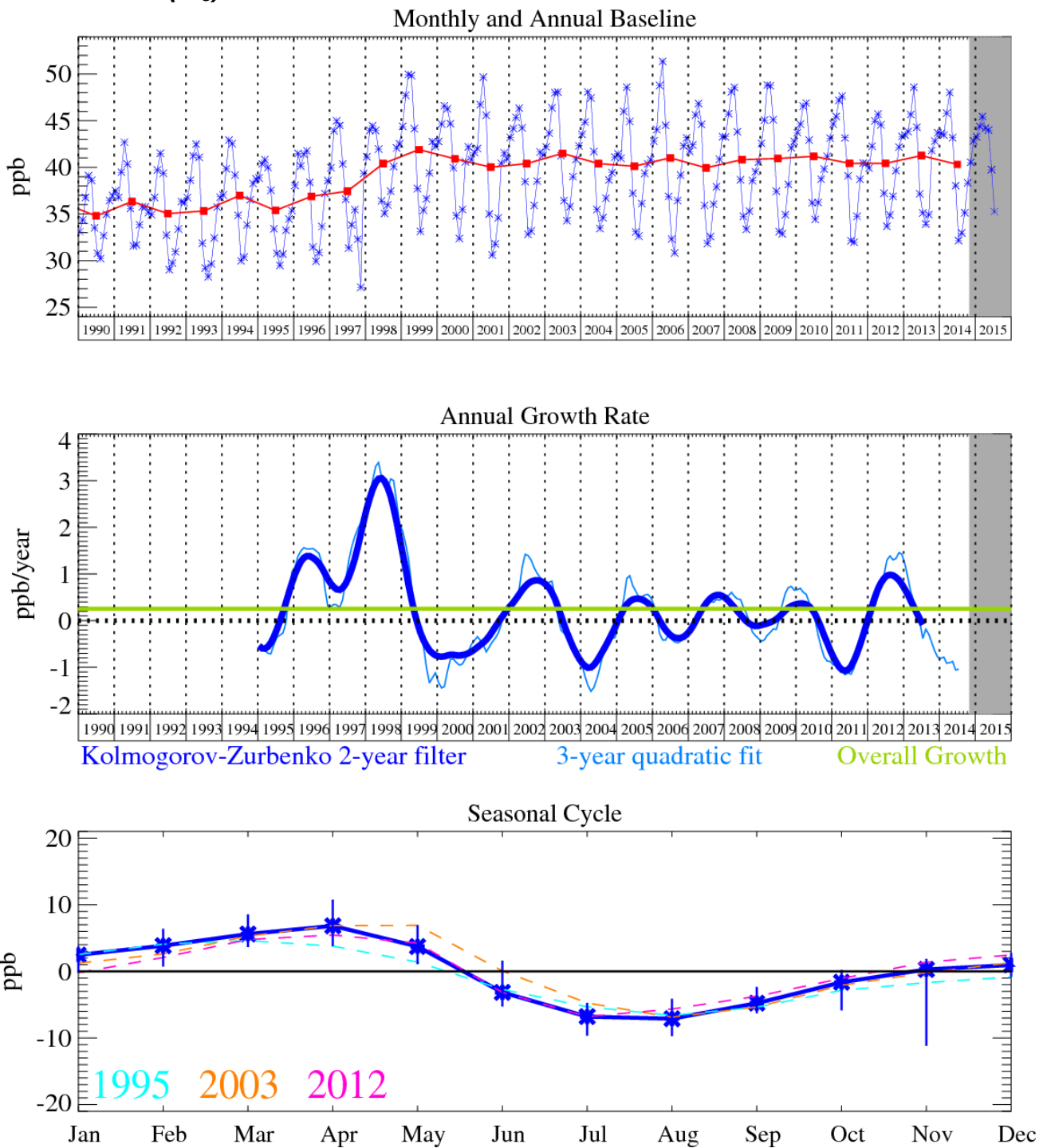


Figure 64: Ozone (O_3): Monthly (blue) and annual (red) baseline mole fractions (top plot). Annual (blue) and overall average growth rate (green) (middle plot). Seasonal cycle (de-trended) with year-to-year variability (lower plot). Grey area covers un-ratified and therefore provisional data.

6.24 Hydrogen

Hydrogen is an oxidation product of methane and isoprene whose main sink is surface uptake mainly in the northern hemisphere. Annual mean baseline levels have remained roughly constant (within measurement uncertainty) for much of the Mace Head record. There is evidence of anomalous growth in 2010-2011 through the influence of the forest fires in the Russian Federation.

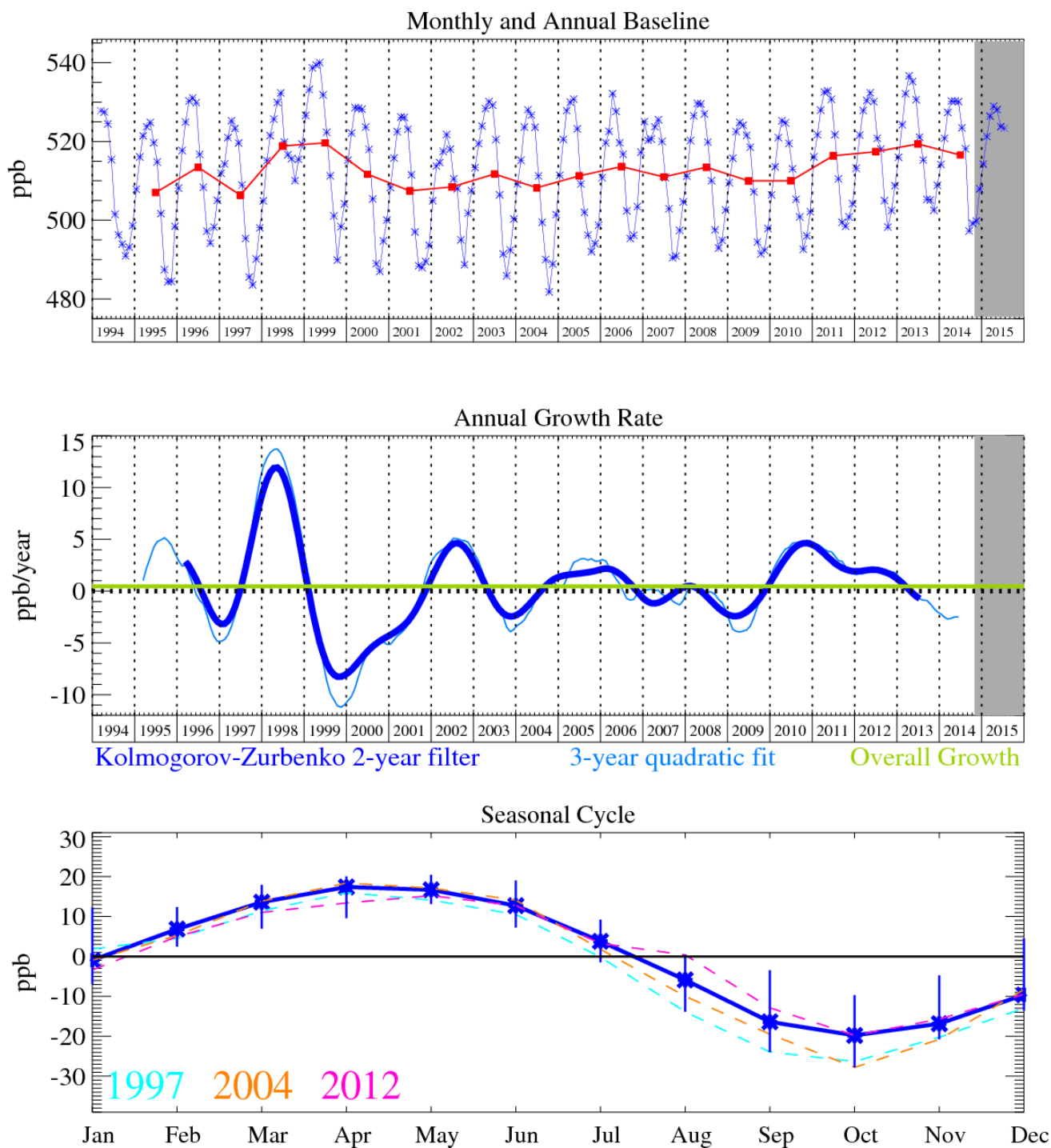


Figure 65: Hydrogen (H_2): Monthly (blue) and annual (red) baseline (top plot). Annual (blue) and overall average growth rate (green) (middle plot). Seasonal cycle (de-trended) with year-to-year variability (lower plot). Grey area covers un-ratified and therefore provisional data.

7 Results from the European InGOS project

7.1 Introduction

InGOS (Integrated non-CO₂ Greenhouse gas Observing System) is an EU funded project with the aim of improving and extending the European observation capacity for non-CO₂ greenhouse gases. The project began in October 2011 and ended in September 2015. InGOS is coordinated by the Energy Research Centre of the Netherlands (ECN) and involves many partners from across the EU (including our team at the Met Office and the University of Bristol). The project as a whole aims to standardise measurements, strengthen existing observation sites, build capacity in new member states, and prepare for integration of the network with other networks. The data set for N₂O and CH₄ from the European InGOS monitoring stations was analysed using InTEM as part of a work package to compare emissions estimates between independent inverse modelling systems from different research groups. This approach aims to provide more realistic estimates of the overall model uncertainties. Four independent inverse modelling frameworks (one of which is InTEM) were also applied to estimate the emissions of halogenated organic compounds and SF₆ in Europe in the year 2011. The main goal was to better characterize the capabilities and limitations of the current monitoring system for estimating European emissions of these compounds.

We utilised a Bayesian inverse methodology, as described in the May 2015 Interim report, using data from in situ instrumentation and flask samples from observatories across Europe. The monitoring sites for N₂O and CH₄ are numerous (20+ sites) and span south to 35.3°N (Finokalia, Greece), north to 78.9°N (Ny-Ålesund, Norway), east to 30.7°E (Voeikovo, Russia) and west to -20.3°E (Heimay, Iceland) but with the majority of sites located in central Europe. The baseline estimate from Mace Head was applied as a prior to each station, however, this was allowed to be perturbed independently for each site in the inversion depending on the relative contributions of background air from the 11 air origin sectors (Figure 4). For the halogenated species, measurements from three sites are assimilated - Mace Head, Jungfraujoch (Switzerland) and Monte Cimone (Italy). Prior emission information from the EDGAR database was used within the inversions for all species as set out in the InGOS protocol supplied to all participating modelling groups.

Here we present a subset of the InTEM (Met Office) results from the InGOS project.

7.2 Halogenated species emissions estimates

The mountainous topography surrounding Jungfraujoch (3580 metres above sea level) in Switzerland makes modelling the movement of air masses to this site extremely challenging. The Monte Cimone observatory is also at a very high altitude (2165 metres above sea level). To minimise this considerable uncertainty, we utilised data only from the early morning period (6am – 9am) for the Jungfraujoch and Monte Cimone stations, when air arriving at the 2 sites was most likely to be represented well by NAME and the underlying meteorology. To prevent our emissions estimates being weighted towards the Mace Head observations we used early afternoon (12pm – 3pm) data for this site (when the boundary layer height is greatest and mixing most significant).

Results for HFC-125, HFC-134a and SF₆ are given in Figure 66 Emissions by country in 2011 for HFC-125 (top), HFC-134a (middle) and SF₆ (bottom) using the Bayesian inversion methodology. Clear uncertainty reductions from the prior to the posterior are demonstrated for HFC-134a and HFC-125 for countries that have significant emissions. For HFC-134a there is general agreement between the posterior values and the prior values from EDGAR. Results for HFC-125, however, show that prior emissions from Spain and Italy could be underestimated in the EDGAR prior: The posterior emissions are significantly larger and are accompanied by an uncertainty reduction. Little improvement could be made beyond the prior emissions estimates for SF₆, primarily due to the poor sensitivity of our measurement sites to the main areas of emissions in Europe i.e. Germany.

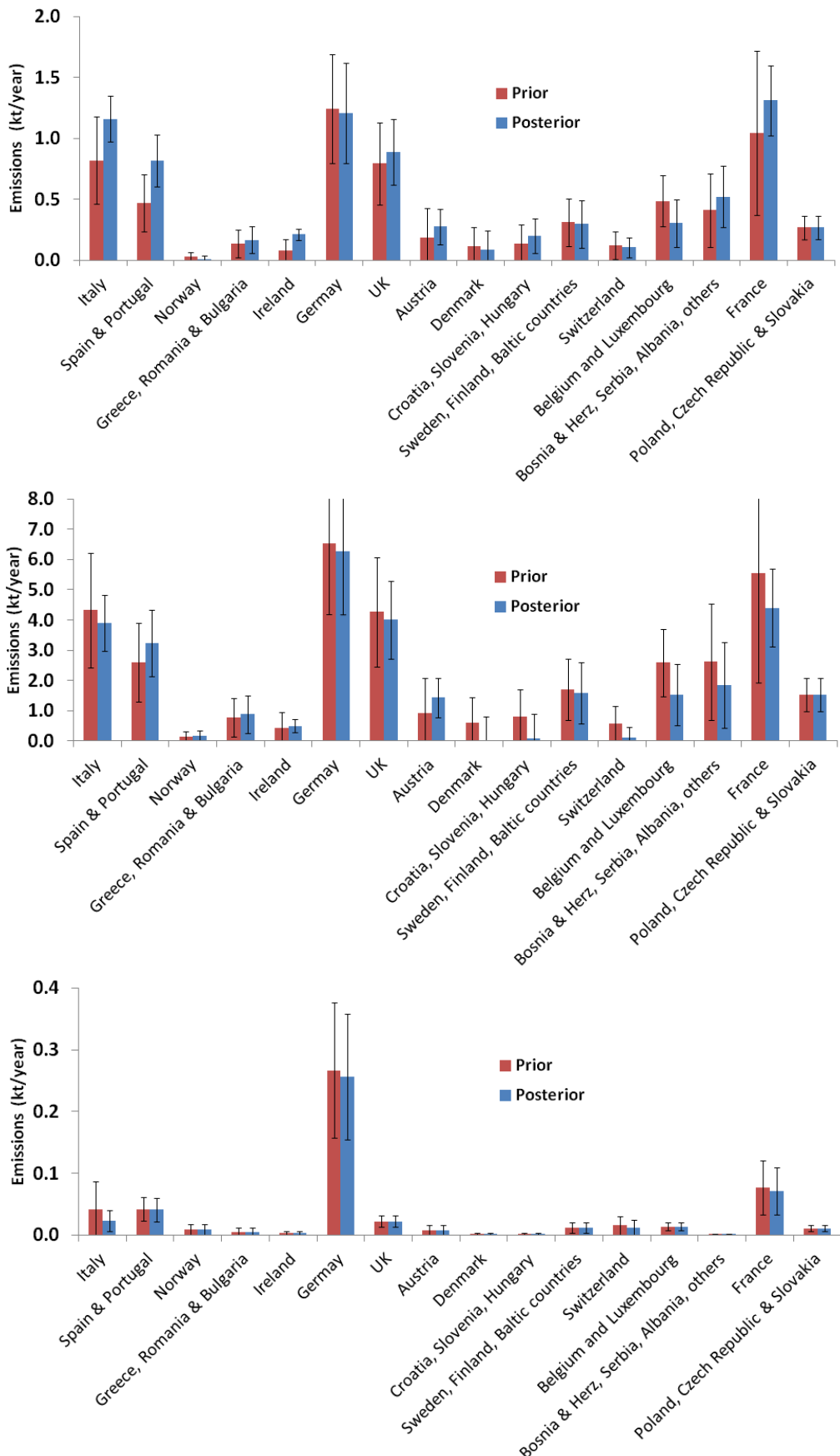


Figure 66 Emissions by country in 2011 for HFC-125 (top), HFC-134a (middle) and SF₆ (bottom) using the Bayesian inversion methodology.

7.3 Methane and nitrous oxide emission estimates

A large number of inversions were performed as set out in the InGOS protocol. For both CH₄ and N₂O the following experiments were made:

- Estimates for each year from 2006-2012 using an EDGAR prior, in situ measurements from 13 sites, and flask sample measurements from 13 sites.
- Estimates for each year from 2010-2012 using an EDGAR prior, in situ measurements from 18 sites, and flask sample measurements from 14 sites.
- Estimates for each year from 2010-2012 without prior information and using in situ measurements from 18 sites and flask sample measurements from 14 sites.
- Estimates for each year from 2010-2012 using an EDGAR prior, and only using in situ measurements from the 18 sites.

Here we have chosen a select number of experiments and years to demonstrate the output from the project. We have selected 2006 from Experiment 1 and 2011 from Experiments 2 and 3 (See Figure 67 and Figure 68). We have not included results from Experiment 4 here as only marginal changes are observed from Experiment 2.

The sensitivity of measurements to emissions from particular regions can be gauged from the relative uncertainties on the posterior estimates when no prior information is used. The region of the Netherlands, Belgium and Luxembourg (BeNeLux), for example, has a very small relative posterior emissions sensitivity. Italy and Spain, however, do not have significant measurement coverage and so have large relative posterior uncertainties. This is reflected in the results of Experiment 2 where very little error reduction or change in absolute emissions is observed for Spain or Italy from the prior to the posterior, yet an increase in absolute emissions accompanied by a large uncertainty reduction is observed for BeNeLux.

Our estimates for the UK for both N₂O (101 ± 30 kt yr⁻¹ for 2006; 100 ± 28 kt yr⁻¹ for 2011) and CH₄ (2900 ± 760 kt yr⁻¹ for 2006; 2470 ± 630 kt yr⁻¹ for 2011) compare well with estimates using the (MHD-only) DECC network ($37\text{--}162$ kt yr⁻¹ and $1560\text{--}3570$ kt yr⁻¹ for N₂O and CH₄, respectively, for 2006, and $17\text{--}149$ kt yr⁻¹ and $1270\text{--}3100$ kt yr⁻¹ for N₂O and CH₄, respectively, for 2011). Without use of a prior (Experiment 3) the magnitude of emissions of CH₄ (1570 kt yr⁻¹ for 2011) is at the lower end of the DECC network uncertainty range.

For NWEU our INGOS estimate of emissions is ~ 524 kt yr⁻¹ and ~ 13300 kt yr⁻¹ for N₂O and CH₄, respectively. For N₂O this is well within the (MHD-only) DECC network estimates, however, for CH₄ this is slightly higher than the (MHD-only) DECC network 95th percentile estimate. Given that NWEU estimates of CH₄ using the extended DECC network are larger than the MHD-only estimates, this InGOS estimate (using further independent observations in Europe) would further suggest that MHD-only CH₄ estimates for NWEU are potentially underestimated. Across all the inversions one of the most significant results is the high estimate of N₂O from France. In 2011 the posterior emissions were 240 ± 20 kt yr⁻¹; up from 140 ± 50 kt yr⁻¹ in the prior.

Our work has been submitted to the project leaders for the halocarbon, and nitrous oxide and methane tasks. The comparison of our results against those of the other modelling groups in Europe will take place in the second half of 2015. How our results compare against independent models and inverse methods will shed light on the significance of our results and highlight shortcomings and strengths in our respective methodologies.

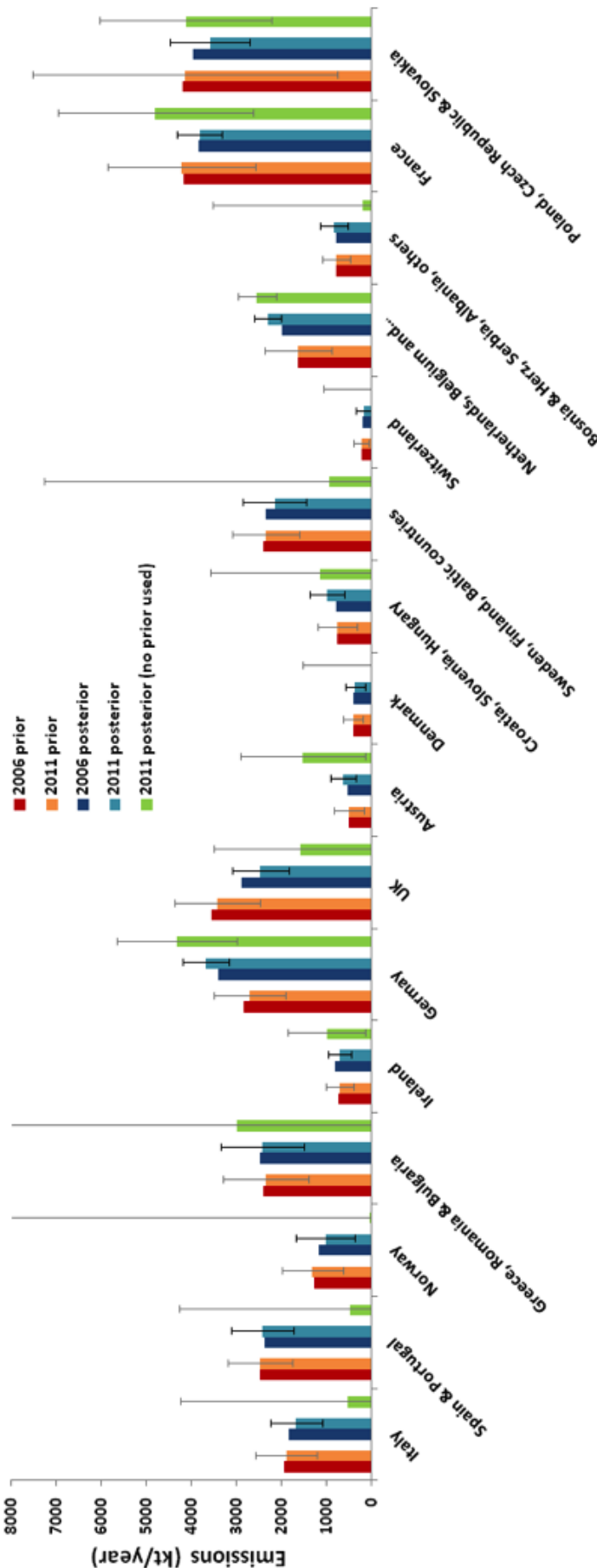


Figure 67 Estimates of CH₄ emissions for the InGOS project. Prior emissions are shown in red for 2006 and 2011 with corresponding posterior emissions in blue. Posterior emissions for the 'no prior' case for 2011 are shown in green.

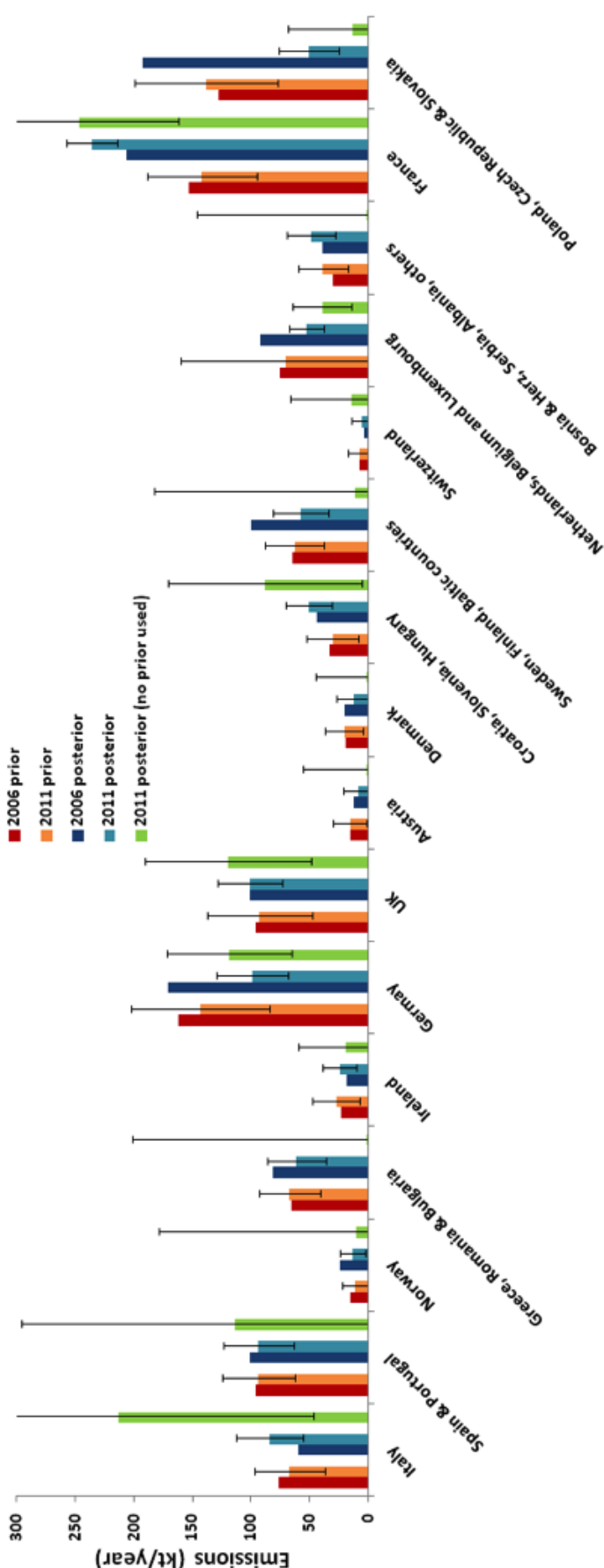


Figure 68 Estimates of N₂O emissions for the InGOS project. Prior emissions are shown in red for 2006 and 2011 with corresponding posterior emissions in blue. Posterior emissions for the 'no prior' case for 2011 are shown in green.

8 Appendix – Additional Site Information

8.1 Mace Head (MHD)

A new local server was installed at Mace Head on 29th June 2015 after a computing issue. The new server had Ubuntu 14.04 LTS installed.

8.1.1 Medusa-GCMS

Overall, the Medusa worked well over the past 16 months. In May 2014, an issue with T2 occurred and it was established that the thermocouple on the trap had become detached. The trap and thermocouple were replaced on 13th May and solved the issue. An issue with HFC-125 and HFC-32 contamination developed after the installation of the new trap in May 2014. The source of the problem is leakage of air conditioner coolant (HFC-32/125) into the lab, resulting in lab levels for these gases at ~1000 times ambient levels. Flushing the sample pump with outside air rectified the contamination issue. Switching pump or air conditioning unit are currently being explored as a long-term solution for the problem. A number of shutdowns occurred due to power outages and UPS shutdowns on 26/06/14, 12/08/14, 23/12/14, 01/03/15 and 03/01/15. A cross-port leak was found on valve 6 on 1st January 2015 and fixed on 22nd January 2015. A computing issue in June 2015 resulted in 10 days data loss. On 30th June, valve 6 was misaligned and caused an alarm email. The valve was realigned the same day. On 1st July 2015, EPC4 pressure was unstable due to the trap icing up. The Cryotiger was switched off and left to warm up. After further investigation, it was found that the Nafion sheath supply was off, causing the pressure instability for EPC4. Whilst the Cryotiger was at ambient temperature, the parker filters were changed.

8.1.2 GC-MD

The MD performed well for the reporting period. Most of the data loss resulted from ancillary equipment failure or a computing issue.

8.2 Ridge Hill (RGL)

The site at Ridge Hill, Herefordshire, has been operational since February 2012 and has collected 43 months of data from two sample inlets at 45 m and 90 m. The local server's operating system was upgraded to Ubuntu 14.04 LTS in February 2015.

8.2.1 GC-ECD

The gas chromatograph (GC) with electron capture detector (ECD), which measures N₂O and SF₆ at Ridge Hill from the 90 m inlet, ran well over the past 16 months. Fortnightly to monthly visits are being made to ensure instrumentation is running well and there are sufficient calibration and carrier gases.

8.2.2 CRDS

The Picarro G2301 Cavity Ring Down Spectrometer (CRDS) has been running well over the last 16 months. The CRDS samples air from the two tower inlets, 45 and 90 m, sequentially, altering every 30 minutes. The CRDS measures CO₂ and CH₄ in an evacuated cavity at very low pressure. Sample valve control and CRDS data is now continuously performed by GCWerks software from the local server, enabling the viewing of data in a similar manner to other GC based instruments. The Nafion drying system was removed from the CRDS in June 2015. H₂O correction coefficients were established using a H₂O droplet test and coefficients implemented in the post-processing of the data. An inter-comparison exercise with the UK GAUGE project was conducted in November 2014.

8.3 Taconeston (TAC)

Taconeston began operation in July 2012 and has collected 38 months of data. The Medusa GC-MS and GC-MD sample from the 100 m inlet, whilst the CRDS samples sequentially from inlets at heights of 54, 100 and 185 m. The local server was upgraded to Ubuntu 14.04 LTS in January 2015.

8.3.1 Medusa-GCMS

The Medusa has generally performed well over the past 16 months. A number of issues with the Cryotiger cooling system have occurred in May and June 2014. The Cryotiger was recharged with refrigerant on 26th June 2014 but a leak occurred with a refrigerant return line and the unit was not fully recharged, resulting in the Medusa being shutdown. A replacement Cryotiger unit and return line were brought up from Bristol and installed on 28th June 2014. A number of problems with loss of internet connection resulted in the site drifting from the Network Time Protocol (NTP). This was noticed on 2nd December 2014, when the difference between mobos1 time (Linux server) and NTP was 12 minutes and 36 seconds. A time correction has been applied to the data.

A problem with the air conditioning unit resulted in the unit not cooling the mobile lab enough. The Medusa-GCMS was shutdown on 6th January 2015 to prevent the instrument overheating. It was discovered that the filters on the external portion of the air conditioning unit were blocked. Access to the external unit was impeded by a fence erected by the site owners. A hole had to be cut in the fence on 16th February 2015 to allow an engineer access to clean the unit. The Medusa-GCMS was restarted on 17th February 2015. As part of the InGOS project, inter-comparison cylinders were run on the Medusa between 23rd and 25th March 2013.

After a number of poor tunes of the Mass Spectrometer (MS) on 24th June 2015, a leak was detected on the MS door. This was finally rectified by cleaning the o-ring that forms the seal on the door and applying a small amount of vacuum grease to the o-ring. This resulted in a couple of hours loss of data. A problem with the helium regulator developed on 13th July 2015 but this was replaced with a temporary regulator until a new regulator was put on the He cylinder on 27th July 2015. In the process of changing over the regulators, the system became contaminated with N₂. The system was bled on 28th July 2015 to remove N₂ contamination of the system. On 16th July, the 100 m line pump failed but was replaced on 17th July, resulting in data being lost in between this time.

8.3.2 GC-MD

The MD has operated well since it was installed. The PP1 system (measures CO and H₂) had to be disconnected from the GC-MD to investigate poor chromatography on 26th June 2014 but was reconnected on 29th July 2014. A problem with the air conditioning unit resulted in the unit not cooling the mobile lab enough. The GC-MD was shut down on 9th January 2015 to prevent the instrument overheating. The instrument was restarted on 28th January 2015.

A leak in the zero air carrier gas for the PP1 system was found on 29th January 2015 and resulted in the carrier gas running out. A new cylinder was put on and the system was leak checked. An internal pressure regulator was discovered to be faulty, so was bypassed and removed upon the suggestion of the system designer. Instrument precision was monitored afterwards to ensure that the removal of the pressure regulator did not have a negative impact on the quality of the data.

8.3.3 CRDS

The Picarro G2301 CRDS at Taconeston has been running well over the past 16 months. The system was upgraded to Windows 7 in June 2014, which fixed a number of instrumental issue previously experienced. The Nafion drying system was removed from the CRDS in June 2015. H₂O correction coefficients were established using a H₂O droplet test and coefficients implemented in the post-processing of the data. An inter-comparison exercise with the UK GAUGE project was conducted in January 2015.

8.4 Angus (TTA)

The University of Bristol (UoB) took over routine operation of Angus in January 2013 and has collected 32 months of data since this transition, sampling from an inlet at 222 m.

8.4.1 CRDS

The Picarro G2301 CRDS has operated well during the past 16 months. The site is visited by a local site operator on a monthly basis to carry out routine maintenance and repairs. The lack of an inlet cup and shield to prevent liquid water entering the sampling line still remains a problem at the site. Windows 7 was installed in November 2014 on the Picarro G2301. A power failure in January 2015 resulted in 4 days loss of data until a hard reboot of the system was done. Inter-comparison exercises with the GAUGE and cucumber projects were conducted in August 2014 and April 2015, respectively.